A COMPARISON OF IDENTIFICATION TECHNIQUES FOR FRACTIONAL ORDER SYSTEMS

by

Rıfat Volkan Şenyuva

B.S., Control Engineering, Istanbul Technical University, 2007

Submitted to the Institute for Graduate Studies in
Science and Engineering in partial fulfillment of
the requirements for the degree of
Master of Science

Graduate Program in Electrical & Electronic Engineering

Boğaziçi University

2009

ACKNOWLEDGEMENTS

I want to thank Assoc. Prof. Yağmur Denizhan, who introduced me to the subject, for her guidance and help during the preparation of this thesis. I have very much benefited from the discussions we had on the subject.

I would like to express my sincere gratitude to my family who have never hesitated to give me all assitance they can throughout my entire life.

This thesis has been supported by TUBİTAK National Scholarship Programme for MSc Students.

ABSTRACT

A COMPARISON OF IDENTIFICATION TECHNIQUES FOR FRACTIONAL ORDER SYSTEMS

This thesis compares the performances of various identification methods of deterministic and linear systems described by fractional order models. A detailed introduction to fractional calculus and fractional differential equations is presented. In this respect, the definitions of fractional calculus by Cauchy, Grünwald-Letnikov, Riemann-Liouville and Caputo as well as their properties and integral transforms are covered. Both analytical and numerical solutions of fractional differential equations as well as the initial condition problem are given in this thesis. Nonparametric and parametric system identification techniques for integer order systems are reviewed. The investigated fractional order identification methods are parametric techniques based on minimizing the prediction error. The modeling is done in black-box approach where the structure of the fractional order differential equation is selected at the start of the identification procedure. The estimation of the parameter vector can be performed in time and frequency domain. Time domain identification is carried out by using linear regression form and Grünwald-Letnikov's definition while the investigated frequency domain methods are Levy's method and Levy's method with Vinagre's weights. As benchmark systems, semi-integrating electrical circuits and Bagley-Torvik's viscoelastic system are used. Identification results have revealed that in general the proposed fractional order models are more successful at predicting the system output than the proposed integer order models. The persistency of excitation from integer order system identification has to be redefined for fractional order system identification. Time domain methods can be applied directly while in frequency domain system's frequency response must first be estimated by nonparametric methods. Original contribution of this thesis is the comparison of integer and fractional order models for the chosen benchmark systems.

ÖZET

KESİRLİ DERECELİ SİSTEMLER İÇİN SİSTEM TANIMA TEKNİKLERİNİN KARŞILAŞTIRILMASI

Bu tezde çesitli sistem tanıma tekniklerinin kesirli dereceli deterministik doğrusal sistemler üzerindeki performansları karşılaştırılmıştır. Bu çalışmanın öncelikli hedeflerinden biri, kesirli dereceli matematiğin tanıtılmasıdır. Bu bağlamda kesirli dereceli matematikte en çok kullanılan Cauchy, Grünwald-Letnikov, Riemann-Liouville ve Caputo türev ve integral tanımları incelenmiştir. Bu tanımların özellikleri ve Laplace dönüşümlerine yer verilmiştir. Kesirli dereceli diferansiyel denklemlerin analitik ve sayısal çözümleri ile birlikte başlangıç koşulu problemi araştırılmıştır. Parametrik ve parametrik olmayan tamsayılı sistem tanıma teknikleri üzerinde çalışılmıştır. İncelenen kesirli dereceli sistem tanıma teknikleri parametriktir ve öngörü hatasını küçültmeye dayanır. Kullanılacak olan kesirli dereceli diferansiyel denklemin yapısı siyah-kutu yöntemi gereği kullanıcı tarafından başta seçilir. Parametre vektörü zaman tanım kümesi ve frekans tanım kümesi metotları ile bulunabilir. Zaman tanım kümesinde doğrusal regresyon formu ve Grünwald-Letnikov tanımı kullanılırken frekans tanım kümesinde Levy'nin metodu ve Vinagre ağırlıklarının bu metoda uygulanması incelenir. Anlatılan tekniklerin karşılaştırılması yarım integral alıcı devreler ve Bagley-Torvik sistemi üzerinde yapılır. Sonuçta önerilen kesirli dereceli modellerin tamsayı karşılıklarına göre dinamik sistemi temsil etmede genelde daha başarılı oldukları görülmüştür. Giriş işaretleri için geçerli olan sürekli uyarma kavramının kesirli dereceli sistem tanıma için tekrar tanımlanması gerektiğini gözlenmiştir. Zaman tanım kümesi metotları doğrudan uygulanabilirken frekans tanım kümesinde ilk önce frekans cevabının parametrik olmayan metotlar ile bulunması gerekir. Bu tez çalışmasında özgün olarak tamsayılı ve kesirli dereceli modeller seçilen örnek sistemler üzerinde karşılaştırılmıştır.

TABLE OF CONTENTS

LIST OF FIGURES

LIST OF TABLES

LIST OF SYMBOLS/ABBREVIATIONS

$\arg\min f(x)$	Value of x that minimized $f(x)$
$E\{x\}$	Mathematical expectation of the random vector x
$\overline{E}\{x(n)\}$	$\lim_{N\to\infty}\frac{1}{N}\sum_{n=1}^{N}E\{x(n)\}$
${}_a\mathscr{D}_t^{\alpha}$	Continuous integro-differential operator
$\mathscr{L}\{\cdot\}$	Laplace transform
$\Re(z)$	Real part of the complex number z
$\Im(z)$	Imaginary part of the complex number z
$\mathbb{R}$	Set of real numbers
$\mathbb{R}^N$	Euclidian N-dimensional space
$\mathbb{Z}$	Set of integer numbers
$R_x(\tau)$	$\overline{E}\left\{x(n)x^T(n-\tau)\right\}$
$R_{x_1x_2}(\tau)$	$\overline{E}\left\{x_1(n)x_2^T(n-\tau)\right\}$
$\Phi_x(\omega)$	Power spectrum of x
$\Phi_{x_1x_2}(\omega)$	Cross power spectrum between x_1 and x_2
$G(e^{j\omega})$	Frequency Response
$G(s)$	Continuous time transfer function from u to y
$G_0(s)$	True continuous time transfer function from u to y
$G(z)$	Discrete time transfer function from u to y
$G(z,\theta)$	Discrete time transfer function from u to y in a model structure, corresponding to the parameter value θ
$G_0(z)$	True discrete time transfer from u to y for a given system
$H(z)$	Discrete time transfer function from e to y
$H(z,\theta)$	Discrete time transfer function from e to y in a model structure, corresponding to the parameter value θ
$L(z)$	Prefilter for prediction errors
$U_N(\omega)$	Fourier transform of u
$V_N(\theta,Z^N)$	Criterion function to be minimized

$W_{\nu\hat{\nu}}(z)$	Discrete time transfer function from ν to $\hat{\nu}$
$W_{u\hat{y}}(z)$	Discrete time transfer function from u to $\hat{\nu}$
$W_{y\hat{y}}(z)$	Discrete time transfer function from y to $\hat{y}$
$Y_N(\omega)$	Fourier transform of y
Z^N	$\{u(0), y(0), \ldots, u(N), y(N)\}$
$\mathscr{E}_\alpha(t)$	One parameter Mittag-Leffler function
$\mathscr{E}_{\alpha,\beta}(t)$	Two parameter Mittag-Leffler function
$e(n)$	Disturbance at discrete time n
$f_e(x,\theta)$	Probability density function of the random variable e
$g(\tau)$	Impulse response of a linear, time-invariant, casual system
q	Commensurate order
$u(n)$	Input variable at discrete time n
$y(n)$	Output variable at discrete time n
$\hat{y}(n\|n-1)$	Predicted output at discrete time n
$\varepsilon(n)$	Prediction error $y(n) - \hat{y}(n\|n-1)$
$\varphi(n)$	Regression vector at discrete time n
$\nu(n)$	Disturbance variable at discrete time n
$\hat{\nu}(n\|n-1)$	Predicted disturbance variable at discrete time n
$\varpi_j^{(\alpha)}$	Binomial coefficients, $\varpi_j^{(\alpha)} = (-1)^j \binom{\alpha}{j}$
θ	Vector used to parametrize models
θ_0	True values of the parameter vector
ζ	Parameter of Levenberg-Marquardt Algorithm
$\Gamma(x)$	Gamma function

ARX	AutoRegressive with eXternal input
ARMAX	AutoRegressive Moving Average with eXternal input
DFT	Discrete Fourier Transform
ETFE	Empirical Transfer Function Estimate
FIR	Finite Impulse Response
FODE	Fractional Order Differential Equation
LSE	Least Squares Estimate

LTI	Linear Time Invariant
PDF	Probability Density Function
PEM	Prediction Error Identification Method
PRBS	Pseudo Random Binary Signal
RL	Riemann-Liouville
SPA	Spectral Analysis
WSS	Wide-sense Stationary

1. INTRODUCTION

Science is based on making observations and building models which best represent the properties deduced from these observations. The aim of modelling is to fit the observations into some structure. System identification studies the techniques of establishing mathematical models by using data gathered from the dynamical systems that are to be identified. Since scientific research is centered on dynamical systems, system identification is an integral part of scientific methodology and thus has a wide application area [1].

Since Newton discovered his laws of motion, and combined them with differential equations to explain Kepler's laws of planetary motion in 1666, various mathematical formalisms have been developed in order to model dynamical systems. Dynamical system models can be categorized according to various criteria. The two main types are differential equations and difference equations. The difference between them is based on their evaluation of time. While differential equations describe the evolution of dynamical systems in continuous time, the time in difference equations is discrete. These two types of mathematical models can be further categorized according to a number of properties such as ordinary or partial, linear or nonlinear, time invariant or time variant, deterministic or stochastic.

Order of a differential equation can also be the basis of categorization. Fractional order differential equations are differential equations which involve derivatives of non integer, fractional order. Although the invention of fractional calculus is as old as the classical calculus going back to the late 1600s, it has not been widely used as a tool for modelling dynamical systems. However, identification on real systems has shown that fractional order models can be more intrinsic and adequate than integer order models in describing the dynamics of many real systems. One of the first such physical systems known to be modelled by a fractional order differential equation is the semi-infinite lossy transmission line. The current going into this line is modelled equal as the $(0.5)^{\text{th}}$ order derivative of the applied voltage [2]. Another electrical dynamical system

example is a capacitor model which uses fractional order calculus in order to better account for losses [3]. Heating dynamics of a heat-rod system can also be modelled by a fractional order differential equation [1].

There exist many more dynamical systems such as viscoelastic systems, electrochemical processes, dielectric polarization, colored noise, electromagnetic waves and boundary layer effects in ducts, the dynamics of which is claimed to be better captured via fractional order models throughout the literature. The fractional-order-nature of the dynamics of these systems is believed to originate from the material and chemical properties found within these systems [2, 4]. However, system identification with fractional order models is an area that has been investigated much less than its integer order counterpart. Thus there remains a wide range of dynamical systems which can benefit from a fractional order model. The aim of this thesis is to identify such systems and observe if they can be better represented by fractional order models.

1.1. Dynamical Systems

A dynamical system is one which upon an interaction with external stimuli produces observable signals, i.e. outputs, based on not only on the current values of the external stimuli but also on their earlier values. This is an important feature which distinguishes a dynamical system from any other system [1]. If a dynamical system always produces the same output for a given starting condition, then it is a deterministic one. The dynamical systems in this thesis are deterministic.

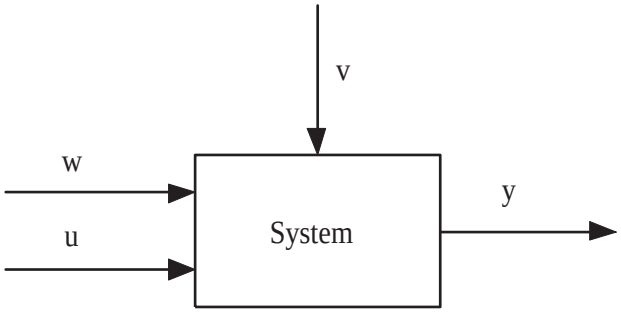

Figure 1.1. A system with output y, input u, measured disturbance w, and unmeasured disturbance v.

The external signals acting on a system are categorized as inputs and disturbances (Figure 1.1). Input signals are signals created intentionally by the user and can be changed by the user while disturbance signals are not controllable. Disturbance signals can also be classified as measured disturbance and unmeasured disturbance (Figure 1.1).

1.2. Dynamical System Models

Models can be classified into many different groups according to the mathematical formalism employed. The problem of driving a car can be solved by the help of a mental model without any mathematical sophistication. Graphical models consisting of numerical tables and plots can be sufficient to describe certain systems. Impulse responses, step responses and frequency responses are graphical models typically used for the linear systems. Even complex dynamics of nonlinear systems can be understood by graphical models called flows.

Mathematical expressions such as difference or differential equations may be considered as advanced mathematical or analytical models and they are preferred to the simpler models mentioned above once the application becomes complicated. Mathematical models are categorized into groups such as time continuous or time discrete, lumped or distributed, deterministic or stochastic, linear or nonlinear. Each of these adjectives marks a property of the used model for the dynamic system and thus determines the type of the equation. Mathematical models are used in almost all fields of science including engineering, physics and even nontechnical areas like economy, ecology and biology [1].

In this thesis only deterministic, lumped-parameter, continuous time linear systems will be considered. Such systems lend themselves to description in terms of ordinary linear differential equations.

1.3. Fractional Order Equations

Fractional calculus is not a new subject. Interest in this subject dates back to a letter written by Leibniz to L'Hôspital in the late 17th century. In the year of 1695 L'Hôspital, referring to the differentiation notation $d^n y/dx^n$, asked Leibniz: "What if n be 1/2?". Leibniz [5] replied: "... This is an apparent paradox from which, one day, useful consequences will be drawn."

First organized studies on fractional calculus were performed in the beginning and middle of the 19th century by Liouville and Riemann. Liouville (1832) expanded functions in series of exponentials and defined the derivative of such a series by operating term-by-term under the assumption of derivative order being a positive integer. Riemann (1847) proposed a different definition which involved a definite integral and was applicable to power series with noninteger exponents [5].

It was Grünwald and Krug who first unified the results of Liouville and Riemann. Grünwald (1867) adopted as his starting point the definition of a derivative as the limit of a difference quotient and arrived at definite integral formulas for differentiation to an arbitrary order. Krug (1890), working through Cauchy's integral formula for ordinary derivatives, showed that Riemann's definite integral had to be interpreted as having a finite lower limit while Liouville's definition corresponded to a lower limit $-\infty$ [5].

Meanwhile the development of the applications of the fractional calculus was moving parallel to these theoretical beginnings. One of the first applications was the tautochrone problem. Abel (1823) solved the integral equation for the tautochrone problem via an integral transform which could be written as a semi-derivative. A powerful boost in the use of fractional calculus to solve problems was provided by Boole. Boole (1844) developed symbolic methods for solving linear differential equations with constant coefficients. The next important step in the application of fractional order calculus was made by Heaviside. Heaviside developed operational calculus to solve certain problems of electromagnetic theory. In the year of 1920 he introduced fractional differentiation in his work on transmission line theory. Later Gemant (1936) extended

Heaviside's approach for problems of elasticity [6].

In the 20th century notable contributions were made to both the theory and application of the fractional calculus. Some of the work worth mentioning was done by Weyl (1917), Hardy and Littlewood (1925, 1928, 1932), Kober (1940), and Kuttner (1953) who examined some properties of both differentiation and integration to an arbitrary order of functions belonging to Lebesgue and Lipschitz classes. Erdélyi (1939, 1940, 1954) and Osler (1970) gave definitions of differentiation and integration to an arbitrary order with respect to arbitrary functions. Post (1930) used difference quotients to define generalized differentiation for operators. Riesz (1949) developed a theory of fractional integration for functions of more than one variable. Erdélyi (1964, 1965) applied the fractional calculus to integral equations and Higgins(1967) used fractional integral operators to solve differential equations [6]. Some of the present-day applications of fractional calculus include fluid flow, rheology, dynamical processes in self-similar and porous structures, diffusive transport akin to diffusion, electrical networks, probability and statistics, control theory of dynamical systems, viscoelasticity, electrochemistry of corrosion, chemical physics, optics and signal processing.

1.4. System Identification

1.4.1. Historical Perspective

The foundations of system identification came from previous work on mathematical statistics. Econometrics and time series analysis can be considered as the mother of system identification. The field of econometrics uses statistics to derive information from economic data. Time series analysis and difference equation modeling are statistical tools developed by econometrics. Time series analysis originated from the efforts of Jevons (1884), Yule (1927) and Wold (1938). Mann and Wald (1943) established the asymptotic theory of the least squares estimator for stochastic linear difference equations. Koopmans et al. (1950) not only expanded the asymptotic estimator theory to multivariable systems, but also solved central identifiability issues and presented Gaussian maximum likelihood estimates [7].

Although preliminary work was long established in the field of econometrics, from control system perspective the term "system identification" was coined by Zadeh (1956). From that point onwards system identification theory took on two different paths. First path dealt with the realization problem which was suggested by Ho and Kalman (1966). Their aim was to implement impulse response in the realization of linear state space models. Before this time control engineers were using graphical models such as Bode, and Nyquist graphs, Ziegler-Nichols charts or step response analysis in the design of dynamic systems. With the introduction of state-space representation there came optimal control theory which formed the basis of model based control design. Later this path was further developed by Akaike (1976), Larimore (1983), Van Overschee and DeMoor (1996). These participations gave birth to methods called as subspace methods [8].

The second path which was more related to statistical time series analysis from econometrics and was given the name of prediction error approach. This approach was pioneered by Åström and Bohlin (1965). Åström and Bohlin applied the Gaussian maximum likelihood framework established from time series analysis to the problem of system identification. This framework comprised of several models given unheard names by the control community like autoregressive moving average or autoregressive moving average with exogenous inputs. Up to that time these models were unknown to control community but they were well known by the statistics community. These models combined with Gaussian maximum likelihood estimate created the framework of prediction error identification [7].

Identification community was under complete influence of the prediction error framework until 1978 and the search for the true system model was the priority. Then in 1978 Anderson et. al., Ljung and Caines suggested that system identification should be seen as finding the best description of the actual system amongst a number of models. The aim of identification became choosing the best approximation of the true system. The priority shifted to the model errors. With the work of the eighties on bias and variance analysis system identification emerged as a design problem. The selection of input, model structure, and criterion became design variables which could

be adjusted in order to achieve the identification objective set for the model [8].

A new paradigm was born in the beginnings of 1990s. In this new approach priority was to design a model based controller. Identification for control was not only based on identification but also on robust control theory. Thus research areas of identification like experiment design, closed-loop identification and frequency domain identification had to be reviewed from control perspective. The development of model-based control design allowed the expansion of control system theory to other areas of application untouched before such as process control, environmental systems, biological systems, biomedical systems and transportation systems [8].

1.4.2. System Identification Procedure

System identification is based on experimentation. Input and output data gathered from the system are analyzed and a model is deduced from this analysis. There are three important objects in system identification [1].

(i) Experiment design. Input and output data are collected during the experiment. The input signal applied to the system, measured signals and time of the measurement are all determined by the user. These choices related with the experiment design determine the quality of the recorded data.

(ii) A set of candidate models. The most important choice in the system identification procedure is the selection of a set of candidate models from a larger collection of models. The user's choice must match the formal properties of the actual system. If some insight of the system's dynamics is available through physical interpretation, the constructed model set is called a "grey-box". Model sets with adjustable parameters are called grey-boxes. Otherwise if there is no known reference to the physical background of the system, a black-box model set is employed. The parameters of the black box indicate no physical interpretation of the system.

(iii) Identification method. Deciding which model is the best in the set is the identification method. The quality of a model is its degree of how well the reproduced

model output matches the measured data.

Once the user makes a decision on the three issues mentioned above, a particular model from the set that best fits the measured data according to the chosen criterion may be found. There remains a last step where the particular model is evaluated to find out whether the model is valid for its purpose. This last step is model validation. If the model is inadequate for its intended use, the model is rejected. Thus it is highly probable that the first model is going to fail the model validation test. Then the user must review the previous steps of the identification procedure and make the necessary adjustments to various steps. A model may fail the model validation test due to a number of reasons [1].

- The numerical procedure applied to find the best model is not good.
- The chosen criterion is inadequate.
- The chosen model set's description of the actual system is poor.
- The collected data from experimentation is not rich enough.

A significant percentage of any identification application is dedicated to handling these validation problems over and over again like a loop. The schema of system identification procedure is given in Figure 1.2.

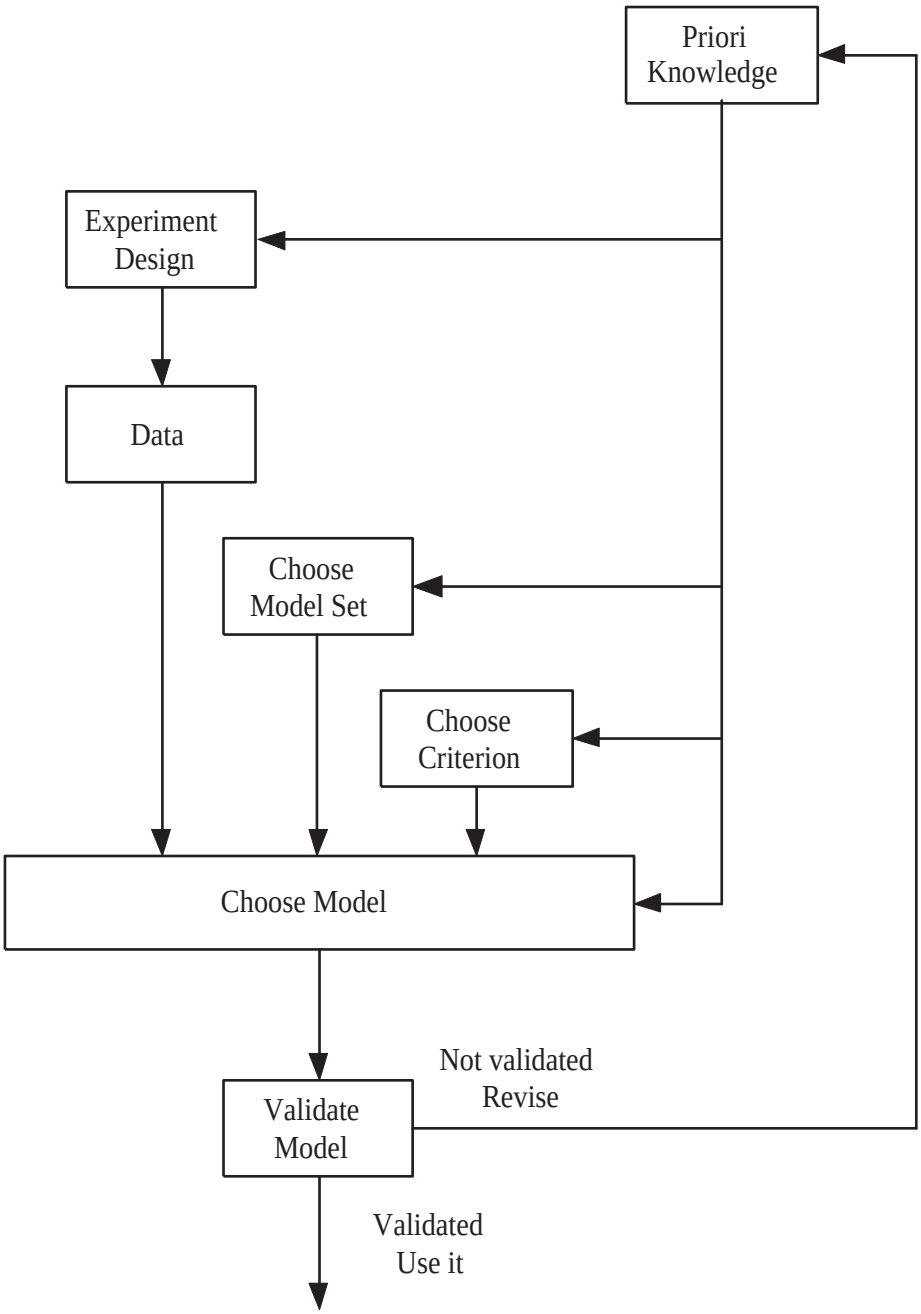

Figure 1.2. Flowchart of the basic system identification method [1].

1.5. Problem Statement

The aim of this thesis is to compare various identification methods for systems that can be described in terms of fractional order models. Some dynamical systems are reported to be better described by fractional order models than integer order models. Some examples of such systems given in the literature are transmission lines, capacitors, thermal systems, viscoelastic systems and electrochemical processes. Integer order differential equations derived from classical calculus are believed to be inadequate for modeling these real systems. Fractional order models developed for these systems are continuous time fractional order differential equations which are linear and time invariant. An n-term fractional order differential equation is given as

$$\mathscr{D}^{\alpha_0}y(t)+a_1\mathscr{D}^{\alpha_1}y(t)+\cdots+a_n\mathscr{D}^{\alpha_n}y(t) = b_0\mathscr{D}^{\beta_0}u(t)+b_1\mathscr{D}^{\beta_1}u(t)+\cdots+b_m\mathscr{D}^{\beta_m}u(t) \quad (1.1)$$

where the operators $\mathscr{D}^{\alpha_k}$ and $\mathscr{D}^{\beta_k}$ are called continuous integro-differential operator (see Section 2) and represents differentiation of the applied function to arbitrary real order. Depending upon the system, not all α_k's and β_k's are required to be integer or noninteger. Differentiation orders, $(\alpha_0, \ldots, \alpha_n, \beta_0, \ldots, \beta_m)$, are supposed to be known by the user as it is the case of many real dynamical systems.

System identification methods that are to be investigated are based on continuous time black-box models (Figure 1.3). Black-box models allow the user to construct models for dynamical systems that are not easily described by known physical laws.

Figure 1.3. Identification approach.

The structure of the model depends upon the selection of the differentiation orders, α_k's and β_k's. Once the orders are fixed for a model, then the model is

parametrized via the coefficients of the differential equation (1.1).

$$\theta = \begin{bmatrix} a_1 & \cdots & a_n & b_0 & \cdots & b_m \end{bmatrix}^T \tag{1.2}$$

The parameter vector, θ, is estimated either analytically or numerically by minimizing prediction error (see Section 3.3.3). User may estimate many model structures with different configurations of the differentiation orders and different parameters. Then the user compares these structures and chooses the model that fits the validation data best.

This thesis investigates how this strategy can be applied with fractional order models and compares various extensions of the identification techniques used with integer order models.

2. FRACTIONAL ORDER LINEAR SYSTEMS

Fractional order calculus is a subject as old as the classical calculus. Although the idea of fractional order calculus was first mentioned in a letter from Leibniz from to L'Hospital in 1695, there would not be any significant work until the beginning of the 19th century. The studies of Liouville, Riemann and Holmgren in the second half of the 19th century could be considered the earliest systematic works on fractional order calculus [6].

There exist many physical systems that can benefit from being described by fractional order models. One of the first physical systems to be recognized for such models is the voltage-current relation of a semi-infinite lossy transmission line. Another example is the diffusion of heat into a semi-infinite solid. Heat flow into the semi-infinite solid is equal to the half-derivative of the temperature. Such physical systems can be better modelled by using fractional order calculus rather than the classical calculus [9].

It is observed that fractional order calculus has been neglected as a mathematical tool for modelling fractional order system dynamics because integer-order models are more suitable for analysis and provide in most cases easier solutions. Understanding the solutions of fractional order differential equations is the key to building better models for fractional order dynamic systems.

For that purpose, fundamentals of the fractional order calculus are introduced first. There exist many different definitions because fractional order calculus is still under development. Only the significant definitions and their useful properties will be presented here. Then fractional order differential equations and their solutions will be given.

2.1. Fractional Order Calculus

Fractional order calculus is a generalization of integration and differentiation to non-integer order fundamental operator ${}_a\mathscr{D}_t^\alpha$, where a and t are the limits of the operation. The continuous integro-differential operator is defined in [9] and α is the order of the operation, generally $\alpha \in \mathbb{R}$.

$$ {}_a\mathscr{D}_t^\alpha = \begin{cases} \frac{\mathrm{d}^\alpha}{\mathrm{d}t^\alpha} & \Re(\alpha) > 0, \\ 1 & \Re(\alpha) = 0, \\ \int_a^t (\mathrm{d}\tau)^{-\alpha} & \Re(\alpha) < 0, \end{cases} \tag{2.1} $$

The development of the fractional order calculus led to various definitions of fractional order differentiations and integrations. Some of the definitions are simply extensions made from classical calculus. The significant definitions consists of the Cauchy integral formula, the Grüwald-Letnikov definition, the Riemann-Liouville definition, and the Caputo definition. Before giving these well-established definitions and their properties, the gamma function which is used in each of these definitions is introduced.

2.1.1. Gamma Function

The complete gamma function $\Gamma(x)$ function is very important in fractional calculus. Certain properties of this function will be presented in this subsection. The Euler limit (2.2) gives a thorough definition of $\Gamma(x)$ [6].

$$ \Gamma(x) \equiv \lim_{N\to\infty} \frac{N!N^x}{x(x+1)(x+2)\dots(x+N)} \tag{2.2} $$

Another definition of $\Gamma(x)$ is the integral transform definition. Although this definition is more practical, x cannot assume negative values (2.3).

$$ \Gamma(x) \equiv \int_0^\infty y^{x-1}e^{-y}\mathrm{d}y, \qquad x > 0 \tag{2.3} $$

The recurrence property can be written down after applying an integration by parts (2.4).

$$\Gamma(x+1) = x\Gamma(x) \tag{2.4}$$

The recurrence property is regarded as the most important property of $\Gamma(x)$ function. This relation can also be derived from the first definition of $\Gamma(x)$ function, the Euler limit definition. By replacing x with positive integer n and using $\Gamma(1) = 1$, the recurrence can be expanded to the factorial of n (2.5).

$$\Gamma(n+1) = n\Gamma(n) = n(n-1)\Gamma(n-1) = \ldots = n \cdot (n-1) \cdots 2 \cdot 1 \cdot \Gamma(1) = n! \tag{2.5}$$

If recurrence property is written as $\Gamma(x-1) = \Gamma(x)/(x-1)$, an analytic continuation is gained and the gamma funtion becomes applicable to negative arguments. According to the new expression not only $\Gamma(0)$ is infinite but also all of the negative integers give infinity because of the recurrence. However the ratios of gamma functions of negative integers are finite (2.6).

$$\frac{\Gamma(-n)}{\Gamma(-N)} = (-N)(-N+1)\cdots(-n-2)(-n-1) = (-n)^{N-n}\frac{N!}{n!} \tag{2.6}$$

The reciprocal $1/\Gamma(x)$ of the gamma function is single valued and finite for all x. The graph of this function for $-4 \leq x \leq 6$ is shown in Figure 2.1. It is observed from Figure 2.1 that the reciprocal changes signs continuously for negative x values. As for the positive x values, the function approaches asymptotically to zero. This approach can be approximated as in (2.7).

$$\frac{1}{\Gamma(x)} \approx \frac{x^{\frac{1}{2}-x}}{\sqrt{2\pi}}e^{x}, \qquad x \to \infty \tag{2.7}$$

While the gamma function of a positive integer n is itself a positive integer, the gamma function of any negative integer is infinite.

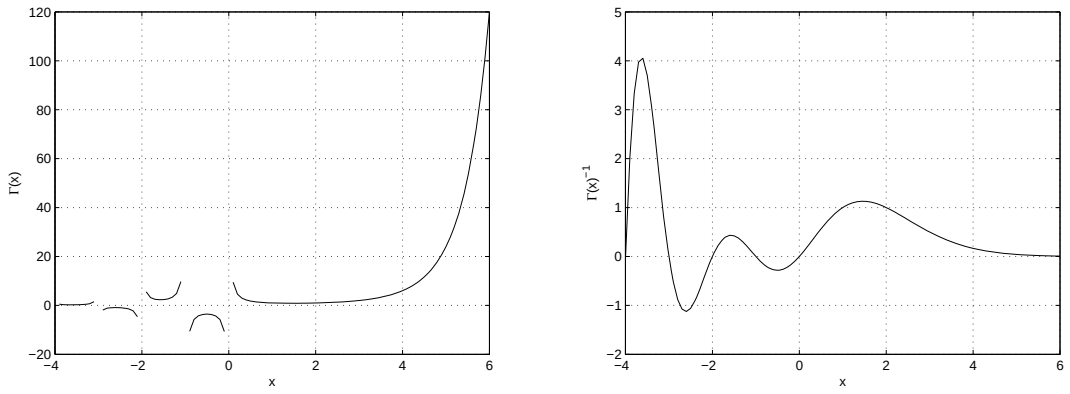

(a) Gamma function (b) The reciprocal of the gamma function

Figure 2.1. Gamma function and its reciprocal for $-4 \leq x \leq 6$.

The gamma functions of $\Gamma(\frac{1}{2}+n)$ and $\Gamma(\frac{1}{2}-n)$ are multiples of $\Gamma(\frac{1}{2}) = \sqrt{\pi}$ (2.8).

$$\Gamma\left(\frac{1}{2} \pm n\right) = \begin{cases} \dfrac{(2n)!\sqrt{\pi}}{4^n n!} \\ \\ \dfrac{(-4)^n n!\sqrt{\pi}}{(2n)!} \end{cases} \tag{2.8}$$

Some values of the gamma function are given in Table 2.1.

Table 2.1. Some values of the gamma function.

$\Gamma(-\frac{3}{2}) = \frac{4}{3}\sqrt{\pi}$	$\Gamma(1) = 1$
$\Gamma(-1) = \pm\infty$	$\Gamma(\frac{3}{2}) = \frac{1}{2}\sqrt{\pi}$
$\Gamma(-\frac{1}{2}) = -2\sqrt{\pi}$	$\Gamma(2) = 1$
$\Gamma(0) = \pm\infty$	$\Gamma(\frac{5}{2}) = \frac{3}{4}\sqrt{\pi}$
$\Gamma(\frac{1}{2}) = \sqrt{\pi}$	$\Gamma(3) = 2$

2.1.2. Definitions and Properties of Fractional Order Calculus

There exist various definitions of fractional order derivative and integral developed by different mathematicians.

2.1.2.1. Fractional-order Cauchy Integral Formula. This is an extension from integer order calculus (2.9).

$$\mathscr{D}^{\alpha} f(t) = \frac{\Gamma(\alpha+1)}{\mathrm{j}2\pi} \int_{\mathbf{C}} \frac{f(\tau)}{(\tau - t)^{\alpha+1}} \mathrm{d}\tau \tag{2.9}$$

C denotes the closed path that encircles the poles of $f(t)$. $\Gamma(\alpha+1)$ is the gamma function (2.1.1). The advantage of the Cauchy's integral formula is that the integrals and derivatives of sinusoidal and cosine functions can be expressed as in (2.10).

$$\begin{aligned} \mathscr{D}^{\alpha} \left[\sin \omega t\right] &= \omega^{\alpha} \sin\left(\omega t + \frac{\alpha\pi}{2}\right) \\ \mathscr{D}^{\alpha} \left[\cos \omega t\right] &= \omega^{\alpha} \cos\left(\omega t + \frac{\alpha\pi}{2}\right) \end{aligned} \tag{2.10}$$

Using Cauchy's formula it can be proved that (2.10) holds for arbitrary α.

2.1.2.2. Grünwald-Letnikov Definition. The fractional order differentiation and integral can be defined in a unified way by Grünwald-Letnikov definition [5, 6, 9, 10].

$${}_{a}\mathscr{D}_{t}^{\alpha} f(t) = \lim_{h \to 0} \frac{1}{h^{\alpha}} \sum_{j=0}^{[(t-a)/h]} (-1)^{j} \binom{\alpha}{j} f(t - jh) \tag{2.11}$$

While the subscripts to the left and right of $\mathscr{D}$ are lower and upper bounds in the integral, $\binom{\alpha}{j}$ are the binomial coefficients. $|\alpha|$ denotes either the order of differentiation, α should be positive, or the order of integration, α should be negative. α can take noninteger values.

The advantage of this definition is that it allows numerical differentiation and integration of a function to an arbitrary order. However as the value of t increases, the computations become more complex and larger memory is required due to the increasing number of past values of the function involved in the summation.

2.1.2.3. Riemann-Liouville Definition. According to Riemann-Liouville (RL) definition [5, 6, 9, 10] the fractional order integral is established as (2.12).

$$ {}_a\mathscr{D}_t^{-\alpha} f(t) = \frac{1}{\Gamma(\alpha)} \int_a^t (t-\tau)^{\alpha-1} f(\tau) \mathrm{d}\tau \tag{2.12} $$

a is the initial limit value and $0 < \alpha < 1$. In the case of $a = 0$, the notation of the integral is simplified to $\mathscr{D}_t^{-\alpha} f(t)$. The RL definition is a widely used definition for fractional order differentiation and integral. Similarly, fractional order differentiation is defined as (2.13) where $n - 1 < \beta \leq n$.

$$ \begin{aligned} {}_a\mathscr{D}_t^{\beta} f(t) &= \frac{\mathrm{d}^n}{\mathrm{d}t^n} \left[{}_a\mathscr{D}_t^{-(n-\beta)} f(t) \right] \\ &= \frac{1}{\Gamma(n-\beta)} \frac{\mathrm{d}^n}{\mathrm{d}t^n} \left[\int_a^t \frac{f(\tau)}{(t-\tau)^{\beta-n+1}} \mathrm{d}\tau \right] \end{aligned} \tag{2.13} $$

The disadvantage of the RL definition is that its integral transform (see Section 2.1.3) introduces initial conditions like $\mathscr{D}^{\alpha-1} f(0), \mathscr{D}^{\alpha-2} f(0), \ldots, \mathscr{D}^{\alpha-n} f(0)$ where $n-1 < \alpha \leq n$. Such initial conditions have no known physical interpretation.

2.1.2.4. Caputo Definition. The Caputo fractional order differentiation [5, 6, 9, 10] is defined in (2.14).

$$ {}_0\mathscr{D}_t^{\alpha} f(t) = \frac{1}{\Gamma(1-\alpha)} \int_0^t \frac{f^{m+1}(\tau)}{(t-\tau)^{\alpha}} \mathrm{d}\tau \tag{2.14} $$

m is an integer and $\alpha = m + \gamma$, $0 < \gamma \leq 1$. Similarly, by Caputo's definition, the integral is described by (2.15).

$$ {}_0\mathscr{D}_t^{-\gamma} f(t) = \frac{1}{\Gamma(\gamma)} \int_0^t \frac{f(\tau)}{(t-\tau)^{1-\gamma}} \mathrm{d}\tau, \quad \gamma > 0 \tag{2.15} $$

The advantage of the Caputo definition is that its integral transform (see Section 2.1.3) implements physically interpretable initial conditions such as $f'(0), f''(0), f'''(0), \ldots$ from integer order calculus and this advantage makes Caputo definition more preferable than the RL definition.

2.1.2.5. Properties of Fractional-Order Calculus. Properties of fractional order calculus [10] are summarized below.

- The fractional order differentiation ${}_a\mathscr{D}_t^{\alpha} f(t)$ of an analytic function $f(t)$ with respect to t is also an analytic function of t and α.
- If $\alpha = n$, where n is a positive integer, the fractional operator is identical to integer order derivative. If α is a negative integer, $\alpha = -n$, then the fractional operator acts like n-fold integration.
- For $\alpha = 0$ the operation ${}_a\mathscr{D}_t^{\alpha} f(t)$ is the identity operator, ${}_a\mathscr{D}_t^{0} f(t) = f(t)$.
- The fractional order differentiation and integration are linear operators (2.16).

$$ {}_a\mathscr{D}_t^{\alpha}[cf(t) + dg(t)] = c\, {}_a\mathscr{D}_t^{\alpha} f(t) + d\, {}_a\mathscr{D}_t^{\alpha} g(t) \tag{2.16} $$

- The semigroup property, commutative-law, is valid under some reasonable constraints on the function $f(t)$ (2.17).

$$ {}_a\mathscr{D}_t^{\alpha}[{}_a\mathscr{D}_t^{\beta} f(t)] = {}_a\mathscr{D}_t^{\beta}[{}_a\mathscr{D}_t^{\alpha} f(t)] = {}_a\mathscr{D}_t^{\alpha+\beta} f(t) \tag{2.17} $$

2.1.3. Integral Transforms of Fractional Operators

The function $F(s)$ of the complex variable s is defined by (2.18).

$$F(s) = \mathscr{L}\{f(t)\} = \int_0^\infty e^{-st} f(t)\mathrm{d}t \tag{2.18}$$

(2.18) is called the Laplace transform of the function, $f(t)$. For the existance of the integral, the function $f(t)$ must be of the exponential order α, which means there exists positive constants M and T satisfying (2.19).

$$e^{-\alpha t}|f(t)| \leq M, \qquad t > T \tag{2.19}$$

The function $f(t)$ can be found from the Laplace transform $F(s)$ with the help of the inverse Laplace trasnform (2.20).

$$f(t) = \mathscr{L}^{-1}\{F(s)\} = \int_{c-j\infty}^{c+j\infty} e^{st} F(s)ds, \qquad c = \Re(s) > c_0 \tag{2.20}$$

c_0 lies in the right half plane of the absolute convergence of the Laplace integral (2.20).

The convolution of two functions $f(t)$ and $g(t)$ which are equal to zero for $t < 0$ is given in (2.21).

$$f(t) * g(t) = \int_0^t f(t-\tau)g(\tau)\mathrm{d}\tau = \int_0^t f(\tau)g(t-\tau)\mathrm{d}\tau \tag{2.21}$$

The Laplace transform of the convolution (2.21) is equal to the product of the Laplace transform of those functions (2.22).

$$\mathscr{L}\{f(t) * g(t)\} = F(s)G(s) \tag{2.22}$$

(2.22) holds under the assumption that both $F(s)$ and $G(s)$ exist.

The Laplace transform of the derivative of an integer order n of the function $f(t)$ can be calculated as (2.23).

$$\begin{aligned}\mathscr{L}\left\{f^n(t)\right\} &= s^n F(s) - \sum_{k=0}^{n-1} s^{n-k-1} f^{(k)}(0) \\ &= s^n F(s) - \sum_{k=0}^{n-1} s^k f^{(n-k-1)}(0) \end{aligned} \tag{2.23}$$

The Laplace tranforms of the fractional integrals and derivatives are given below. The lower terminal of the fractional operators is assumed to be zero, $a = 0$.

2.1.3.1. Laplace Transform of Integrals. The RL fractional integral of order $\alpha > 0$ can be rewritten as a convolution of the functions $g(t) = t^{\alpha-1}$ and $f(t)$ [11].

$$\mathscr{D}_t^{-\alpha} f(t) = \frac{1}{\Gamma(\alpha)} \int_0^t (t-\tau)^{\alpha-1} f(\tau) \mathrm{d}\tau = t^{\alpha-1} * f(t) \tag{2.24}$$

The Laplace transform of the function $t^{\alpha-1}$ is given in (2.25).

$$G(s) = \mathscr{L}\left\{t^{\alpha-1}\right\} = \Gamma(\alpha) s^{-\alpha} \tag{2.25}$$

Thus, we can obtain the Laplace transform of the RL and the Grünwald-Letnikov fractional integral by using the Laplace transform of the convolution (2.26).

$$\mathscr{L}\left\{\mathscr{D}_t^{-\alpha} f(t)\right\} = s^{-\alpha} F(s) \tag{2.26}$$

2.1.3.2. Laplace Transform of Fractional Derivatives. The fractional derivative definition by RL can be rewritten in the given form [11]

$$\begin{aligned}&\mathscr{D}_t^{\alpha} f(t) \equiv g^{(n)}(t) \\ &g(t) = \mathscr{D}_t^{-(n-\alpha)} f(t) \frac{1}{\Gamma(k-\alpha)} \int_0^t (t-\tau)^{n-\alpha-1} f(\tau) \mathrm{d}\tau, \qquad n-1 \le \alpha < n \end{aligned} \tag{2.27}$$

If the Laplace transform of an integer-order derivative is applied to (2.27), the result is shown in (2.28).

$$\mathscr{L}\left\{\mathscr{D}_t^{\alpha} f(t)\right\} = s^n G(s) - \sum_{k=0}^{n-1} s^k g^{n-k-1}(0) \tag{2.28}$$

The Laplace transform of the function $g(t)$ can be evaluated as (2.29).

$$G(s) = s^{-(n-\alpha)} F(s) \tag{2.29}$$

According to the RL definition, $g^{(n-k-1)}(t)$ can be written as (2.30).

$$g^{(n-k-1)}(t) = \frac{\mathrm{d}^{n-k-1}}{\mathrm{d}t^{n-k-1}} \mathscr{D}_t^{-(n-\alpha)} f(t) = \mathscr{D}_t^{\alpha-k-1} f(t) \tag{2.30}$$

Once (2.29) and (2.30) is substituted into (2.28), the Laplace transform of the RL fractional derivative of order $\alpha > 0$ is obtained (2.31).

$$\mathscr{L}\left\{\mathscr{D}_t^{\alpha} f(t)\right\} = s^{\alpha} F(s) - \sum_{k=0}^{n-1} s^k \left[\mathscr{D}_t^{\alpha-k-1} f(t)\right]_{t=0}, \qquad n-1 \leq \alpha < n \tag{2.31}$$

Although this Laplace transform of the RL fractional derivative is well-known, there is a limitation due to the absence of the physical interpretation of the limit values of fractional derivatives, $\mathscr{D}_t^{\alpha-1} f(0), \mathscr{D}_t^{\alpha-2} f(0), \ldots, \mathscr{D}_t^{\alpha-n} f(0)$. The RL definition was revised by Caputo's definiton because the applications such as viscoelasticity, solid mechanics, and rheology require physically interpretable initial conditions such as $f(0), f^{'}(0), f^{''}(0)$.

The Laplace transform of the Caputo fractional derivative is given in (2.32).

$$\mathscr{L}\left\{\mathscr{D}_t^{\alpha} f(t)\right\} = s^{\alpha} F(s) - \sum_{k=0}^{n-1} s^{\alpha-k-1} f^{(k)}(0), \qquad n-1 \leq \alpha < n \tag{2.32}$$

The Caputo's definition provides the physically realistic initial data required by the applications.

2.1.4. Numerical Evaluation of Fractional Order Differentiation

2.1.4.1. Using Grünwald-Letnikov Definition. The most straightforward way of evaluating the fractional order derivatives is to use the Grünwald-Letnikov definition [12]

$$ {}_a\mathscr{D}_t^{\alpha} f(t) = \lim_{h\to 0} \frac{1}{h^{\alpha}} \sum_{j=0}^{[(t-a)/h]} (-1)^j \binom{\alpha}{j} f(t-jh) \approx \frac{1}{h^{\alpha}} \sum_{j=0}^{[(t-a)/h]} \varpi_j^{(\alpha)} f(t-jh) \qquad (2.33) $$

The binomial coefficients $\varpi_j^{(\alpha)} = (-1)^j \binom{\alpha}{j}$ can be computed recursively from [12]

$$ \varpi_0^{(\alpha)} = 1,\ \varpi_j^{(\alpha)} = \left(1 - \frac{\alpha+1}{j}\right) \varpi_{j-1}^{(\alpha)},\ j = 1, 2, \ldots \qquad (2.34) $$

If the step size h is small enough, (2.33) can be used directly to calculate approximately the values of the fractional order derivatives. For example the 0.75th order derivative of the function $f(t) = \sin(3t+1)$ can be computed numerically for a step size of $h = 0.01$. Using Cauchy's formula (2.9) with (2.10), the 0.75th order derivative of the function can also be obtained analytically as [12]

$$ {}_0\mathscr{D}_t^{0.75} f(t) = 3^{0.75} \sin(3t + 1 + 0.75\pi/2) \qquad (2.35) $$

It can be seen from Figure 2.2 that there exists a significant difference between the Cauchy and Grünwald-Letnikov definitions. This is due to the different interpretation of the function,$f(t)$ for $t < 0$. In Cauchy's formula it is assumed that the function $f(t) = \sin(3t+1)$ is defined for $t < 0$ while Grünwald-Letnikov definition assumes that $f(t) = 0$ for $t < 0$. The difference at $t = 0$ is caused by this fact [12].

2.1.4.2. Using Backward Differences. The fractional derivative of order α of a function $f(t)$, which is defined in $[a, b]$ such that $f(t) \equiv 0$ for $t < a$, is given as the equation (2.36) [13].

$$ {}_a\mathscr{D}_t^{\alpha} f(t) = \frac{1}{\Gamma(n-\alpha)} \left(\frac{\mathrm{d}}{\mathrm{d}t}\right)^n \int_a^t \frac{f(\tau)\mathrm{d}\tau}{(t-\tau)^{\alpha-n+1}}, \quad a < t < b, \quad n-1 \le \alpha < n \qquad (2.36) $$

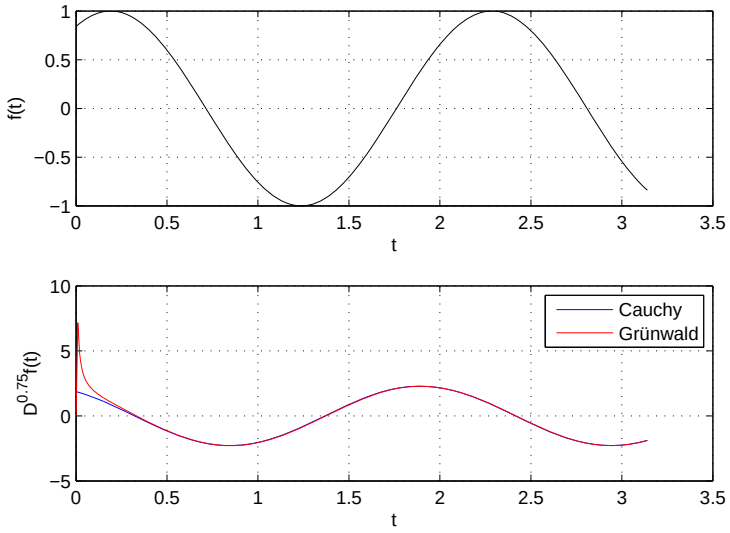

Figure 2.2. Comparison of Cauchy and Grünwald-Letnikov definition of a fractional derivative to the order 0.75 for $f(t) = \sin(3t + 1)$.

Equidistant nodes with the step h : $t_k = kh\,(k = 0, 1, \ldots, N)$, are taken in the interval $[a, b]$ where $t_0 = a$ and $t_N = b$. Using the backward fractional difference approximation for the α-th derivative at the points t_k, $k = 0, 1, \ldots, N$ the equation (2.37) can be obtained [13].

$$ {}_a\mathscr{D}^{\alpha}_{t_k} f(t) \approx \frac{\nabla^{\alpha} f(t_k)}{h^{\alpha}} = h^{-\alpha} \sum_{j=0}^{k} (-1)^j \binom{\alpha}{j} f_{k-j}, \quad k = 0, 1, \ldots, N \tag{2.37} $$

The equation (2.37) can be evaluated for each of the $N + 1$ nodes and represented in the given matrix form (2.38) [13].

$$ \begin{bmatrix} h^{-\alpha}\nabla^{\alpha} f(t_0) \\ h^{-\alpha}\nabla^{\alpha} f(t_1) \\ h^{-\alpha}\nabla^{\alpha} f(t_2) \\ \vdots \\ h^{-\alpha}\nabla^{\alpha} f(t_{N-1}) \\ h^{-\alpha}\nabla^{\alpha} f(t_N) \end{bmatrix} = \frac{1}{h^{\alpha}} \begin{bmatrix} \varpi_0^{(\alpha)} & 0 & 0 & 0 & \cdots & 0 \\ \varpi_1^{(\alpha)} & \varpi_0^{(\alpha)} & 0 & 0 & \cdots & 0 \\ \varpi_2^{(\alpha)} & \varpi_1^{(\alpha)} & \varpi_0^{(\alpha)} & 0 & \cdots & 0 \\ \ddots & \ddots & \ddots & \ddots & \cdots & \cdots \\ \varpi_{N-1}^{(\alpha)} & \ddots & \varpi_2^{(\alpha)} & \varpi_1^{(\alpha)} & \varpi_0^{(\alpha)} & 0 \\ \varpi_N^{(\alpha)} & \varpi_{N-1}^{(\alpha)} & \ddots & \varpi_2^{(\alpha)} & \varpi_1^{(\alpha)} & \varpi_0^{(\alpha)} \end{bmatrix} \begin{bmatrix} f_0 \\ f_1 \\ f_2 \\ \vdots \\ f_{N-1} \\ f_N \end{bmatrix} $$

$$ \varpi_j^{(\alpha)} = (-1)^j \binom{\alpha}{j}, \quad j = 0, 1, \ldots, N \tag{2.38} $$

The column vector of function values $f_k\,(k = 0, \ldots, N)$ (2.38) is multiplied by the matrix (2.39) [13].

$$B_N^{\alpha} = \frac{1}{h^{\alpha}} \begin{bmatrix} \varpi_0^{(\alpha)} & 0 & 0 & 0 & \cdots & 0 \\ \varpi_1^{(\alpha)} & \varpi_0^{(\alpha)} & 0 & 0 & \cdots & 0 \\ \varpi_2^{(\alpha)} & \varpi_1^{(\alpha)} & \varpi_0^{(\alpha)} & 0 & \cdots & 0 \\ \ddots & \ddots & \ddots & \ddots & \cdots & \cdots \\ \varpi_{N-1}^{(\alpha)} & \ddots & \varpi_2^{(\alpha)} & \varpi_1^{(\alpha)} & \varpi_0^{(\alpha)} & 0 \\ \varpi_N^{(\alpha)} & \varpi_{N-1}^{(\alpha)} & \ddots & \varpi_2^{(\alpha)} & \varpi_1^{(\alpha)} & \varpi_0^{(\alpha)} \end{bmatrix} \tag{2.39}$$

The result of the multiplication is the column vector of approximated values of the fractional derivative ${}_a\mathscr{D}_{t_k}^{\alpha} f(t)$, $k = 0, 1, \ldots, N$. The matrix B_N^{α} can be considered as a discrete analogue of fractional differentiation of order α [13].

For B_N^{α} and B_N^{β} the following property holds (2.40) [13].

$$B_N^{\alpha} B_N^{\beta} = B_N^{\beta} B_N^{\alpha} = B_N^{\alpha+\beta} \tag{2.40}$$

In order for B_N^{α} and B_N^{β} to be used as the discrete analogues of the fractional derivatives ${}_a\mathscr{D}_t^{\alpha}$ and ${}_a\mathscr{D}_t^{\beta}$ where $n - 1 \leq \alpha < n$ and $m - 1 \leq \alpha < m$ the following equation must be satisfied (2.41) [13].

$$\begin{aligned} &{}_a\mathscr{D}_t^{\alpha}\left({}_a\mathscr{D}_t^{\beta} f(t)\right) =_a \mathscr{D}_t^{\beta}\left({}_a\mathscr{D}_t^{\alpha} f(t)\right) =_a \mathscr{D}_t^{\alpha+\beta} f(t) \\ &f^{(k)}(a) = 0, \quad k = 1, 2, \ldots, r-1, \quad r = \max\{n, m\} \end{aligned} \tag{2.41}$$

The function $f(t) = \sin(3t + 1)$ is solved numerically this time using backward difference technique with the same step size of $h = 0.01$ (Figure 2.3).

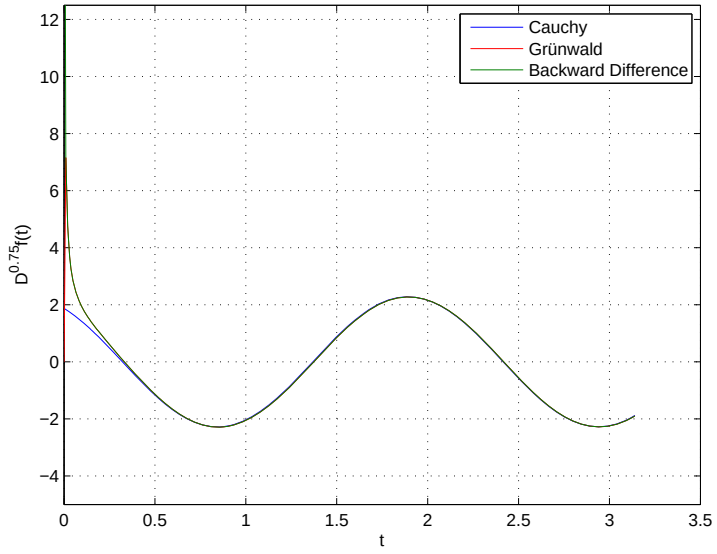

Figure 2.3. Comparison of Grünwald-Letnikov and backward difference definition of a fractional derivative to the order 0.75 for $f(t) = \sin(3t + 1)$.

2.2. Fractional Order Linear Differential Equations

2.2.1. Mittag-Leffler Function

The exponential function, e^{-t}, plays a very important role in the theory of integer order differential equations. One parameter generalization of this function was introduced by G. M. Mittag-Leffler [9, 10].

$$\mathscr{E}_\alpha(t) = \sum_{k=0}^{\infty} \frac{t^k}{\Gamma(\alpha k + 1)} \tag{2.42}$$

A plot of one parameter Mittag-Leffler function of $\mathscr{E}_\alpha(-t^\alpha)$ for various values of α is given in Figure 2.4. As it is seen from Figure 2.4, for $\alpha = 1$ one parameter Mittag-Leffler function behaves like e^{-t} is the basis for the solution of integer order differential equations.

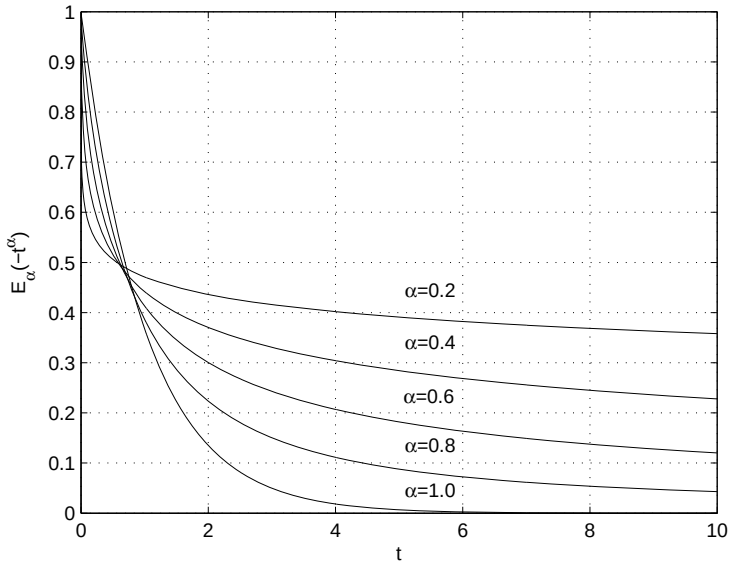

Figure 2.4. One-parameter Mittag-Leffler function as α varies from 0.2 to 1.0 in 0.2 increments.

The two parameter function of the Mittag-Leffler type, which plays a very important role in the fractional calculus, was introduced by Agarwal [9]. A number of relationships for this function were obtained by Humbert and Agarwal using the Laplace transform technique. A two parameter function of the Mittag-Leffler type is defined by the series expansion [9, 10].

$$\mathscr{E}_{\alpha,\beta}(t) = \sum_{k=0}^{\infty} \frac{t^k}{\Gamma(\alpha k + \beta)}, \qquad (\alpha > 0, \beta > 0) \tag{2.43}$$

By using the definition (2.43), the following equations can be derived (2.44).

$$\begin{aligned}
\mathscr{E}_{1,1}(t) &= \sum_{k=0}^{\infty} \frac{t^k}{\Gamma(k+1)} = \sum_{k=0}^{\infty} \frac{t^k}{k!} = e^t \\
\mathscr{E}_{1,2}(t) &= \sum_{k=0}^{\infty} \frac{t^k}{\Gamma(k+2)} = \sum_{k=0}^{\infty} \frac{t^k}{(k+1)!} = \frac{e^t - 1}{t} \\
\mathscr{E}_{1,3}(t) &= \sum_{k=0}^{\infty} \frac{t^k}{\Gamma(k+3)} = \sum_{k=0}^{\infty} \frac{t^k}{(k+2)!} = \frac{e^t - 1 - t}{t^2}
\end{aligned} \tag{2.44}$$

Once the first parameter is fixed to one, the function can be generalized (2.45).

$$\mathscr{E}_{1,m}(t) = \frac{1}{t^{m-1}} \left\{ e^t - \sum_{k=0}^{m-2} \frac{t^k}{k!} \right\} \tag{2.45}$$

The hyperbolic sine and cosine are also particular cases of the Mittag-Leffler function (2.46).

$$\begin{aligned} \mathscr{E}_{2,1}(t^2) &= \sum_{k=0}^{\infty} \frac{t^{2k}}{\Gamma(2k+1)} = \cosh(t) \\ \mathscr{E}_{2,2}(t^2) &= \sum_{k=0}^{\infty} \frac{t^{2k}}{\Gamma(2k+2)} = \frac{\sinh(t)}{t} \end{aligned} \tag{2.46}$$

For $\beta = 1$ the two parameter Mittag-Leffler function turns into the one parameter Mittag-Leffler function (2.47).

$$\mathscr{E}_{\alpha,1}(t) = \sum_{k=0}^{\infty} \frac{t^k}{\Gamma(\alpha k+1)} \equiv \mathscr{E}_{\alpha}(t) \tag{2.47}$$

2.2.2. Numerical Methods of Solving FODEs

The general procedure of numerical solution of fractional order differential equations (FODE) consists of two steps. First initial conditions are used to reduce a given initial-value problem to a problem with zero initial conditions. At this stage a modified equation with zero initial conditions is obtained. Then the system of algebraic equations is obtained by replacing all derivatives in the modified equation by the corresponding discrete analogues, B_N^{α} [13].

An m-term linear FODE is shown as

$$\sum_{k=1}^{m} p_k(t) \mathscr{D}^{\alpha_k} y(t) = f(t), \quad 0 \leq \alpha_1 < \alpha_2 < \ldots < \alpha_m, \quad n-1 < \alpha_m < n \tag{2.48}$$

$\mathscr{D}^{\alpha_k}$ (2.48) denotes either RL or Caputo fractional derivative of order α_k. Using the following notations given as

$$
\begin{aligned}
P_N^{(k)} &= \begin{bmatrix} p_k(t_0) & 0 & \dots & 0 \\ 0 & p_k(t_1) & 0 & \vdots \\ 0 & \dots & \ddots & 0 \\ 0 & \dots & 0 & p_k(t_N) \end{bmatrix} \\
Y_N &= \begin{bmatrix} y(t_0) & y(t_1) & \dots & y(t_N) \end{bmatrix}^T \\
F_N &= \begin{bmatrix} f(t_0) & f(t_1) & \dots & f(t_N) \end{bmatrix}^T
\end{aligned} \tag{2.49}
$$

and taking into account that the discrete analogue of $\mathscr{D}^{\alpha_k}$ is $B_N^{\alpha_k}$, the FODE (2.48) can be written in the following form

$$
\sum_{k=1}^{m} P_N^{(k)} B_N^{\alpha_k} Y_N = F_N \tag{2.50}
$$

If $n-1 < \alpha_m < n$, then the RL and the Caputo versions of the equation (2.48) become equivalent under the assumption of zero initial values of the function $y(t)$ and its $n-1$ derivatives [13].

$$
y^{(k)}(t_0) = 0, \quad k = 0, 1, \dots, n-1 \tag{2.51}
$$

Approximating the derivatives in the initial conditions by backward differences, the equation (2.52) can be obtained [13].

$$
y(t_0) = y(t_1) = \dots = y(t_{n-1}) = 0 \tag{2.52}
$$

In order to determine $y_n, \dots, y_N$ from the linear algebraic system (2.50), the first n rows must be omitted and these rows must be substituted with the zero values from (2.52).

This can be achieved by introducing the eliminator operator, $S_{0,1,\ldots,n-1}$ [13].

$$\left\{ S_{0,1,\ldots,n-1} \left\{ \sum_{k=1}^{m} P_N^{(k)} B_N^{\alpha_k} \right\} S_{0,1,\ldots,n-1}^T \right\} \{ S_{0,1,\ldots,n-1} Y_N \} = S_{0,1,\ldots,n-1} F_N \tag{2.53}$$

The solution of the linear algebraic system (2.53) along with the zero starting values (2.52) gives the numerical solution of the FODE (2.48) with zero initial conditions.

If the coefficients $p_k(t)$ are constant, $p_k(t) \equiv p_k$, then the system of equations (2.53) becomes even more simpler

$$\sum_{k=1}^{m} p_k B_{N-n}^{\alpha_k} \{ S_{0,1,\ldots,n-1} Y_N \} = S_{0,1,\ldots,n-1} F_N \tag{2.54}$$

Now three examples from [13] will be given to demonstrate how this technique can be applied to the FODEs. A two term FODE, 2-FODE, will be solved numerically with three different initial condition scenarios: zero initial conditions, Caputo's initial conditions and the RL intial conditions. The numerical solutions will be compared to the analytical solution obtained by the Laplace transform method. The theorems for the existance and uniqueness of the solutions are given in Appendix A.

Example 1. At first a 2-FODE with zero initial conditions is considered

$$y^{(\alpha)}(t) + y(t) = 1, \quad y(0) = 0 \quad y^{'}(0) = 0 \tag{2.55}$$

The analytical solution of the 2-FODE with zero initial conditions [13] is given as

$$y(t) = t^{\alpha} \mathscr{E}_{\alpha,\alpha+1}(-t^{\alpha}) \tag{2.56}$$

The numerical solution of the problem can be found from the system, where $m = 2$, $\alpha_1 = \alpha$, $\alpha_2 = 0$, $n = 2$, $p_1 = p_2 = 1$, $B_{N-n}^{\alpha_1} = B_{N-2}^{\alpha}$, $B_{N-n}^{\alpha_2} = I_{N-2}$, $F_N = (1, 1, \ldots, 1)^T$ [13]. The numerical solution for these values can be obtained from the system of

algebraic equations given as

$$\left\{B^{\alpha}_{N-2} + I_{N-2}\right\}\left\{S_{0,1}Y_N\right\} = S_{0,1}F_N \tag{2.57}$$

The analytical and numerical solutions of the problem with zero initial conditions, $y(0) = y^1(0) = 0$, for $\alpha = 1.8$ are plotted in Figure 2.5. Simulation step size is $h = 0.01$.

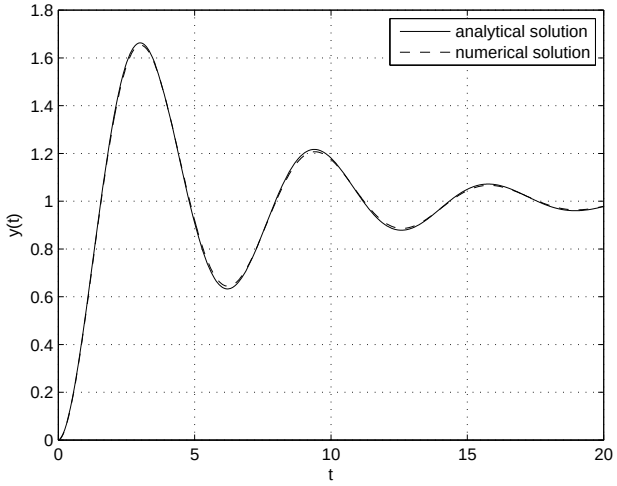

Figure 2.5. Analytical and numerical solutions of two-term FODE for $\alpha = 1.8$.

Example 2. The two-term FODE is now considered with given initial conditions

$$y^{(\alpha)}(t) + y(t) = 1, \quad y(0) = c_0 \quad y^{'}(0) = c_1 \tag{2.58}$$

The analytical solution is obtained by applying Laplace transform to Caputo's fractional derivative definition (2.59).

$$y(t) = c_0\mathscr{E}_{\alpha,1}(-t^{\alpha}) + c_1 t\mathscr{E}_{\alpha,2}(-t^{\alpha}) + t^{\alpha}\mathscr{E}_{\alpha,\alpha+1}(-t^{\alpha}) \tag{2.59}$$

Then the problem (2.58) is transformed to the problem with zero initial conditions in order to obtain the numerical solution. An auxiliary function $y_*(t)$ is introduced (2.60).

$$y(t) = c_0 + c_1 t + y_*(t) \tag{2.60}$$

The new problem with zero initial conditions is formed as

$$y_*^{(\alpha)}(t) + y_*(t) = 1 - c_0 - c_1 t, \quad y_*(0) = 0, \quad y_*'(0) = 0 \tag{2.61}$$

The analytical and numerical solutions of the 2-FODE for $\alpha = 1.8$ with the given initial conditions $c_0 = 1$ and $c_1 = -1$ are shown in Figure 2.6.

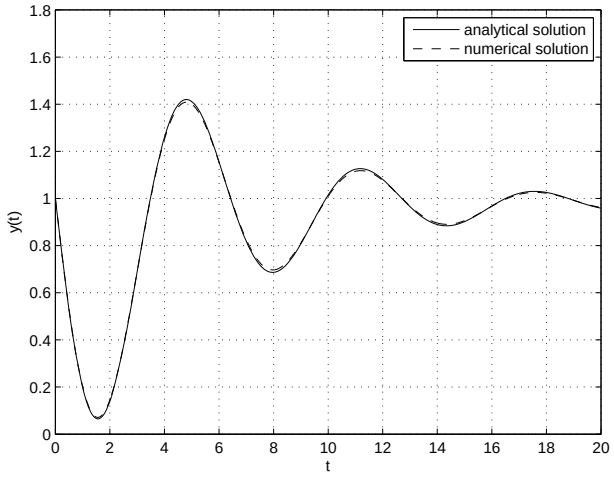

Figure 2.6. Analytical and numerical solutions of the 2-FODE with Caputo initial conditions.

Example 3. Finally the 2-FODE is considered with the RL initial conditions (2.62).

$$y^{(\alpha)}(t) + y(t) = 1, \quad y^{(\alpha-1)}(0) = c_0, \quad y^{(\alpha-2)}(0) = c_1 \tag{2.62}$$

The analytical solution can be found by applying the Laplace transform as

$$y(t) = c_0 t^{\alpha-1} \mathscr{E}_{\alpha,\alpha}(-t^\alpha) + c_1 t^{\alpha-2} \mathscr{E}_{\alpha,\alpha-1}(-t^\alpha) + t^\alpha \mathscr{E}_{\alpha,\alpha+1}(-t^\alpha) \tag{2.63}$$

For numerical solution the problem must first be converted to the problem with zero initial conditions. In order to accomplish this, the auxiliary function $y_*(t)$ is needed

$$y(t) = c_0 t^{\alpha-1} + c_1 t^{\alpha-2} + y_*(t) \tag{2.64}$$

Substituting this expression into the equation with the initial conditions, the problem of finding $y_*(t)$ can be formulated as

$$y_*^{(\alpha)}(t) + y_*(t) = 1 - c_0 t^{\alpha-1} - c_1 t^{\alpha-2}, \quad y_*(0) = 0, \quad y_*'(0) = 0 \tag{2.65}$$

The analytical and numerical solutions of the 2-FODE for $\alpha = 1.8$ with the given RL initial conditions $c_0 = 1$ and $c_1 = -1$ are shown in Figure 2.7.

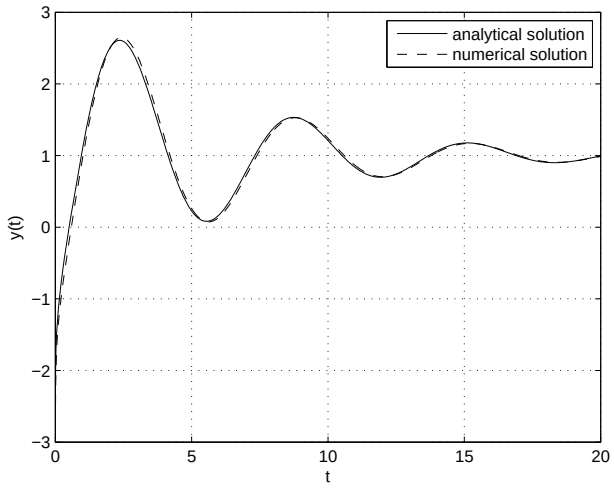

Figure 2.7. Analytical and numerical solutions of the 2-FODE with the RL initial conditions.

3. INTEGER ORDER SYSTEM IDENTIFICATION TECHNIQUES

Here identification techniques for integer order time invariant linear systems will be presented. Although these systems represent many idealizations that do not exist in real life processes, they constitute the most important class of dynamical systems considered not only in the academic study but also in practice. The reason behind this is not only the justified approximations or the simplification of the analysis. Models estimations based on linear theory often lead to good results in practice.

Thus a review of linear systems theory is neccessary before moving on to the identification techniques.

3.1. Review of Linear Systems

3.1.1. Impulse Response

It is well known that a linear, time invariant (LTI), casual system can be described by its impulse response $g(\tau)$ (3.1).

$$y(t) = \int_{\tau=0}^{\infty} g(\tau)u(t-\tau)\mathrm{d}\tau \tag{3.1}$$

Knowing $\{g(\tau)\}_{\tau=0}^{\infty}$, the output can be computed for any input. The impulse response is a complete characterization of the system.

Identification deals with observations of inputs and outputs in discrete time because the data acquisition takes place in discrete time. The output signal $y(t)$ is assumed to be observed at the sampling instants $t_n = nT$, $n = 1, 2, \ldots$ (3.2).

$$y(nT) = \int_{\tau=0}^{\infty} g(\tau)u(nT-\tau)\mathrm{d}\tau \tag{3.2}$$

The interval T is called the sampling interval. Sampling instants are equally distributed. The input signal $u(t)$ is kept constant between the sampling instants (3.3).

$$u(t) = u_n, \quad nT \leq t < (n+1)T \tag{3.3}$$

Keeping the input signal constant between the sampling instants (3.3) simplifies the analysis of the system (3.4).

$$\begin{aligned} y(nT) &= \int_{\tau=0}^{\infty} g(\tau)u(nT-\tau)\mathrm{d}\tau = \sum_{l=1}^{\infty} \int_{\tau=(l-1)T}^{lT} g(\tau)u(nT-\tau)\mathrm{d}\tau \\ &= \sum_{l=1}^{\infty} \left[\int_{\tau=(l-1)T}^{lT} g(\tau)\mathrm{d}\tau \right] u_{n-l} = \sum_{l=1}^{\infty} g_T(l)u_{n-l} \end{aligned} \tag{3.4}$$

$g_T(l)$ is defined as (3.5).

$$g_T(l) = \int_{\tau=(l-1)T}^{lT} g(\tau)\mathrm{d}\tau \tag{3.5}$$

The expression (3.4) can be used to compute the output at the sampling instants. If the input is subject to (3.3), it is sufficient to know $\{g_T(l)\}_{l=1}^{\infty}$ in order to compute the system's response. The relationship (3.4) describes a sampled data system and the sequence $\{g_T(l)\}_{l=1}^{\infty}$ is called the impulse response of the system.

From here on for easing the notation T is assumed to be one time unit and n is used to enumerate the sampling instants (3.6).

$$y(n) = \sum_{k=1}^{\infty} g(k)u(n-k), \quad n = 0, 1, 2, \ldots \tag{3.6}$$

3.1.2. Disturbance Framework

According to the equation (3.6) the output can be exactly calculated if the input is known. For real life processes this is not true. There always exist signals which are beyond our control and those signals have undesirable effects on the system. In linear system framework the undesirable effects imposed by those signals are lumped into a additive term $\nu(n)$ at the output (3.7).

$$y(n) = \sum_{k=1}^{\infty} g(k)u(n-k) + \nu(n) \tag{3.7}$$

The source of this disturbance term can be sensor measurement noise or an input that is not contrallable by the user. The most characteristic feature of a disturbance is that its value is not known beforehand. Information about past disturbance values may be used to make guesses about future values. Thus a probabilistic framework is employed in order to describe future disturbances. Let $\nu(n)$ be given as (3.8).

$$\nu(n) = \sum_{k=0}^{\infty} h(k)e(n-k) \tag{3.8}$$

$e(n)$ (3.8) is a sequence of independent identically distributed random variables with a certain probability density function. For reasons of normalization, one can assume that $h(0) = 1$ since the variance of e can be adjusted.

$e(n)$ and $\nu(n)$ are realizations of stochastic processes (see Appendix B), sequences of random variables. On the other hand, it can be assumed that the input sequence is deterministic while disturbances on the system are described by random variables. Thus the system output, $y(n)$ is a mixed signal, a realization of a stochastic processes with deterministic components (Figure 3.1). In system identification this configuration is called the open loop operation where $u(n)$ and $\nu(n)$ are independent. G and H (Figure 3.1) represent the transfer functions (see Appendix C) of the LTI dynamical system and the disturbance respectively.

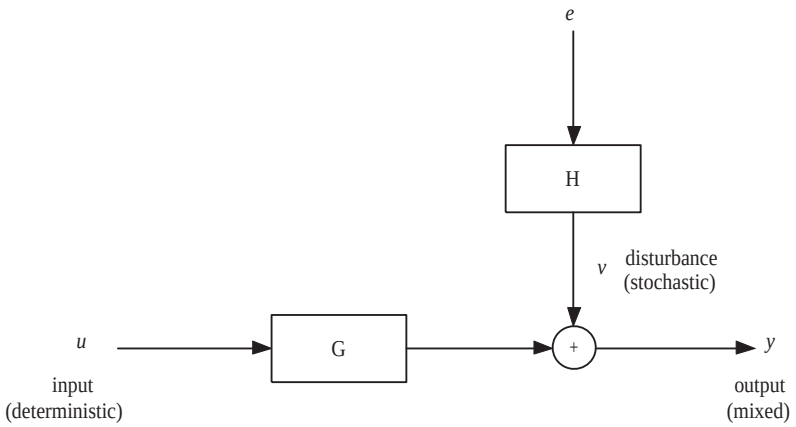

Figure 3.1. A framework for linear systems with disturbances.

3.2. Nonparametric Identification

Nonparametric identification methods consist of direct techniques that aim at finding the best description of the LTI model. The description is either in time domain as an estimate of the system's impulse response, $\hat{g}(n)$, or in frequency domain as an estimate of the system's frequency response, $\hat{G}(e^{j\omega})$.

3.2.1. Time Domain Methods

Time domain methods can be categorized as transient response analysis and correlation analysis. For both categories, it is assumed that the system to be identified operates in open loop configuration. Open loop configuration means that the sequences $u(n)$ and $\nu(n)$ are independent.

3.2.1.1. Impulse Response Analysis. An LTI system described by (3.7) is subjected to a pulse input (3.9).

$$u(n) = \begin{cases} a, & n = 0 \\ 0, & n \neq 0 \end{cases} \tag{3.9}$$

The output of the system is given in (3.10).

$$y(n) = ag(n) + \nu(n) \tag{3.10}$$

If the noise level is low, it is possible to determine the impulse response coefficients $g(n)$ from an experiment with a pulse input. The estimate and the error are given as

$$\hat{g}(n) = \frac{y(n)}{a} \tag{3.11}$$

$$|g(n) - \hat{g}(n)| = \frac{|\nu(n)|}{a} \tag{3.12}$$

This simple method is called impulse response analysis. Although the analysis is simple, this method has a major drawback that it cannot be applied easily to physical processes. Such pulse inputs are not easy to generate in real time and even if they are generated, they cause the error of the estimate to be significant. Moreover they make the system exhibit nonlinear effects which destroy our assumption of a linear model [1, 14].

3.2.1.2. Step Response Analysis. If the input signal is selected as a step

$$u(n) = \begin{cases} a, & n \geq 0 \\ 0, & n < 0 \end{cases}$$

the output of the LTI system is given as (3.13).

$$y(n) = a \sum_{k=1}^{n} g(k) + \nu(n) \tag{3.13}$$

By using (3.13) the estimate of $g(n)$ can be obtained as (3.14).

$$\hat{g}(n) = \frac{y(n) - y(n-1)}{a} \tag{3.14}$$

$$|g(n) - \hat{g}(n)| = \frac{|\nu(n) - \nu(n-1)|}{a} \tag{3.15}$$

Similarly step response analysis suffers from large estimation errors in pratical applications. However if the goal is to recover some basic control related characteristics such as delay time, static gain, and dominating time constants, the accuracy of the step response analysis is sufficient [1, 14].

3.2.1.3. Correlation Analysis. If the input of an LTI system is a quasi-stationary sequence and the system operates in open-loop configuration

$$\overline{E}\left\{u(n)u(n-\tau)\right\} = R_u(\tau)$$
$$\overline{E}\left\{u(n)\nu(n-\tau)\right\} \equiv 0$$

then the correlation of output and input [1] is given as

$$\overline{E}\left\{y(n)u(n-\tau)\right\} = R_{yu}(\tau) = \sum_{k=1}^{\infty} g(k)R_u(k-\tau) = g * R_u(\tau) \tag{3.16}$$

If the input is chosen as white noise so that

$$R_u(\tau) = a\delta_{\tau 0}$$

then an estimate of the impulse response is obtained by using an estimate of $R_{yu}(\tau)$ [1].

$$g(\tau) = \frac{R_{yu}(\tau)}{a} \Rightarrow \hat{g}(\tau) = \frac{\hat{R}^N_{yu}(\tau)}{a} = \frac{\frac{1}{N}\sum_{n=\tau}^{N} y(n)u(n-\tau)}{\frac{1}{N}\sum_{n=0}^{N} u^2(n)} \tag{3.17}$$

If the input is not white noise, the correlation between output and input

$$\hat{R}^N_{yu}(\tau) = \sum_{k=1}^{M} \hat{g}(k)\hat{R}^N_u(k-\tau) \tag{3.18}$$

yields an algebraic system of equations where $\hat{R}_u^N(\tau) = \hat{R}_u^N(-\tau)$

$$\begin{bmatrix} \hat{R}_{yu}^N(0) \\ \vdots \\ \hat{R}_{yu}^N(M-1) \end{bmatrix} = \begin{bmatrix} \hat{R}_u^N(0) & \hat{R}_u^N(-1) & \dots & \hat{R}_u^N(-(M-1)) \\ \hat{R}_u^N(1) & \hat{R}_u^N(0) & \dots & \hat{R}_u^N(-(M-2)) \\ \vdots & \ddots & \ddots & \vdots \\ \hat{R}_u^N(M-1) & \dots & \dots & \hat{R}_u^N(0) \end{bmatrix} \begin{bmatrix} \hat{g}(0) \\ \vdots \\ \hat{g}(M-1) \end{bmatrix} \tag{3.19}$$

Once the algebraic system of equations (3.19) is solved, the estimate can be calculated

$$\hat{g}(\tau) = \sum_{k=0}^{M-1} \hat{g}(k) z^{-k} \tag{3.20}$$

3.2.2. Frequency Domain Methods

If the input to the LTI system without the disturbance term (3.6) is a sinusoidal signal,

$$u(n) = a\cos\omega n = a\Re(e^{j\omega n})$$

the corresponding output [1] is given as

$$\begin{aligned} y(n) &= a\sum_{k=1}^{\infty} g(k)\Re(e^{j\omega(n-k)}) = a\Re\left\{\sum_{k=1}^{\infty} g(k)e^{j\omega(n-k)}\right\} \\ &= a\Re\left\{e^{j\omega n}\sum_{k=1}^{\infty} g(k)e^{-j\omega k}\right\} = a\Re\left\{e^{j\omega n}G(e^{j\omega})\right\} \\ &= a|G(e^{j\omega})|\cos(\omega n + \phi), \quad \phi = \angle G(e^{j\omega}) \end{aligned} \tag{3.21}$$

In (3.21) the input cosine is defined since time minus infinity. If $u(n) = 0$, $n < 0$, then an additional term is obtained (3.22).

$$-\Re\left\{e^{j\omega n}\sum_{k=n}^{\infty} g(k)e^{-j\omega k}\right\} \tag{3.22}$$

This term (3.22) is of transient nature and tends to go to zero as time goes to infinity provided that $G(z)$ is stable.

If the input is applied to the system with the disturbance term, the output is given in (3.23).

$$y(n) = a|G(e^{j\omega})|\cos(\omega n + \phi) + \nu(n) + \text{transient}, \quad \phi = \angle G(e^{j\omega}) \tag{3.23}$$

The system output (3.23) is always a cosine of the same frequency but with an amplitude magnified by $|G(e^{j\omega})|$ and a phase shift of $\angle G(e^{j\omega})$. The complex valued function

$$G(e^{j\omega}), \quad -\pi \leq \omega \leq \pi \tag{3.24}$$

denotes the transfer function evaluated at the point $z = e^{j\omega}$. This function is called the frequency function of the system because it gives information as to what will happen in stationarity [1, 14].

The frequency domain analysis comprises of methods aiming at the determination of an estimate of $G(e^{j\omega})$. Using the amplitude and phase shift imposed on the output signal, an estimate $\hat{G}_N(e^{j\omega})$ can be calculated. However, this calculation is just for one frequency. Thus, the calculations must be repeated for a number of frequencies in the frequency band specified by the user [1, 14].

3.2.2.1. Frequency Analysis by Correlation Method. With the noise component $\nu(n)$ present in (3.23), it is not easy to determine $|G(e^{j\omega})|$ and ϕ accurately by graphic methods. The part of the output that is a cosine function of known frequency can be correlated from the noise. By inserting the sums [14]

$$I_c(N) = \frac{1}{N}\sum_{n=1}^{N} y(n)\cos\omega n, \quad I_s(N) = \frac{1}{N}\sum_{n=1}^{N} y(n)\sin\omega n$$

into (3.23), once the transient term is ignored, the $I_c(N)$ and $I_s(N)$ are obtained (3.25).

$$\begin{aligned} I_c(N) &= \frac{a}{2}|G(e^{j\omega})|\cos\phi + a|G(e^{j\omega})|\frac{1}{2}\frac{1}{N}\sum_{n=1}^{N}\cos(2\omega n+\phi) \\ &\quad + \frac{1}{N}\sum_{n=1}^{N}\nu(n)\cos\omega n \\ I_s(N) &= -\frac{a}{2}|G(e^{j\omega})|\sin\phi + a|G(e^{j\omega})|\frac{1}{2}\frac{1}{N}\sum_{n=1}^{N}\sin(2\omega n+\phi) \\ &\quad + \frac{1}{N}\sum_{n=1}^{N}\nu(n)\sin\omega n \end{aligned} \tag{3.25}$$

The second term goes to zero as N goes to infinity. The third term also tends to zero if $\nu(n)$ does not contain a pure periodic component of frequency ω.

These two expressions suggest the following estimate of $|G(e^{j\omega})|$ and ϕ [14].

$$\begin{aligned} |\hat{G}_N(e^{j\omega})| &= \frac{\sqrt{I_c^2(N)+I_s^2(N)}}{a/2} \\ \hat{\phi}_N &= \angle\hat{G}_N(e^{j\omega}) = -\tan^{-1}\frac{I_s(N)}{I_c(N)} \end{aligned} \tag{3.26}$$

By repeating the procedure for a number of frequencies, the frequency response of the system can be obtained. However, many industrial processes do not admit sinusoidal inputs in normal operation. Moreover, the experimentation time is long due to the repeated procedure [1, 14].

3.2.2.2. Fourier Analysis. For a finite sequence of inputs $u(n)$, $n = 1, 2, \ldots, N$ the discrete Fourier transform (DFT) is given as

$$U_N(\omega) = \frac{1}{\sqrt{N}}\sum_{n=1}^{N}u(n)e^{-j\omega n} \tag{3.27}$$

DFT gives values calculated for $\omega = 2\pi k/N$, $k = 1, \ldots, N$. $U_N(\omega)$ is periodic with period 2π.

$$U_N(\omega + 2\pi) = U_N(\omega)$$

The inverse DFT can be applied to get $u(n)$ (3.28).

$$u(n) = \frac{1}{\sqrt{N}} \sum_{k=1}^{N} U_N \left(\frac{2\pi k}{N} \right) e^{j2\pi kn/N} \tag{3.28}$$

For a linear system an estimate of the frequency function can be computed by applying DFT (3.29).

$$\hat{G}_N(e^{j\omega}) = \frac{Y_N(\omega)}{U_N(\omega)} \tag{3.29}$$

Here ω is precisely the frequency of the input signal. In a linear system different frequencies pass through the system independently of each other. It is therefore quite natural to extend the frequency analysis estimate to the case of multifrequency inputs (3.30).

$$\hat{\hat{G}}_N(e^{j\omega}) = \frac{Y_N(\omega)}{U_N(\omega)} \tag{3.30}$$

$\hat{\hat{G}}_N(e^{j\omega})$ is called the empirical transfer function estimate (ETFE). In (3.30) it is assumed that $U_N(\omega) \neq 0$. If for some frequencies DFT yields zero, then the ETFE is undefined for those frequencies.

In the case of a periodic input signal, ETFE yields very good estimates at the frequencies that are present in the input. However when the input is not periodic the ETFE becomes a very crude estimate. For inputs that are not periodic the variance of ETFE does not decrease as N increases unlike the case of periodic inputs. The estimates at different frequencies are asymptotically uncorrelated [1, 14].

With the help of ETFE, the discrete time transfer function can also be estimated from the following procedure [1, 14].

(i) Calculate $\hat{\hat{G}}_N(e^{j\frac{2\pi}{N}k})$ for $k = 1, \ldots, N$.

(ii) Apply the inverse DFT, $\hat{\hat{g}}(n) = \dfrac{1}{N}\displaystyle\sum_{k=1}^{N} \hat{\hat{G}}_N(e^{j\frac{2\pi}{N}k})e^{j\frac{2\pi}{N}nk}, \quad n = 1, \ldots, N$

(iii) Define $\hat{\hat{G}}(z) = \displaystyle\sum_{k=1}^{N} \hat{\hat{g}}(k)z^{-k}$.

3.2.2.3. Spectral Analysis. If the output signal $y(n)$ and the input signal $u(n)$ are jointly quasi-stationary (see Appendix B), then the power spectrum of $y(n)$ is defined as

$$\Phi_y(\omega) = \sum_{\tau=-\infty}^{\infty} R_y(\tau)e^{-j\tau\omega} \tag{3.31}$$

while the cross spectrum between the output and the input signals is expressed as

$$\Phi_{yu}(\omega) = \sum_{\tau=-\infty}^{\infty} R_{yu}(\tau)e^{-j\tau\omega} \tag{3.32}$$

In case $u(n)$ is a quasi-stationary, deterministic signal with spectrum $\Phi_u(\omega)$ and $e(n)$ is white noise with variance λ, spectrum of $y(n)$ and cross spectrum of $y(n)$ and $u(n)$ is given as

$$\begin{aligned} \Phi_y(\omega) &= |G(e^{j\omega})|^2\Phi_u(\omega) + \lambda|H(e^{j\omega})|^2 \\ \Phi_{yu}(\omega) &= G(e^{j\omega})\Phi_u(\omega) \end{aligned} \tag{3.33}$$

Thus the estimate is the ratio of two spectral estimates

$$\hat{G}_N(e^{j\omega}) = \frac{\hat{\Phi}^N_{yu}(\omega)}{\hat{\Phi}^N_u(\omega)} \tag{3.34}$$

The steps of the spectral analysis method is shown below [1, 14].

(i) Compute the covariances and cross-covariance from $u(n)$ and $y(n)$

$$\hat{R}_u^N(\tau) = \frac{1}{N}\sum_{n=1}^{N} u(n+\tau)u(n), \qquad \hat{R}_{yu}^N(\tau) = \frac{1}{N}\sum_{n=1}^{N} y(n+\tau)u(n)$$

(ii) Apply DFT to covariance and cross-covariance in order to obtain spectrum and cross spectrum

$$\hat{\Phi}_u^N(\omega) = \sum_{\tau=-M}^{M} \hat{R}_u^N(\tau)W_M(\tau)e^{-j\omega\tau}, \qquad \hat{\Phi}_{yu}^N(\omega) = \sum_{\tau=-M}^{M} \hat{R}_{yu}^N(\tau)W_M(\tau)e^{-j\omega\tau}$$

$W_M(\tau)$ is called the lag window with the width M.

(iii) The ratio of the spectra gives the estimate, $\hat{G}_N(e^{j\omega})$.

3.3. Parametric Identification

Parametric identification is based on estimation methods using a parameter vector θ. A set of candidate models is selected first and then the parameter vector of each model is estimated. Then the best model within the set is chosen to represent the dynamical system. This section concentrates on the decision of whether a model is good or not. Within this context the concept of prediction is addressed first. Next various model structures for the LTI systems are introduced. Finally minimization of the prediction error is given.

3.3.1. Prediction

The idea of how to predict future output values is essential for the development of parameter identification methods. In a LTI system described by (3.7) the prediction of $\nu(n)$ [1] is given as

$$\nu(n) = \sum_{k=0}^{\infty} h(k)e(n-k) \tag{3.35}$$

It is further assumed that $H(z)$ is stable (3.36).

$$\sum_{k=0}^{\infty} |h(k)| < \infty \tag{3.36}$$

A crucial property of (3.35) is that $H(z)$ should be invertible in order to compute $e(n)$ once $\nu(n)$ is known for $n-1, n-2, \ldots$ (3.37).

$$e(n) = \sum_{k=0}^{\infty} \widetilde{h}(k)\nu(n-k), \quad \widetilde{H}(z) = \sum_{k=0}^{\infty} \widetilde{h}(k)z^{-k}, \quad \sum_{k=0}^{\infty} |\widetilde{h}(k)| < \infty \tag{3.37}$$

$\widetilde{H}(z) = H^{-1}(z)$ is satisfied provided that the function $1/H(z)$ be analytic in $|z| \geq 1$. $H(z)$ must have no zeros on or outside the unit circle.

One-step-ahead prediction of $\nu(n)$ [1] can be done if the observations up to $n-1$ are present. Since $h(0) = 1$, $\nu(n)$ can expressed as

$$\nu(n) = \sum_{k=0}^{\infty} h(k)e(n-k) = e(n) + \sum_{k=1}^{\infty} h(k)e(n-k) \tag{3.38}$$

The knowledge of $\nu(n)$ for $n-1, n-2, \ldots$ implies the knowledge of $e(n)$ for $n-1, n-2, \ldots$. Therefore the second term of (3.38) is known up to $n-1$. The conditional expectation of $\nu(n)$ denoted by $\hat{\nu}(n|n-1)$ [1] can be calculated as

$$\hat{\nu}(n|n-1) = \sum_{k=1}^{\infty} h(k)e(n-k) \tag{3.39}$$

since $e(n)$ has zero mean. The transfer function of the one-step-ahead disturbance predictor [1] is given as

$$W_{\nu\hat{\nu}}(z) = \frac{H(z)-1}{H(z)} = [1 - H^{-1}(z)] \tag{3.40}$$

Using this transfer function the one-step-ahead prediction of $\nu(n)$ can be computed as shown in Figure 3.2.

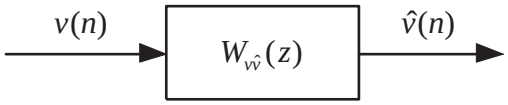

Figure 3.2. One-step-ahead prediction of $\nu(n)$.

One-step-ahead prediction of $y(n)$ assumes that the values of the output and input are known up to $n-1$th step. The one-step-ahead prediction of $y(n)$ then can be calculated using the transfer functions

$$W_{u\hat{y}}(z) = H^{-1}(z)G(z), \qquad W_{y\hat{y}}(z) = 1 - H^{-1}(z) \tag{3.41}$$

as shown in Figure 3.3.

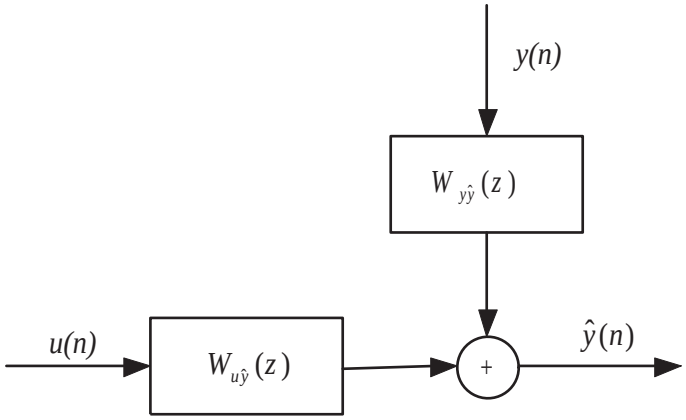

Figure 3.3. One-step-ahead prediction of $y(n)$.

3.3.2. Parametrized Model Structures

An LTI model is specified by the impulse response, the spectrum of the additive disturbance and the PDF of the disturbance. A complete model is thus given by $G(z,\theta)$, $H(z,\theta)$, and $f_e(x,\theta)$ the PDF of $e(n)$. θ denotes the parameter vector to be determined by the identification procedure. Parameters are the unknown coefficients of the mathematical model that govern the system behaviour. One-step-ahead prediction of a complete model can be computed by using (3.41) (Figure 3.3). The prediction does not depend on $f_e(x,\theta)$ [1].

There are different ways of describing a complete model in terms of θ. One obvious way of parametrizing G and H is to represent them in rational functions and then the coefficients of the numerator and denominator are taken as parameters.

3.3.2.1. Equation Error Model Structure. The most simple linear difference equation that describes the input-output relationship is given by

$$y(n) + a_1 y(n-1) + \cdots + a_{n_a} y(n-n_a) = b_1 u(n-1) + \cdots + b_{n_b} u(n-n_b) + e(n) \quad (3.42)$$

The model (3.42) is called an equation error model due to the noise term which acts like a direct error in the equation. The parameter vector is shown as

$$\theta = \begin{bmatrix} a_1 & \dots & a_{n_a} & b_1 & \dots & b_{n_b} \end{bmatrix}^T \quad (3.43)$$

By introducing

$$A(z) = 1 + a_1 z^{-1} + \cdots + a_{n_a} z^{-n_a} \quad (3.44)$$

$$B(z) = b_1 z^{-1} + \cdots + b_{n_b} z^{-n_b} \quad (3.45)$$

$G(z,\theta)$ and $H(z,\theta)$ can be expressed as

$$G(z,\theta) = \frac{B(z)}{A(z)}, \quad H(z,\theta) = \frac{1}{A(z)} \quad (3.46)$$

This model is also known as an ARX model (Figure 3.4), where AR refers to the autoregressive part $A(z)y(n)$ and X to the extra input $B(z)u(n)$. In the special case where $n_a = 0$, $y(n)$ is modeled as a finite impulse response (FIR).

The most important property of the equation error model is that the predictor can be written as a linear regression. By inserting (3.46) into (3.41) the predictors for

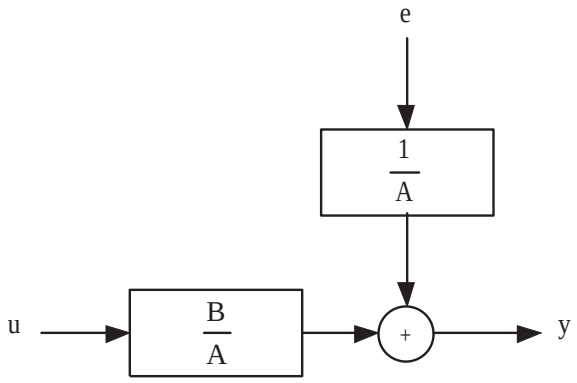

Figure 3.4. ARX model structure [1].

the equation error model can be obtained as

$$W_{u\hat{y}}(z) = B(z), \qquad W_{y\hat{y}}(z) = 1 - A(z) \tag{3.47}$$

By using the vector

$$\varphi(n) = \begin{bmatrix} -y(n-1) & \cdots & -y(n-n_a) & u(n-1) & \cdots & u(n-n_b) \end{bmatrix}^T \tag{3.48}$$

the predictor (3.47) can be expressed as

$$\hat{y}(n|n-1) = \theta^T \varphi(n) = \varphi^T(n)\theta \tag{3.49}$$

This form is known as linear regression in statistics and the vector $\varphi(n)$ is the regression vector.

3.3.2.2. ARMAX Model Structure. The equation error model structure lacks the freedom in describing the properties of the disturbance term. If the equation error is defined as a moving average of white noise, then the model is given as

$$\begin{aligned} &y(n) + a_1 y(n-1) + \cdots + a_{n_a} y(n-n_a) \\ &= b_1 u(n-1) + \cdots + b_{n_b} u(n-n_b) + e(n) + c_1 e(n-1) + \cdots + c_{n_c} e(n-n_c) \end{aligned} \tag{3.50}$$

Introducing

$$C(z) = 1 + c_1 z^{-1} + \cdots + c_{n_c} z^{-n_c} \tag{3.51}$$

$G(z,\theta)$ and $H(z,\theta)$ can be given as

$$G(z,\theta) = \frac{B(z)}{A(z)}, \quad H(z,\theta) = \frac{C(z)}{A(z)} \tag{3.52}$$

ARMAX model structure is shown in Figure 3.5.

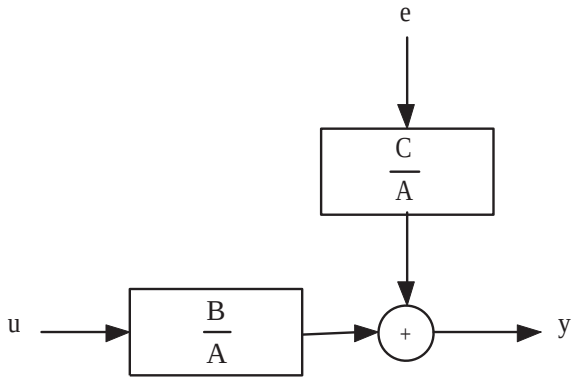

Figure 3.5. ARMAX model structure [1].

The parameter vector for ARMAX is

$$\theta = \begin{bmatrix} a_1 & \dots & a_{n_a} & b_1 & \dots & b_{n_b} & c_1 & \dots & c_{n_c} \end{bmatrix}^T \tag{3.53}$$

The predictors for ARMAX model structure (Figure 3.5) are obtained by inserting (3.52) into (3.41)

$$W_{u\hat{y}}(z) = \frac{B(z)}{C(z)}, \qquad W_{y\hat{y}}(z) = 1 - \frac{A(z)}{C(z)} \tag{3.54}$$

The predictor can be rewritten like (3.49)

$$\hat{y}(n|n-1) = \varphi^T(n,\theta)\theta \tag{3.55}$$

The regression vector is defined as

$$\varphi(n,\theta) = [-y(n-1) \quad \dots \quad -y(n-n_a) \quad u(n-1) \quad \dots \quad u(n-n_b) \\ \varepsilon(n-1,\theta) \quad \dots \quad \varepsilon(n-n_c,\theta)]^T \tag{3.56}$$

where the prediction error

$$\varepsilon(n,\theta) = y(n) - \hat{y}(n|n-1) \tag{3.57}$$

is used. The equation (3.55) is called pseudolinear regression due to θ being an argument of the regression vector.

3.3.2.3. Output Error Model Structure. The transfer functions of all previous model structures, both G and H share the polynomial A as a common factor in the denominators. The relation between input and undisturbed output w can be expressed as a linear difference equation

$$w(n) + f_1 w(n-1) + \cdots + f_{n_f} w(n-n_f) = b_1 u(n-1) + \cdots + b_{n_b} u(n-n_b) \tag{3.58}$$

$$y(n) = w(n) + e(n) \tag{3.59}$$

With $F(z)$ given as

$$F(z) = 1 + f_1 z^{-1} + \cdots + f_{n_f} z^{-n_f} \tag{3.60}$$

y(n) can be written as

$$y(n) = \frac{B(z)}{F(z)} u(n) + e(n) \tag{3.61}$$

Output error (OE) model structure can be seen from Figure 3.6.

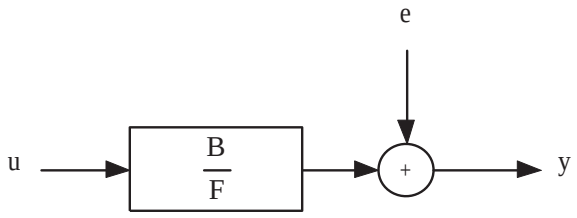

Figure 3.6. OE model structure [1].

The parameter vector for the OE model structure is given as

$$\theta = \begin{bmatrix} b_1 & b_2 & \dots & b_{n_b} & f_1 & f_2 & \dots & f_{n_f} \end{bmatrix}^T \tag{3.62}$$

Since $H(z,\theta) = 1$, the predictor is

$$\hat{y}(n|n-1) = w(n) \tag{3.63}$$

The predictor can be rewritten as in formal agreement with the ARMAX model predictor

$$\hat{y}(n|n-1) = \varphi^T(n,\theta)\theta \tag{3.64}$$

where the regression vector is given as

$$\varphi(n,\theta) = \begin{bmatrix} u(n-1) & \dots & u(n-n_b) & -w(n-1,\theta) & \dots & -w(n-n_f,\theta) \end{bmatrix}^T \tag{3.65}$$

3.3.2.4. General Family of Model Structures. All of the model structures given so far and more can be derived from a generalized model structure shown as

$$G(z,\theta) = \frac{B(z)}{A(z)F(z)}, \qquad H(z,\theta) = \frac{C(z)}{A(z)D(z)} \tag{3.66}$$

If the dynamics contain a delay of n_k samples from input to output, then this results in some zero coefficients for polynomial B.

In this case the generalized model (see Figure 3.7) can be described by

$$G(z,\theta) = z^{-n_k}\frac{\overline{B}(z)}{A(z)F(z)}, \qquad H(z,\theta) = \frac{C(z)}{A(z)D(z)} \tag{3.67}$$

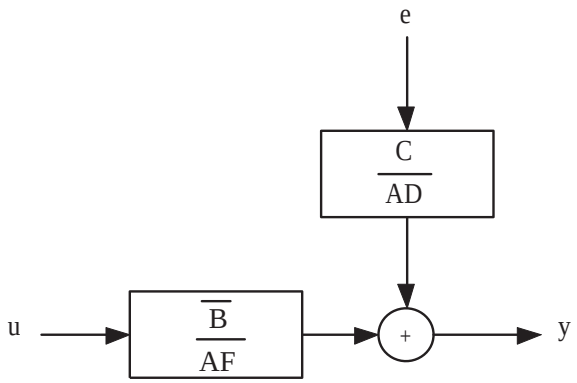

Figure 3.7. Generalized model structure.

The predictor can also be generalized as

$$W_{u\hat{y}}(z) = \frac{D(z)B(z)}{C(z)F(z)}, \qquad W_{y\hat{y}}(z) = 1 - \frac{D(z)A(z)}{C(z)} \tag{3.68}$$

3.3.3. Prediction Error Framework

There exists various model structures as seen in Section 3.3.2. In order to distinguish a model from a set of candidate models a test is needed to evaluate a model's ability to describe the observed data. The essence of a model is its prediction aspect and thus a model's performance can be judged in this respect. The prediction error of a certain model is defined as

$$\varepsilon(n,\theta) = y(n) - \hat{y}(n|\theta) \tag{3.69}$$

When the input-output data set $Z^n = [y(1), u(1), y(2), u(2), \ldots, y(N), u(N)]$ is known, the prediction error of a certain model can be computed for $n = 1, 2, \ldots, N$.

A good model produces small prediction errors when applied to the observed data. The problem is to qualify what "small" should mean. One approach is to form a criterion function that measures the size of ε. The prediction-error sequence is a vector in $\mathbb{R}^N$. The size of this vector can be measured using any norm in $\mathbb{R}^N$.

The prediction error sequence is filtered through a stable linear filter $L(z)$ which yields the filtered prediction error $\varepsilon_F(n,\theta)$. The aim of filtering is to remove high frequency disturbances. The filter L acts like a frequency weighting which enchances or suppresses certain frequencies. Once the filtered prediction error is subject to the following norm

$$V_N(\theta, Z^N) = \frac{1}{N}\sum_{n=1}^{N} l(\varepsilon_F(n,\theta)) \tag{3.70}$$

where $l(\cdot)$ is a scalar valued positive function. For the choice of $l(\cdot)$, a first candidate is a quadratic norm

$$l(\varepsilon) = \frac{1}{2}\varepsilon^2 \tag{3.71}$$

which is convenient both for computation and analysis.

The function $V_N(\theta, Z^N)$ is a well-defined scalar-valued function of the model parameter θ. The estimate $\hat{\theta}_N$ is defined by minimization

$$\hat{\theta}_N = \hat{\theta}_N(Z^N) = \arg\min V_N(\theta, Z^N) \tag{3.72}$$

Here arg min means the minimizing argument of the function. If the minimum is not unique, then arg min denote the set of minimizing arguments. The procedures used in this way of estimating θ is known as prediction error identification methods (PEM).

3.3.3.1. Linear Regression and Least-Squares Method. Linear regression is a special case of PEM. Linear regression model structures are very useful in describing both

linear and nonlinear systems. The linear regression employs a predictor that is linear in θ

$$\hat{y}(n|\theta) = \varphi^T(n)\theta + \mu(n) \tag{3.73}$$

$\mu(n)$ represents the known parameters. φ is the vector of regressors, the regression vector. For example the regression vector of an ARX model structure is given as

$$\varphi(n) = \begin{bmatrix} -y(n-1) & \dots & -y(n-n_a) & u(n-1) & \dots & u(n-n_b) \end{bmatrix}^T \tag{3.74}$$

Once $\mu(n)$ is considered zero for notational simplicity, the prediction error for (3.73) becomes

$$\varepsilon(n,\theta) = y(n) - \varphi^T(n)\theta \tag{3.75}$$

If the frequency filtering and error criterion is taken as $L(z) = 1$ and $l(\varepsilon) = \frac{1}{2}\varepsilon^2$ respectively, then

$$V_N(\theta, Z^N) = \frac{1}{N}\sum_{n=1}^{N}\frac{1}{2}[y(n) - \varphi^T(n)\theta]^2 \tag{3.76}$$

This is the least squares criterion for linear regression. The most important feature of this criterion is that it is a quadratic function of θ. Therefore it can be minimized analytically

$$\hat{\theta}_N^{LS} = \arg\min V_N(\theta, Z^N) = \left[\frac{1}{N}\sum_{n=1}^{N}\varphi(n)\varphi^T(n)\right]^{-1}\frac{1}{N}\sum_{n=1}^{N}\varphi(n)y(n) \tag{3.77}$$

which gives the least squares estimate (LSE) provided that the inverse exits.

If the $d \times d$ matrix $R(N)$ and the d-dimensional column vector $f(N)$ is introduced as

$$R(N) = \frac{1}{N} \sum_{n=1}^{N} \varphi(n)\varphi^T(n) \tag{3.78}$$

$$f(N) = \frac{1}{N} \sum_{n=1}^{N} \varphi(n)y(n) \tag{3.79}$$

the entries of (3.78) and (3.79) will consist of estimates of the covariance function of output and input sequence.

$$[R(N)]_{ij} = \frac{1}{N} \sum_{n=1}^{N} y(n-i)y(n-j), \quad 1 \leq i,\, j \leq n_a \tag{3.80}$$

The LSE can be computed using only such estimates.

Under the assumption that the observed data is generated by

$$y(n) = \varphi^T(n)\theta_0 + \nu_0(n) \tag{3.81}$$

where θ_0 and ν_0 are considered the true values of the parameter vector and the disturbance respectively. Then the LSE (3.77) can be expressed as

$$\hat{\theta}_N^{LS} = \theta_0 + [R(N)]^{-1} \frac{1}{N} \sum_{n=1}^{N} \varphi(n)\nu_0(n) \tag{3.82}$$

Desired properties of $\hat{\theta}_N$ are given as

- It is close to θ_0.
- It converges to θ_0 as N goes to infinity.

If $\nu_0(n)$ is small compared to $\varphi(n)$, then the error term

$$[R(N)]^{-1}\frac{1}{N}\sum_{n=1}^{N}\varphi(n)\nu_0(n) \tag{3.83}$$

will be small and the first property is satisfied.

In order to investigate the case where N goes to infinity, $\nu_0(n)$ is assumed to be a realization of a stationary stochastic process. If the input is quasi stationary so that the sums like

$$\hat{R}_u^N(\tau) = \frac{1}{N}\sum_{n=1}^{N}u(n)u(n-\tau) \to R_u(\tau) = \overline{E}\left\{u(n-\tau)u(n)\right\} \tag{3.84}$$

converge as N tends to infinity. Then $R(N)$ converges as $R(N) \to R^*$. Also under weak conditions

$$\frac{1}{N}\sum_{n=1}^{N}\varphi(n)\nu_0(n) \to h^*$$

Thus the LSE (3.82) converges as

$$\hat{\theta}_N \to \theta_0 + (R^*)^{-1}h^* \tag{3.85}$$

The requirements for (3.85) to be valid is given as

- R^* is nonsingular. If the input and disturbance sequences are independent, open loop configuration, and the $m \times m$ matrix whose i, j entry is $R_u(i-j)$ is non-singular, then R^* becomes nonsingular. In this case the input is called to be persistently exciting of order n_b.
- $h^* = 0$. This can be realized in two ways
  - (i) $\nu_0(n)$ is a sequence of independent random variables with zero mean values, white noise. Then $\nu_0(n)$ does not depend on what has happened up to $n-1$-th step and hence $E\left\{\varphi(n)\nu_0(n)\right\} = 0$

(ii) The input sequence is independent of the zero mean noise sequence and $n_a = 0$. Then $\varphi(n)$ contains only u terms and hence $E\{\varphi(n)\nu_0(n)\} = 0$.

3.4. Persistence of Excitation

A quasi-stationary input signal $u(n)$, with spectrum $\Phi_u(\omega)$, is persistently exciting of order n if, for all filters of the form

$$W_n(z) = w_1 z^{-1} + \cdots + w_n z^{-n} \tag{3.86}$$

the equation

$$|W_n(e^{j\omega})|^2 \Phi_u(\omega) \equiv 0 \Rightarrow W_n(e^{j\omega}) \equiv 0 \tag{3.87}$$

is satisfied [1]. The equation (3.87) indicates that $W_n(z)W_n(z^{-1})$ can have at most $n-1$ different zeros on the unit circle due to symmetry. Hence $u(n)$ is persistently exciting of order n, if $\Phi_u(\omega)$ is different from zero at least n points in the interval $-\pi < \omega \leq \pi$ [1].

Another definition of persistence of excitation is given in terms of the covariance function $R_u(\tau)$. The quasi-stationary input signal $u(n)$ is persistently exciting of order n if and only if $n \times n$ matrix of $\overline{R}_n$

$$\overline{R}_n = \begin{bmatrix} R_u(0) & R_u(1) & \cdots & R_u(n-1) \\ R_u(1) & R_u(0) & \cdots & R_u(n-2) \\ \vdots & \vdots & \ddots & \vdots \\ R_u(n-1) & R_u(n-2) & \cdots & R_u(0) \end{bmatrix} \tag{3.88}$$

is nonsingular [1].

Excitation orders for input signal commonly used in identification are given below.

- Step Input. Persistently exciting of order 1.
- Pseudo Random Binary Signal. Pseudo random binary signal (PRBS) is a periodic signal with period M that can only take two different values, $\mp a$, in a certain way. A PRBS of length $n \leq M$ is persistently exciting of order n. By using the covariance function for the PRBS of length $n \leq M$

$$R_u(\tau) = \begin{cases} a^2 & \tau = 0, \mp M, \mp 2M, \dots \\ -\dfrac{a^2}{M} & \text{otherwise} \end{cases} \tag{3.89}$$

it can be shown that $\overline{R}_n$

$$\overline{R}_n = \begin{bmatrix} a^2 & -\frac{a^2}{M} & \cdots & -\frac{a^2}{M} \\ -\frac{a^2}{M} & a^2 & \cdots & -\frac{a^2}{M} \\ \vdots & \vdots & \cdots & \vdots \\ -\frac{a^2}{M} & -\frac{a^2}{M} & \cdots & a^2 \end{bmatrix} \tag{3.90}$$

is nonsingular [1].

- Periodic Sum of Sinusoids Signal. Periodic sum of sinusoids signal is the sum of sinusoids at m different frequencies.

$$u(n) = \sum_{j=1}^{m} a_j \cos(\omega_j t + \phi_j) \tag{3.91}$$

Periodic sum of sinusoids signal is persistently exciting of order n if $\Phi_u(\omega)$

$$\Phi_u(\omega) = \sum_{j=1}^{m} \frac{a_j}{2} \left[\delta(\omega - \omega_j + \delta(\omega + \omega_j))\right] \tag{3.92}$$

is nonzero at exactly n different frequencies

$$0 \leq \omega_1 < \omega_2 < \cdots < \omega_n \leq \pi$$
$$n = \begin{cases} 2m & 0 < \omega_1, \omega_n < \pi \\ 2m-1 & 0 < \omega_1 \ \otimes \ \omega_n = \pi \\ 2m-2 & 0 = \omega_1 \ \& \ \omega_n = \pi \end{cases} \tag{3.93}$$

3.5. Comparison of Integer Order Identification Methods

For example assume that the transfer function of the system to be identified is as follows

$$G(s) = \frac{1}{s^2 + 0.2s + 1} e^{-2s} \tag{3.94}$$

This system (3.94), which is a second order process model with underdamped modes (complex poles) and a peak frequency response at 1 rad/s, is simulated at a sampling interval of 1 s and a large enough set of input-output data is gathered. A random binary signal of 100 sample length that is persistently exciting of order 100 (see Section 3.4) is used as an input signal. As for a disturbance term, white noise with a standard deviation of 0.2 is applied which results in a signal-to-noise ratio of about 20 dB. A plot of the gathered input-output data is given in Figure 3.8.

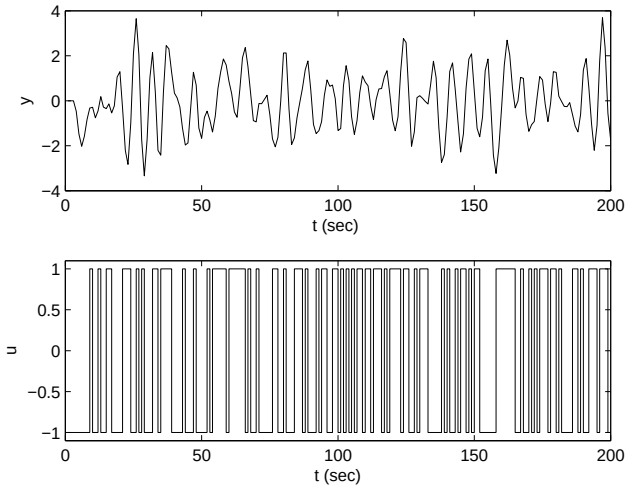

Figure 3.8. System response to random binary signal.

As a first step, the mean values of both output and input signal is subtracted in order to remove any offsets. This operation is known as detrending. The linear model we are trying to build describe deviations from a physical equilibrium. With steady-state data, it is reasonable to assume that the mean levels of the signals correpond to such an equilibrium. Thus, detrending is required to avoid modeling the absolute equilibrium levels in physical units. Once detrending is applied, the input-output data is split into two parts: the first part of the data to be used in estimation and the second part of the data to be used for validation (Figure 3.9).

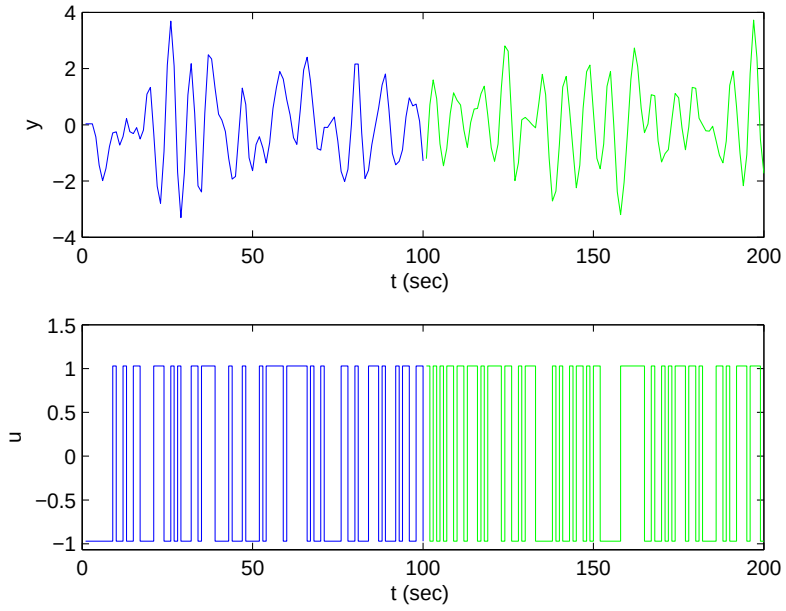

Figure 3.9. Detrended output signal (y) and the random binary input signal (u).

Using correlation analysis the impulse response of the system is obtained. System's true and estimated impulse responses are shown in Figure 3.10. The system's first response to the input outside the 3-standard deviation confidence region occurs at the third lag. The fact that the system's first response does not occur at the zero lag indicates that there is a nonzero delay in the system.

Step response of the system can also be estimated from correlation analysis. Estimated step response (Figure 3.11) confirms the existence of a delay in the system. Moreover, the overshoot clearly indicates that the system has complex poles and hence the order of the system should be greater than one.

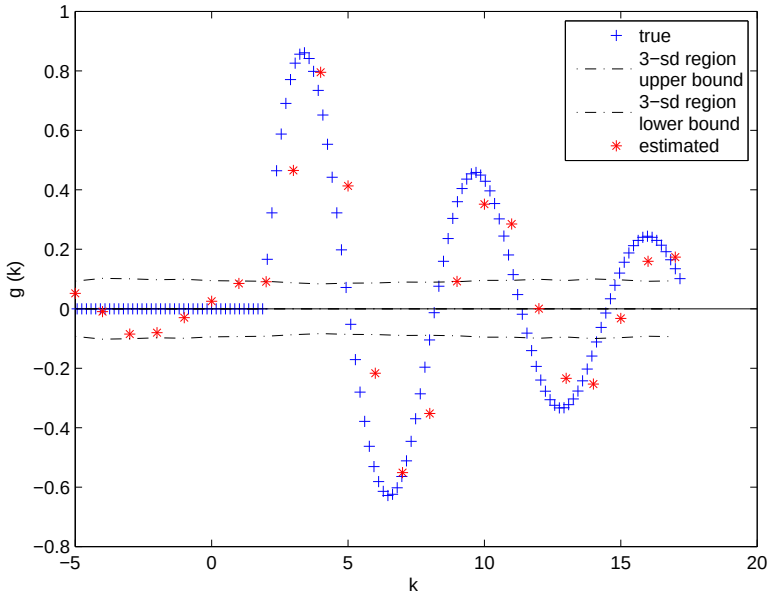

Figure 3.10. Estimated Impulse response by correlation analysis.

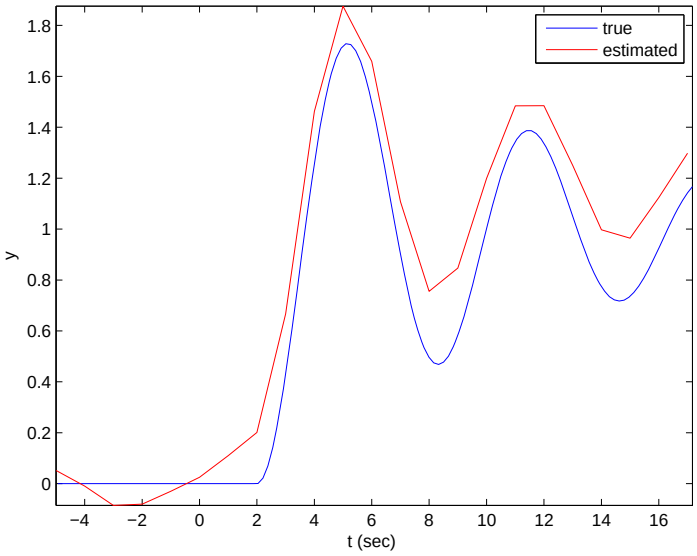

Figure 3.11. Estimated Step Response by Correlation Analysis.

Frequency response of the system is estimated using both ETFE and SPA. The amplitude peaks at the frequency of about 1 rad/s (Figure 3.12). This suggests a possible resonant behaviour of the complex poles.

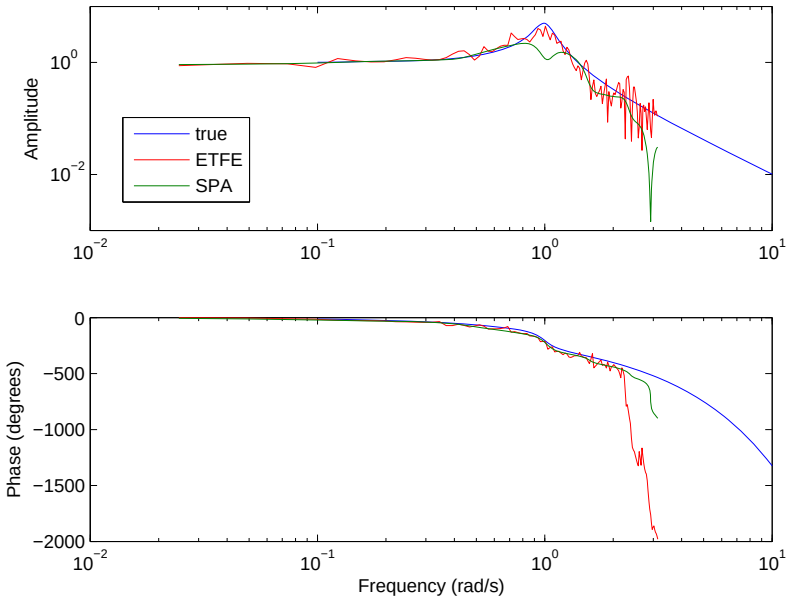

Figure 3.12. Estimated Frequency Response by ETFE and SPA.

As it is observed from the identification methods applied so far, nonparametric identification is very useful in giving the user information about some properties of the system which can be useful for choosing the form of the model. From time domain identification methods of impulse and step analysis, it is inferred that the system has a three sample delay from input to output. Frequency domain methods have shown that the system order is 2 and the poles are complex. Now by using these facts a parametrized model for the system may be constructed using output error (OE) model structure

$$G(z,\theta) = z^{-n_k}\frac{\overline{B}(z)}{F(z)} = z^{-3}\frac{b_1 + b_2 z^{-1}}{1 + f_1 z^{-1} + f_2 z^{-2}}, \qquad H(z,\theta) = 1 \tag{3.95}$$

The prediction error of this model (3.95) can be written in pseudolinear regression form (see Section 3.3.2.3)

$$\hat{y}(n|n-1) = \varphi^T(n,\theta)\theta, \qquad \hat{\theta} = \begin{bmatrix} b_1 & b_2 & f_1 & f_2 \end{bmatrix}^T$$
$$\varphi(n,\theta) = \begin{bmatrix} u(n-3) & u(n-4) & -\hat{y}(n-1,\theta) & -\hat{y}(n-2,\theta) \end{bmatrix}^T \tag{3.96}$$

The parameters of the model (3.95) are estimated as

$$\hat{\theta} = \begin{bmatrix} 0.44 & 0.39 & -0.98 & 0.81 \end{bmatrix}^T \tag{3.97}$$

The comparison of the estimated OE model and the validation data is shown in Figure 3.13. The estimated OE model fits the validation data by 78.34 per cent.

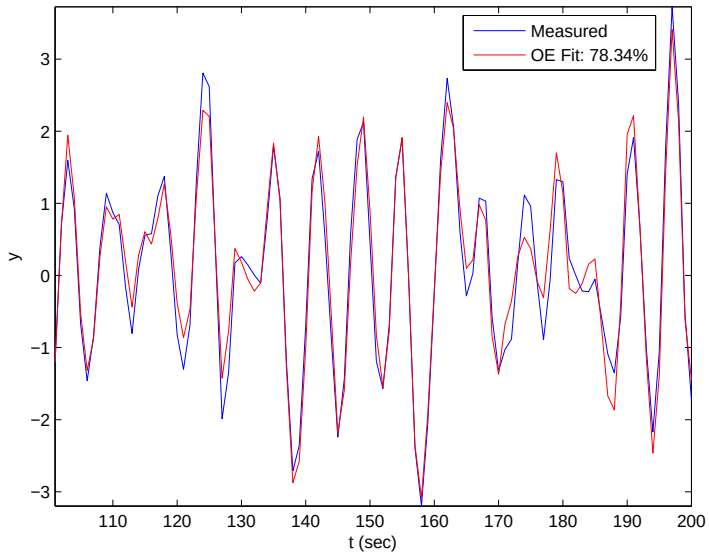

Figure 3.13. Comparison of the measured output and the OE model output.

The estimated OE model is a discrete time model and this discrete time OE model must be converted to continuous time since the system to be identified is a continuous time process.

$$\hat{G}(z) = \frac{0.44z^{-3} + 0.39z^{-4}}{1 - 0.98z^{-1} + 0.81z^{-2}} \Rightarrow \hat{G}(s) = \frac{0.008573s + 0.9998}{s^2 + 0.217s + 1.003}e^{-2s} \tag{3.98}$$

If the parameter vector is rewritten for the continuous time process model, the parametric identification procedure may be evaluated in continuous time as

$$\theta_0 = \begin{bmatrix} 1 & 0.2 & 1 & 1 & 0 & 2 \end{bmatrix}^T$$
$$\hat{\theta} = \begin{bmatrix} 1.003 & 0.217 & 1 & 0.9998 & 0.008573 & 2 \end{bmatrix}^T \tag{3.99}$$

The constructed OE model structure (3.95) is inadequate in modeling the noise as it is seen from the comparison (Figure 3.13). The identification can be improved by using ARMAX model structure (see Section 3.3.2.2) which allows more flexibility in modeling the noise. Hence, the noise model is changed to a second order moving average process while the system model is kept same.

$$G(z,\theta) = z^{-n_k}\frac{\overline{B}(z)}{F(z)} = z^{-3}\frac{b_1 + b_2 z^{-1}}{1 + f_1 z^{-1} + f_2 z^{-2}}, \qquad H(z,\theta) = 1 + c_1 z^{-1} + c_2 z^{-2} \tag{3.100}$$

The parameters of the ARMAX model (3.100) are estimated as

$$\hat{\theta} = \begin{bmatrix} f_1 & f_2 & b_1 & b_2 & c_1 & c_2 \end{bmatrix}^T = \begin{bmatrix} -0.99 & 0.81 & 0.43 & 0.41 & 0.88 & -0.03 \end{bmatrix}^T$$

yields the following model

$$\hat{G}(z,\theta) = \frac{0.43z^{-3} + 0.41z^{-4}}{1 - 0.99z^{-1} + 0.81z^{-2}}, \qquad \hat{H}(z,\theta) = 1 + 0.88z^{-1} - 0.03z^{-2} \tag{3.101}$$

The 5-step-ahead comparison of the two models and the validation data is shown in Figure 3.14. While the OE model fits the validation data by 78.34 per cent, the fit of the ARMAX model is 81.55 per cent. It is seen clearly that the ARMAX model due to better modeling noise is more successful at fitting the validation data than the OE model.

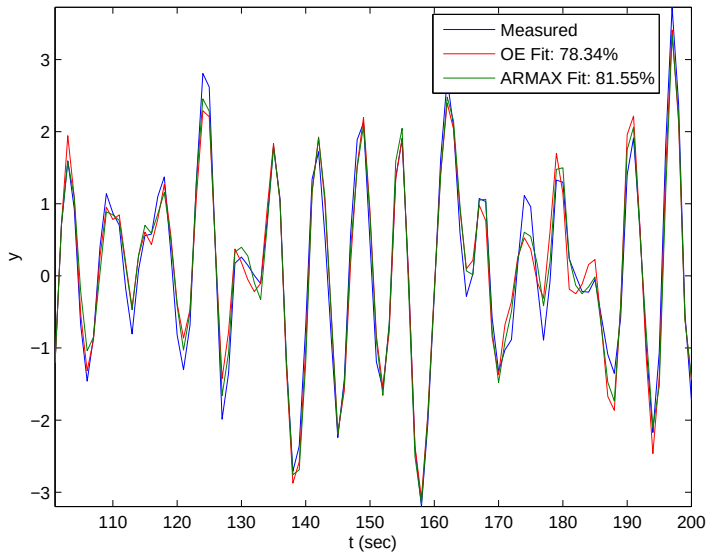

Figure 3.14. 5-step-ahead comparison of the measured output and the OE and ARMAX model outputs.

While none of the applied identification methods is perfect, all of them give some insight into the system. Each identification method has its own set of advantages and disadvantages. All of the nonparametric methods depend on their inputs being persistently exciting. Time domain methods of impulse and step response analysis are simple to apply and may yet give critical information such as delay time, gain, dominating time constant, order and complexity of system poles but they are subject to significant errors due to noise that cannot be neglected. Correlation analysis gives the same estimate regardless of the noise as long as the input remains persistently exciting. Frequency domain methods composed of frequency, fourier and spectral analysis also depend on the the type of the input signals and do not yield satisfactory results for poor input signals such as impulse and step. Although frequency analysis method is easy to apply and allows focusing on a specified frequency range, the method must be repeated for the given number of frequencies which may cause long experimentation time and requires sinusoidal input signal which in practice cannot be applied to many real processes. While fourier analysis results in good estimates for periodic inputs, the nonperiodic inputs gives crude estimates. Spectral analysis attempts to smooth the frequency response estimated from fourier analysis by using frequency windows. The selection of the frequency window determines the quality of the estimates by spectral

analysis. A comparison of the nonparametric linear identification methods is presented in Table 3.1.

Table 3.1. Comparison of nonparametric linear identification methods

Domain	Methods	Advantages	Disadvantages
Time	Impulse Resp.	simple to apply can be used to determine delay	impulse is hard to generate noise neglected large estimation error may evoke nonlinear modes
	Step Resp.	allows determination of delay, gain, order	noise neglected, large estimation error
	Corr. Anal.	gives same estimation error regardless of noise	input signal must be persistently exciting
Freq.	Freq. Anal.	easy, allows to focus on a specified frequency range	only works with sinusoidal input, experiment must be repeated for each frequency
	Fourier Anal.	estimations are good only for periodic inputs	estimations are crude for nonperiodic inputs
	Spec. Anal.	can smooth estimations by windowing	smoothing not guaranteed

On the other hand, parametric methods are not as sensitive to the type of input signals as the nonparametric methods. The success of the parametric methods depends on the selection of the correct model structure. Equation error model structure also known as ARX is the most simple model structure. Although from a physical point of view this model structure may seem unnatural to model the noise through the denominator dynamics of the system, the advantage of this model which makes it a prime choice for many applications is its predictor that can be written in a linear regression form. The disadvantage of the ARX model is lack of adequate freedom in describing the disturbance term. The ARMAX model structure gives the user flexibility by describing the noise as a moving average (MA) process. However, this flexibility comes at a price. The predictor for ARMAX model structure cannot be written in

a linear regression form. OE model structure allows independent parametrization of the system and disturbance transfer functions. Like ARMAX model structure, the predictor of OE cannot be written in a linear regression form. A comparison of the parametric identification of black-box model structures is given in Table 3.2.

Table 3.2. Comparison of parametric identification of black-box model structures.

Model Structures	Advantages	Disadvantages
ARX	prediction error is in linear regression form, parameters may be calculated by LS	noise model is fixed and cannot be changed
ARMAX	noise may be modeled as a MA process of any order	prediction error is not in linear regression form, parameter can only be calculated numerically
OE	parametrization of system and noise model is independent	

4. FRACTIONAL ORDER SYSTEM IDENTIFICATION TECHNIQUES

The fractional order system identification techniques that are covered in this section are parametric identification methods with fractional order models. Since the nonparametric identification methods given in Section 3.2 do not use a mathematical model, they can be directly applied to any linear system without any modification. The parametric methods should be extended to fractional order models. As benchmark systems semi-integrating circuits and viscoelastic system of Bagley-Torvik are analyzed in detail. The given parametric identification methods with fractional order models are compared using the benchmark systems.

4.1. Parametric Identification with Fractional Order Models

There exist both time domain and frequency domain parametric identification methods using fractional order models.

4.1.1. Time Domain Methods

4.1.1.1. Linear Regression. The linear regression method from integer order system identification can be extended to fractional order models as well. The fractional order system that is to be identified is assumed to be governed by the following fractional order differential equation

$$\mathscr{D}^{\alpha_0}y(t)+a_1\mathscr{D}^{\alpha_1}y(t)+\cdots+a_n\mathscr{D}^{\alpha_n}y(t) = b_0\mathscr{D}^{\beta_0}u(t)+b_1\mathscr{D}^{\beta_1}u(t)+\cdots+b_m\mathscr{D}^{\beta_m}u(t) \quad (4.1)$$

The fractional orders,$(\alpha_0,\ldots,\alpha_n,\beta_0,\ldots,\beta_m)$, are supposed to be known as is the case of many systems such as thermal systems [15]. If no insight is available regarding the fractional orders, they are to be chosen by trial and error. The parameter vector that is to be estimated by linear regression is composed of the coefficients of the fractional

order differential equation

$$\theta = \begin{bmatrix} a_1 & \cdots & a_n & b_0 & \cdots & b_m \end{bmatrix}^T \tag{4.2}$$

Isolating the term $\mathscr{D}^{\alpha_0} y(t)$ allows us to rewrite the fractional order differential equation in linear regression form [16]

$$\begin{aligned} \mathscr{D}^{\alpha_0} y(t) &= -a_1 \mathscr{D}^{\alpha_1} y(t) - \cdots - a_n \mathscr{D}^{\alpha_n} y(t) + b_0 \mathscr{D}^{\beta_0} u(t) + \cdots + b_m \mathscr{D}^{\beta_m} u(t) \\ &= \begin{bmatrix} -\mathscr{D}^{\alpha_1} y(t) & \ldots & -\mathscr{D}^{\alpha_n} y(t) & \mathscr{D}^{\beta_0} u(t) & \ldots & \mathscr{D}^{\beta_m} u(t) \end{bmatrix} \theta \end{aligned} \tag{4.3}$$

Since the data acquisition takes place at the sampling intervals, numerical schemes of fractional order differentiation (see Section 2.1.4) can be applied to the sampled output and input to form the regression vector [16]

$$\underbrace{\begin{bmatrix} \mathscr{D}^{\alpha_0} y(0) \\ \mathscr{D}^{\alpha_0} y(h) \\ \vdots \\ \mathscr{D}^{\alpha_0} y(Kh) \end{bmatrix}}_{\hat{y}(kh)} = \underbrace{\begin{bmatrix} -\mathscr{D}^{\alpha_1} y & \cdots & -\mathscr{D}^{\alpha_n} y & \mathscr{D}^{\beta_0} u & \cdots & \mathscr{D}^{\beta_m} u \end{bmatrix}}_{\varphi(kh)} \underbrace{\begin{bmatrix} a_1 \\ \vdots \\ a_n \\ b_0 \\ \vdots \\ b_m \end{bmatrix}}_{\theta} \tag{4.4}$$

$$\mathscr{D}^{\alpha_i} y = \begin{bmatrix} \mathscr{D}^{\alpha_i} y(0) \\ \mathscr{D}^{\alpha_i} y(h) \\ \vdots \\ \mathscr{D}^{\alpha_i} y(Kh) \end{bmatrix} \qquad \mathscr{D}^{\alpha_i} u = \begin{bmatrix} \mathscr{D}^{\alpha_i} u(0) \\ \mathscr{D}^{\alpha_i} u(h) \\ \vdots \\ \mathscr{D}^{\alpha_i} u(Kh) \end{bmatrix} \tag{4.5}$$

The LS solution of linear regression is given as

$$\hat{\theta} = \left(\varphi^T \varphi\right)^{-1} \varphi^T \hat{y}(kh) \tag{4.6}$$

provided that the inverse exists. Fractional order models based on (4.1) have been developed by Mathieu (1996), Le Lay (1998), Trigeassou (1999) and Cois (2000) [15, 17].

The calculation of the regression vector (4.4) requires differentiating the output and input signals of the system to an arbitrary real order. The Grünwald-Letnikov definition may be used for numerical evaluation of fractional order differentiation (see Section 2.1.4.1). Using Grünwald-Letnikov definition the predictor (4.4) can be rewritten as

$$\hat{y}(kh) = -\frac{\sum_{i=1}^{n} \frac{a_i}{h^{\alpha_i}} \sum_{j=0}^{k} (-1)^j \binom{\alpha_i}{j} y(kh-jh)}{\sum_{i=1}^{n} \frac{a_i}{h^{\alpha_i}}} + \frac{\sum_{l=0}^{m} \frac{b_l}{h^{\beta_l}} \sum_{j=0}^{k} (-1)^j \binom{\beta_l}{j} u(kh-jh)}{\sum_{i=1}^{n} \frac{a_i}{h^{\alpha_i}}} \tag{4.7}$$

The equation (4.7) is nonlinear with respect to the parameters given in (4.2). This nonlinearity can be adressed by defining a new set of parameters

$$a_i^* = \frac{\frac{a_i}{h^{\alpha_i}}}{\sum_{i=1}^{n} \frac{a_i}{h^{\alpha_i}}},\ 1 \le i \le n \qquad b_l^* = \frac{\frac{b_l}{h^{\beta_l}}}{\sum_{i=1}^{n} \frac{a_i}{h^{\alpha_i}}},\ 0 \le l \le m \tag{4.8}$$

Now the predictor can be expressed in a linear form with the new set of parameters

$$\hat{y}(kh) = -\sum_{i=1}^{n} a_i^* y_i^*(kh) + \sum_{l=0}^{m} b_l^* u_l^*(kh) \tag{4.9}$$

$y_i^*(kh)$ and $u_l^*(kh)$ are defined from (4.7) and represent past values of the output and input variables respectively. This method is desribed in [18].

4.1.1.2. Iterative Search By Grünwald-Letnikov Definition. By using (4.7) and (4.8) the predictor (4.9) can also be written as

$$\hat{y}(kh) = -\sum_{i=1}^{n} a_i^* \sum_{j=0}^{k} (-1)^j \binom{\alpha_i}{j} y(kh-jh) + \sum_{l=0}^{m} b_l^* \sum_{j=0}^{k} (-1)^j \binom{\beta_l}{j} u(kh-jh) \tag{4.10}$$

According to commensurate order form [19], in which α's and β's are multiple of a real $q \in \mathbb{R} \setminus \mathbb{Z}$, the predictor (4.10) can be reorganized as

$$\hat{y}(kh,\theta) = -\sum_{i=1}^{n} a_i^* \sum_{j=0}^{k} (-1)^j \binom{iq}{j} y(kh-jh) + \sum_{l=0}^{m} b_l^* \sum_{j=0}^{k} (-1)^j \binom{lq}{j} u(kh-jh) \quad (4.11)$$

A modal decomposition of this form (4.11) has been suggested by Cois, et. al. [20]. The predictor allows the parametrization of the commensurate order along with the coefficients. Parameter vector is given as

$$\theta^T = \begin{bmatrix} q & a_1^* & \cdots & a_n^* & b_0^* & \cdots & b_m^* \end{bmatrix} \quad (4.12)$$

The parameter vector (4.12) can be estimated numerically by minimizing the prediction error. With $\hat{\theta}$ being an estimation of θ the prediction error for a kth sample of total K number of system output data, $y(kh)$, is

$$\varepsilon(kh,\hat{\theta}) = y(kh) - \hat{y}(kh,\hat{\theta}) \quad (4.13)$$

The optimal value of $\hat{\theta}$ can be obtained through minimization of the quadratic criterion applied to the prediction error

$$V_K(\hat{\theta}, Z^K) = \frac{1}{K} \sum_{k=0}^{K-1} \frac{1}{2}\, \varepsilon^2(kh,\hat{\theta}) \quad (4.14)$$

Since the predictor $\hat{y}(kh,\hat{\theta})$ is nonlinear with respect to $\hat{\theta}$, a nonlinear numerical search routine must be used in order to find the optimal parameters that minimize the quadratic criterion. Numerical minimization of the quadratic criterion update the estimate of the minimizing point iteratively according to

$$\hat{\theta}_{i+1} = \hat{\theta}_i + \lambda f_i \quad (4.15)$$

where i denotes the current iteration and f_i is a search direction based on information about $V_K(\hat{\theta}, Z^K)$ acquired at previous iterations and λ is a positive constant deter-

mined so that an appropriate decrease in the value of $V_K(\hat{\theta}, Z^K)$ is obtained. Methods using values of the function, $V_K(\hat{\theta}, Z^K)$, of its gradient, and of its Hessian, the second derivative matrix, are called "Newton" algorithms [1]. The Newton algorithms use the following search direction

$$f_i = -\left[V''(\hat{\theta}_i)\right]^{-1} V'(\hat{\theta}_i) \tag{4.16}$$

which is known as Newton search direction [1]. Some well-known algorithms using the Newton search direction (4.16) are trust-region reflective, Levenberg-Marquardt and Gauss-Newton algorithms. These algorithms are implemented in Matlab's Optimization Toolbox which has been used in minimizing (4.14). The implementation of these algorithms are described in [21]. Levenberg-Marquardt algorithm is chosen for simulations.

4.1.2. Frequency Domain Methods

If the frequency response of the fractional order system is estimated successfully by parametric identification methods, then the estimated frequency response can be modeled by using a transfer function

$$\hat{G}(s) = \frac{b_m s^{\beta_m} + \cdots + b_2 s^{\beta_2} + b_1 s^{\beta_1} + b_0}{a_n s^{\alpha_n} + \cdots + a_2 s^{\alpha_2} + a_1 s^{\alpha_1} + 1} = \frac{\sum_{k=0}^{m} b_k s^{kq}}{1 + \sum_{k=1}^{n} a_k s^{kq}} \tag{4.17}$$

where m and n are the orders of the numerator and denominator. This transfer function has a specific form and so the order is commensurate which means that all powers of the Laplace variable, α's and β's, are multiple of a real $q \in \mathbb{R} \setminus \mathbb{Z}$ [22, 23].

By replacing $s = j\omega$ the frequency response of the transfer function can be expressed as

$$\hat{G}(j\omega) = \frac{\sum_{k=0}^{m} b_k (j\omega)^{kq}}{1 + \sum_{k=1}^{n} a_k (j\omega)^{kq}} = \frac{N(j\omega)}{D(j\omega)} = \frac{\chi(\omega) + j\gamma(\omega)}{\eta(\omega) + j\kappa(\omega)} \tag{4.18}$$

$N(j\omega)$ and $D(j\omega)$ are complex while $\chi, \gamma, \eta, \kappa$ are real [22, 23].

The prediction error between the model and the actual system is given for a specific frequency

$$\varepsilon(j\omega) = G(j\omega) - \hat{G}(j\omega) = G(j\omega) - \frac{N(j\omega)}{D(j\omega)} \tag{4.19}$$

It is possible to minimize the norm of this prediction error but the minimization problem is difficult. In order to simplify the problem, the prediction error has to be redefined [22, 23].

4.1.2.1. Levy's Identification Method. Levy's method tries to minimize the square of the norm of

$$\varepsilon(j\omega)D(j\omega) = G(j\omega)D(j\omega) - N(j\omega) \tag{4.20}$$

This form of prediction error leads to a set of equations easily solvable. For simplifying notation, a new variable E is introduced and the frequency argument of the variables is omitted [22, 23].

$$\begin{aligned} E = GD - N &= [\Re(G) + j\Im(G)]\,(\eta + j\kappa) - (\chi + j\gamma) \\ &= [\Re(G)\eta - \Im(G)\kappa - \chi] + j\,[\Re(G)\kappa + \Im(G)\eta - \gamma] \end{aligned} \tag{4.21}$$

The square of the norm of E is

$$|E|^2 = [\Re(G)\eta - \Im(G)\kappa - \chi]^2 + [\Re(G)\kappa + \Im(G)\eta - \gamma]^2 \tag{4.22}$$

It is observed from (4.18) that

$$\chi(\omega) = \sum_{k=0}^{m} b_k \Re\left[(j\omega)^{kq}\right] \qquad \gamma(\omega) = \sum_{k=0}^{m} b_k \Im\left[(j\omega)^{kq}\right] \tag{4.23}$$

$$\eta(\omega) = 1 + \sum_{k=1}^{n} a_k \Re\left[(j\omega)^{kq}\right] \quad \kappa(\omega) = \sum_{k=1}^{n} a_k \Im\left[(j\omega)^{kq}\right] \tag{4.24}$$

Differentiating $|E|^2$ with respect to b_k and a_k $(k = 0, 1, \ldots, m)$ yields

$$\begin{aligned}\frac{\partial |E|^2}{\partial b_k} = 0 \Leftrightarrow\ & [\Re(G)\eta - \Im(G)\kappa - \chi]\Re\left[(j\omega)^{kq}\right] \\ & + [\Re(G)\kappa + \Im(G)\eta - \gamma]\Im\left[(j\omega)^{kq}\right] = 0 \end{aligned} \tag{4.25}$$

$$\begin{aligned}\frac{\partial |E|^2}{\partial a_k} = 0 \Leftrightarrow\ & \eta\left\{[\Im(G)]^2 + [\Re(G)]^2\right\}\Re[(j\omega)^{kq}] + \kappa\left\{[\Im(G)]^2 + [\Re(G)]^2\right\}\Im[(j\omega)^{kq}] \\ & + \chi\left\{\Im(G)\Im[(j\omega)^{kq}] - \Re(G)\Re[(j\omega)^{kq}]\right\} \\ & - \gamma\left\{-\Im(G)\Re[(j\omega)^{kq}] - \Re(G)\Im[(j\omega)^{kq}]\right\} = 0 \end{aligned} \tag{4.26}$$

The $m+1$ equations from (4.25) and the n equation from (4.26) together form a linear system of equations which can be solved to find the parameters [23].

$$\begin{bmatrix} A & B \\ C & D \end{bmatrix} \begin{bmatrix} b \\ a \end{bmatrix} = \begin{bmatrix} f \\ g \end{bmatrix} \tag{4.27}$$

The linear system of equation is summed for each frequency supposing that the frequency response is estimated at N frequencies [23].

$$\begin{aligned} A_{l,c} = & \sum_{p=1}^{N} \left\{-\Re\left[(j\omega_p)^{lq}\right]\Re\left[(j\omega_p)^{cq}\right] - \Im\left[(j\omega_p)^{lq}\right]\Im\left[(j\omega_p)^{cq}\right]\right\}, \\ & l = 0, 1, \ldots, m \wedge c = 0, 1, \ldots, m \end{aligned} \tag{4.28}$$

$$B_{l,c} = \sum_{p=1}^{N} \left\{ \Re\left[(j\omega_p)^{lq}\right] \Re\left[(j\omega_p)^{cq}\right] \Re\left[G(j\omega_p)\right] + \Im\left[(j\omega_p)^{lq}\right] \Re\left[(j\omega_p)^{cq}\right] \Im\left[G(j\omega_p)\right] \right.$$
$$\left. -\Re\left[(j\omega_p)^{lq}\right] \Im\left[(j\omega_p)^{cq}\right] \Im\left[G(j\omega_p)\right] + \Im\left[(j\omega_p)^{lq}\right] \Im\left[(j\omega_p)^{cq}\right] \Re\left[G(j\omega_p)\right] \right\},$$
$$l = 0, 1, \ldots, m \wedge c = 1, \ldots, n \tag{4.29}$$

$$C_{l,c} = \sum_{p=1}^{N} \left\{ -\Re\left[(j\omega_p)^{lq}\right] \Re\left[(j\omega_p)^{cq}\right] \Re\left[G(j\omega_p)\right] + \Im\left[(j\omega_p)^{lq}\right] \Re\left[(j\omega_p)^{cq}\right] \Im\left[G(j\omega_p)\right] \right.$$
$$\left. -\Re\left[(j\omega_p)^{lq}\right] \Im\left[(j\omega_p)^{cq}\right] \Im\left[G(j\omega_p)\right] - \Im\left[(j\omega_p)^{lq}\right] \Im\left[(j\omega_p)^{cq}\right] \Re\left[G(j\omega_p)\right] \right\},$$
$$l = 1, \ldots, n \wedge c = 0, 1, \ldots, m$$

$$D_{l,c} = \sum_{p=1}^{N} \left(\left\{\Re[G(j\omega_p)]\right\}^2 + \left\{\Im[G(j\omega_p)]\right\}^2 \right)$$
$$\left\{\Re[(j\omega_p)^{lq}]\Re[(j\omega_p)^{cq}] + \Im[(j\omega_p)^{lq}]\Im[(j\omega_p)^{cq}]\right\}, \; l = 1, \ldots, n \wedge c = 1, \ldots, n \tag{4.30}$$

$$b = \begin{bmatrix} b_0 & \cdots & b_m \end{bmatrix}^T \tag{4.31}$$

$$a = \begin{bmatrix} a_1 & \cdots & a_n \end{bmatrix}^T \tag{4.32}$$

$$f_{l,1} = \sum_{p=1}^{N} -\Re[(j\omega_p)^{lq}]\Re[G(j\omega_p)] - \Im[(j\omega_p)^{lq}]\Im[G(j\omega_p)], \qquad l = 0, 1, \ldots, m \tag{4.33}$$

$$g_{l,1} = \sum_{p=1}^{N} -\Re[(j\omega_p)^{lq}] \left(\left\{\Re[G(j\omega_p)]\right\}^2 + \left\{\Im[G(j\omega_p)]\right\}^2 \right), \qquad l = 1, \ldots, n \tag{4.34}$$

Another way to deal with the issue of N frequencies is to assign a system for each frequency and then stack them [23].

$$\begin{bmatrix} A_1 & B_1 \\ C_1 & D_1 \\ A_2 & B_2 \\ C_2 & D_2 \\ \vdots & \vdots \\ A_N & B_N \\ C_N & D_N \end{bmatrix} \begin{bmatrix} b \\ a \end{bmatrix} = \begin{bmatrix} f_1 \\ g_1 \\ f_2 \\ g_2 \\ \vdots \\ f_N \\ g_N \end{bmatrix} \tag{4.35}$$

This is an overdetermined system and so the least squares solution can be used.

$$\begin{bmatrix} b \\ a \end{bmatrix} = \left(\begin{bmatrix} A_1 & B_1 \\ C_1 & D_1 \\ A_2 & B_2 \\ C_2 & D_2 \\ \vdots & \vdots \\ A_N & B_N \\ C_N & D_N \end{bmatrix}^T \begin{bmatrix} A_1 & B_1 \\ C_1 & D_1 \\ A_2 & B_2 \\ C_2 & D_2 \\ \vdots & \vdots \\ A_N & B_N \\ C_N & D_N \end{bmatrix} \right)^{-1} \begin{bmatrix} A_1 & B_1 \\ C_1 & D_1 \\ A_2 & B_2 \\ C_2 & D_2 \\ \vdots & \vdots \\ A_N & B_N \\ C_N & D_N \end{bmatrix}^T \begin{bmatrix} f_1 \\ g_1 \\ f_2 \\ g_2 \\ \vdots \\ f_N \\ g_N \end{bmatrix} \tag{4.36}$$

In simulations Levy's method is applied via Fractional Control Toolbox developed by Valerio [24].

4.1.2.2. Enhancing Levy's Identification with Weights. Levy's method has a disadvantage. The Levy's method often leads to models well fitted to high frequencies but poorly fitted to low frequencies. Using well-chosen weights the influence of low frequency data can be increased and thus this issue may be counterbalanced [22].

If $g(t)$ is the step response of the fractional order system to be identified, according to Vinagre [22]

$$\int_0^\infty |g(t) - \hat{g}(t)|^2 \mathrm{d}t = \int_0^\infty \left| \mathscr{L}^{-1}\left[G(s)\frac{1}{s} \right] - \mathscr{L}^{-1}\left[\hat{G}(s)\frac{1}{s} \right] \right|^2 \mathrm{d}t \tag{4.37}$$

and Parseval's theorem [22] allows this to be written as

$$\int_{-\infty}^{+\infty} \left| G(j\omega)\frac{1}{j\omega} - \hat{G}(j\omega)\frac{1}{j\omega} \right|^2 \mathrm{d}\omega = \int_{-\infty}^{+\infty} \frac{|\varepsilon(\omega)|^2}{\omega^2} \mathrm{d}\omega \tag{4.38}$$

Applying trapezoidal numerical integration rule [22] gives

$$\sum_{p=1}^{N-1} \left\{ \frac{1}{2}(\omega_{p+1} - \omega_p) \left[\frac{|\varepsilon(\omega_{p+1})|^2}{\omega_{p+1}^2} + \frac{|\varepsilon(\omega_p)|^2}{\omega_p^2} \right] \right\} = \sum_{p=1}^{N} |\varepsilon(\omega_p)|^2 \omega_p^* \tag{4.39}$$

where

$$\omega_p^* = \begin{cases} (\omega_2 - \omega_1)/2\omega_1^2 & \text{if } p = 1 \\ (\omega_{p+1} - \omega_{p-1})/2\omega_p^2 & \text{if } 1 < p < N \\ (\omega_f - \omega_{f-1})/2\omega_f^2 & \text{if } p = N \end{cases} \tag{4.40}$$

Instead of minimizing $\sum_{p=1}^{N} |E(\omega_p)|^2$, the new cost function $\sum_{p=1}^{N} |E(\omega_p)|^2 \omega_p^*$ is going to be minimized [22]. The weights that decrease with frequency clearly increases the influence of low frequencies. The new weights do not depend on the coefficients and so differentiating the prediction error with respect to the coefficients does not yield dramatic changes. The matrices and the vectors for the new weights [22] can be calculated from

$$A_{l,c} = \sum_{p=1}^{N} \left\{ -\Re\left[(j\omega_p)^{lq}\right] \Re\left[(j\omega_p)^{cq}\right] - \Im\left[(j\omega_p)^{lq}\right] \Im\left[(j\omega_p)^{cq}\right] \right\} \omega_p,$$

$$l = 0, 1, \ldots, m \wedge c = 0, 1, \ldots, m \tag{4.41}$$

$$B_{l,c} = \sum_{p=1}^{N} \left\{ \Re\left[(j\omega_p)^{lq}\right] \Re\left[(j\omega_p)^{cq}\right] \Re\left[G(j\omega_p)\right] + \Im\left[(j\omega_p)^{lq}\right] \Re\left[(j\omega_p)^{cq}\right] \Im\left[G(j\omega_p)\right] \right.$$

$$\left. -\Re\left[(j\omega_p)^{lq}\right] \Im\left[(j\omega_p)^{cq}\right] \Im\left[G(j\omega_p)\right] + \Im\left[(j\omega_p)^{lq}\right] \Im\left[(j\omega_p)^{cq}\right] \Re\left[G(j\omega_p)\right] \right\} \omega_p,$$

$$l = 0, 1, \ldots, m \wedge c = 1, \ldots, n \tag{4.42}$$

$$C_{l,c} = \sum_{p=1}^{N} \left\{ -\Re\left[(j\omega_p)^{lq}\right] \Re\left[(j\omega_p)^{cq}\right] \Re\left[G(j\omega_p)\right] + \Im\left[(j\omega_p)^{lq}\right] \Re\left[(j\omega_p)^{cq}\right] \Im\left[G(j\omega_p)\right] \right.$$

$$\left. -\Re\left[(j\omega_p)^{lq}\right] \Im\left[(j\omega_p)^{cq}\right] \Im\left[G(j\omega_p)\right] - \Im\left[(j\omega_p)^{lq}\right] \Im\left[(j\omega_p)^{cq}\right] \Re\left[G(j\omega_p)\right] \right\} \omega_p,$$

$$l = 1, \ldots, n \wedge c = 0, 1, \ldots, m \tag{4.43}$$

$$D_{l,c} = \sum_{p=1}^{N} \left(\{\Re[G(j\omega_p)]\}^2 + \{\Im[G(j\omega_p)]\}^2 \right)$$

$$\left\{ \Re[(j\omega_p)^{lq}] \Re[(j\omega_p)^{cq}] + \Im[(j\omega_p)^{lq}] \Im[(j\omega_p)^{cq}] \right\} \omega_p,$$

$$l = 1, \ldots, n \wedge c = 1, \ldots, n \tag{4.44}$$

$$f_{l,1} = \sum_{p=1}^{N} \left\{ -\Re[(j\omega_p)^{lq}]\Re[G(j\omega_p)] - \Im[(j\omega_p)^{lq}]\Im[G(j\omega_p)] \right\} \omega_p, \; l = 0, 1, \ldots, m \quad (4.45)$$

$$g_{l,1} = \sum_{p=1}^{N} \left\{ -\Re[(j\omega_p)^{lq}] \left(\{\Re[G(j\omega_p)]\}^2 + \{\Im[G(j\omega_p)]\}^2 \right) \right\} \omega_p, \qquad l = 1, \ldots, n \quad (4.46)$$

In simulations Levy's method with Vinagre's weights is applied via Fractional Control Toolbox developed by Valerio [24].

4.2. Benchmark Systems

The fractional order models of semi-integrating circuits and viscoelastic system of Bagley-Torvik will be analysed in this section.

4.2.1. Semi-integrating Circuits

Electrical circuits have long been used to perform the operations of differentiation and integration. A simple circuit (Figure 4.1) with a capacitor can be used to provide a voltage output that is proportional to the integral of the applied input current under the assumption of $v(0) = 0$.

$$v(t) = \frac{1}{C} \frac{\mathrm{d}^{-1}}{\mathrm{d}t^{-1}} i(t) \quad (4.47)$$

Circuits that perform differentiation and integration to noninteger orders can also be designed. One such circuit is called semi-integrating circuit or semi-integrator. Although these circuits can perform semi-integration, they have two design considerations: accuracy and limited operation time. Response of a semi-integrating circuit is approximately proportional to the semi-integral of the input signal meaning the circuit has a degree of accuracy. Secondly the semi-integrating circuit can approximate the behaviour of a real semi-integrator only over a limited time interval which has a finite upper limit and a nonzero lower limit. In other words, the semi-integrating circuit has a frequency bandpass. Although these two issues may be improved by selecting better components and increasing the number of components, the cost of the design

will inevitably increase [6].

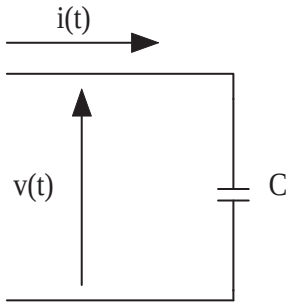

Figure 4.1. An integrating circuit.

First the simple circuit in Figure 4.2 is considered. The input current $i(t)$ flows through the resistor R_1 and then continues through a parallel combination of the capacitor C_0 and the resistor R_0. It is assumed that at $t = 0$ the circuit is at rest which implies that both the applied input current and the potential output are both zero.

$$i(t \leq 0) = v(t \leq 0) = 0 \tag{4.48}$$

A nonzero input current is applied after $t = 0$.

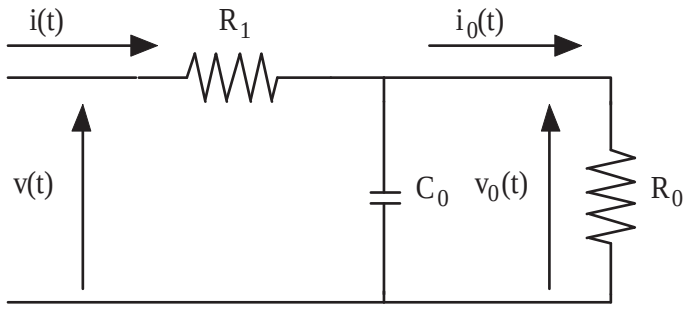

Figure 4.2. A simple 3-component circuit [6].

The current i_0 flows through the resistor R_0 and according to Ohm's law, i_0 is

$$i_0 = \frac{v_0}{R_0}$$

The current that flows through the capacitor can be written as

$$i(t) - i_0(t) = C_0 \frac{\mathrm{d}v_0}{\mathrm{d}t}$$

where using Ohm's law the input current $i(t)$ is given as

$$i(t) = \frac{v(t) - v_0(t)}{R_1}$$

The differential equation that govens the input current $i(t)$ and the output voltage $v(t)$ is

$$[R_0 + R_1]i(t) + R_0 R_1 C_0 \frac{\mathrm{d}i(t)}{\mathrm{d}t} = v(t) + R_0 C_0 \frac{\mathrm{d}v(t)}{\mathrm{d}t} \tag{4.49}$$

If the Laplace transform is applied to (4.49),

$$\frac{V(s)}{R_1 I(s)} = 1 + \frac{\dfrac{1}{R_1 C_0}}{s + \dfrac{1}{R_0 C_0}} \tag{4.50}$$

provided that the initial conditions are zero.

Next two additional components, a series resistor R_2 and a capacitor C_1, are added to the simple 3-component circuit. The new circuit is shown in Figure 4.3.

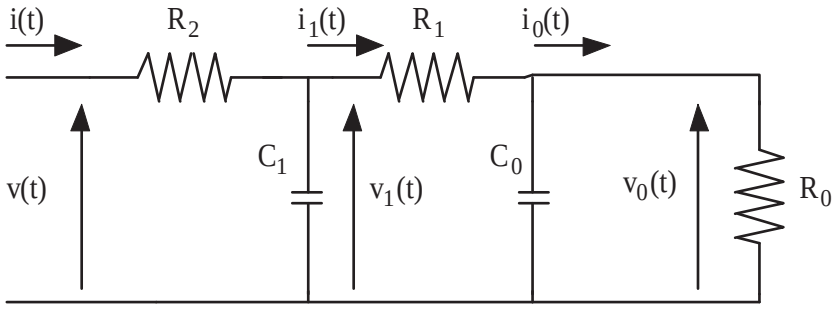

Figure 4.3. 5-component circuit [6].

The transfer function of the 5-component circuit is given as

$$\frac{V(s)}{R_2 I(s)} = 1 + \frac{\dfrac{1}{R_2 C_1}}{s + \dfrac{I_1(s)}{C_1 V_1(s)}} \tag{4.51}$$

$I_1(s)/V_1(s)$ is the inverse of the transfer function of the three component circuit. Inserting (4.50) into (4.51) yields

$$\frac{V(s)}{R_2 I(s)} = 1 + \frac{\omega_3}{s + \dfrac{\omega_2}{1 + \dfrac{\omega_1}{s + \omega_0}}} \tag{4.52}$$

where the frequencies are defined as

$$\omega_0 \equiv \frac{1}{R_0 C_0} \quad \omega_1 \equiv \frac{1}{R_1 C_0} \quad \omega_2 \equiv \frac{1}{R_1 C_1} \quad \omega_3 \equiv \frac{1}{R_2 C_1} \tag{4.53}$$

The transfer function (4.52) can also be represented in the notation of continued fractions [6]

$$\frac{V(s)}{R_2 I(s)} = 1 + \frac{\omega_3}{s+}\,\frac{\omega_2}{1+}\,\frac{\omega_1}{s+}\,\frac{\omega_0}{1} \tag{4.54}$$

The transfer function (4.54) can be generalized to cover $(2n-1)$-component circuit shown in Figure 4.4. The transfer function of the $(2n-1)$-component circuit can be expressed as

$$\frac{E(s)}{R_n I(s)} = 1 + \frac{\omega_{2n-1}}{s+}\,\frac{\omega_{2n-2}}{1+} \cdots \frac{\omega_2}{1+}\,\frac{\omega_1}{s+}\,\frac{\omega_0}{1} \tag{4.55}$$

where the frequencies are

$$\omega_{2k} = \frac{1}{R_k C_k} \qquad \omega_{2k+1} = \frac{1}{R_{k+1} C_k} \tag{4.56}$$

Circuit design seen in Figure 4.4 is also known as an arithmetic ladder network [6].

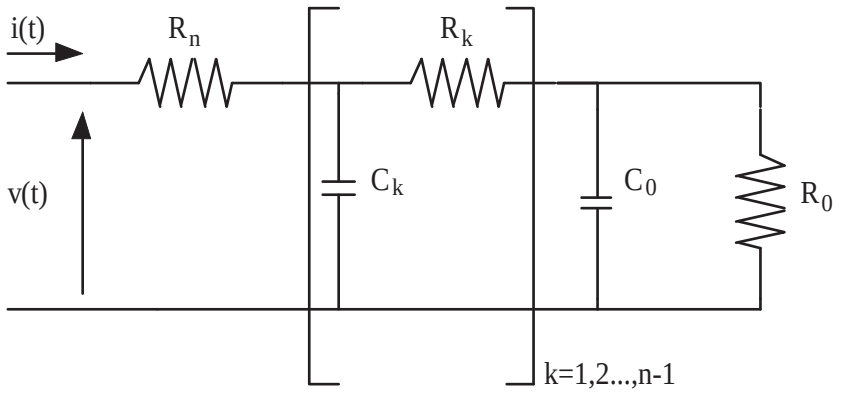

Figure 4.4. A semi-integrating circuit [6].

ω_j can be nondimensionalized through division by s [6]

$$\frac{\omega_j}{s} \equiv \upsilon_j \tag{4.57}$$

Then (4.55) can simplified as

$$\frac{V(s)}{R_n I(s)} = 1 + \frac{\upsilon_{2n-1}}{1+}\,\frac{\upsilon_{2n-2}}{1+}\cdots\frac{\upsilon_2}{1+}\,\frac{\upsilon_1}{1+}\,\frac{\upsilon_0}{1} \tag{4.58}$$

The transfer function (4.58) can take more convenient forms for certain values of R and C. For examples if all capacitors have a common capacitance value and all resistors except the last one have a common resistance value [6]

$$\begin{aligned} &C_0 = C_1 = \ldots = C_{n-1} = C \\ &R_0 = R_1 = \ldots = R_{n-1} = R, \qquad R_n = \frac{1}{2}R \end{aligned} \tag{4.59}$$

Redefining υ [6] for this case

$$\upsilon_0 = \upsilon_1 = \ldots = \upsilon_{2n-3} = \upsilon_{2n-2} = \frac{1}{RCs} \equiv \upsilon, \quad \upsilon_{2n-1} = \frac{2}{RCs} \equiv 2\upsilon \tag{4.60}$$

Using (4.60) the transfer function (4.58) can be written as

$$\frac{2V(s)}{RI(s)} = 1 + 2\frac{\upsilon}{1+}\,\frac{\upsilon}{1+}\cdots\frac{\upsilon}{1+}\,\frac{\upsilon}{1} \tag{4.61}$$

According to Oldham [6], it can be established inductively that the continued fraction (4.61) of $2n$ numeratorial υ's is equal to

$$\frac{\upsilon}{1+}\,\frac{\upsilon}{1+}\cdots\frac{\upsilon}{1+}\,\frac{\upsilon}{1}=\frac{\sqrt{4\upsilon+1}}{1+\left[\dfrac{\sqrt{4\upsilon+1}-1}{\sqrt{4\upsilon+1}+1}\right]^{2n+1}}-\frac{\sqrt{4\upsilon+1}}{2}-\frac{1}{2} \tag{4.62}$$

Combining (4.61) and (4.62) and then through division by $2\sqrt{\upsilon}$ the following [6] can be obtained

$$\frac{V(s)}{I(s)}\sqrt{\frac{Cs}{R}}=\underbrace{\sqrt{\frac{4\upsilon+1}{4\upsilon}}\left[\frac{[\sqrt{4\upsilon+1}+1]^{2n+1}-[\sqrt{4\upsilon+1}-1]^{2n+1}}{[\sqrt{4\upsilon+1}+1]^{2n+1}+[\sqrt{4\upsilon+1}-1]^{2n+1}}\right]}_{f(\upsilon)} \tag{4.63}$$

A plot of the right-hand side of equation, $f(\upsilon)$, versus logarithmicly scaled υ for various values of n is shown in Figure 4.5. It can be observed that as n grows larger the function takes values closer to unity over a wide range of υ values. The function lies within 2% of unity for n values larger than 10 [6].

$$\frac{V(s)}{I(s)}\sqrt{\frac{Cs}{R}}\approx 1,\qquad \text{for } 6\le\upsilon\le\frac{1}{6}n^2 \tag{4.64}$$

Using the definition of υ (4.57) the transfer function of the semi-integrating circuit is expressed as

$$\frac{V(s)}{I(s)}\approx\sqrt{\frac{R}{C}}\frac{1}{s^{0.5}},\qquad \text{for } 6RC\le\frac{1}{s}\le\frac{1}{6}n^2RC \tag{4.65}$$

Time domain expression of (4.65) can be obtained by applying inverse Laplace transform rigorously

$$v(t)\approx\sqrt{\frac{R}{C}}\frac{\mathrm{d}^{-0.5}i}{\mathrm{d}t^{-0.5}}(t),\qquad \text{for } 6RC\le t\le\frac{1}{6}n^2RC \tag{4.66}$$

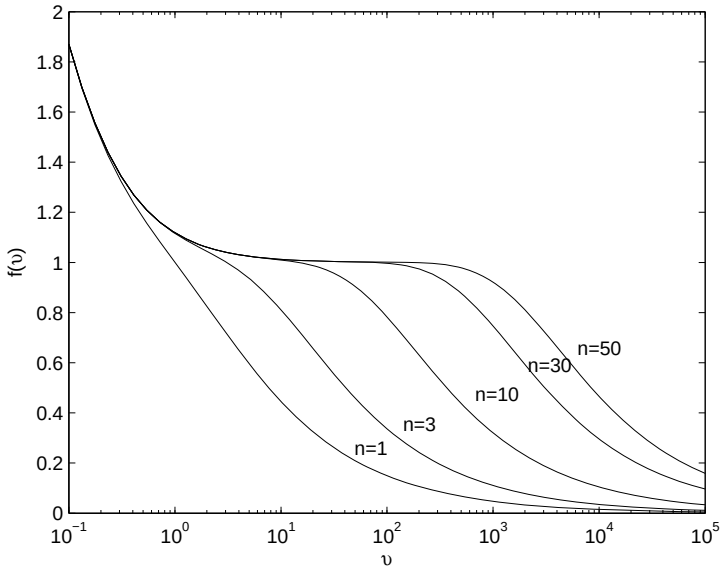

Figure 4.5. A semi-logarithmic plot of $f(\upsilon)$ for various values of n.

Simulation is carried out with two different n values, $n_1 = 30$ and $n_2 = 50$ in order to verify (4.66). The values of the resistor and capacitor in both designs are selected equal

$$\left.\begin{array}{l} C_0 = C_1 = \ldots = C_{n-1} = 0.1\text{F} \\ R_0 = R_1 = \ldots = R_{n-1} = 0.1\Omega, R_n = 0.05\Omega \end{array}\right\} \frac{V(s)}{I(s)} \approx \sqrt{\frac{0.1}{0.1}} \frac{1}{s^{0.5}} \approx \frac{1}{s^{0.5}} \qquad (4.67)$$

The frequency response of the two designs is shown in Figure 4.6. As it is observed from the frequency response, the slope in the magnitude plot is -10 dB/decade which can also be expressed as -0.5×20 dB/decade. On the other hand, phase plot shows that the phase between the specified frequency interval, $[1, 10]$, is approximately half of 90 degrees, -0.5×90 degrees.

The simulation results are in agreement with the analytical analysis. If the transfer function of an ideal fractional order integrator is given as

$$I_\alpha(s) = \frac{1}{s^\alpha} \qquad (4.68)$$

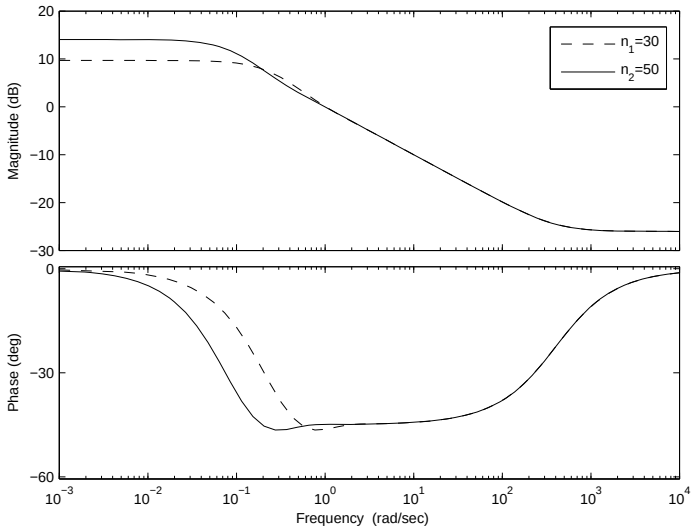

Figure 4.6. Frequency response of semi-integrators for $n_1 = 30$ and $n_2 = 50$.

then magnitude and phase can be computed analytically [25, 26] from

$$I_\alpha(j\omega) = \frac{1}{(j\omega)^\alpha} \Rightarrow |I_\alpha(j\omega)| = \left|\frac{1}{(j\omega)^\alpha}\right| = \frac{1}{\omega^\alpha}, \quad \angle I_\alpha(j\omega) = \alpha \times \frac{\pi}{2} \tag{4.69}$$

In the case of semi-integrators, $\alpha = 0.5$, the magnitude and phase are found as

$$|I_{0.5}(j\omega)| = \frac{1}{\sqrt{\omega}}, \qquad \angle I_{0.5}(j\omega) = \frac{\pi}{4} \tag{4.70}$$

The poles and zeros of the semi-integrator circuit for $n_1 = 30$ is shown in Figure 4.7. All of these poles and zeros are all real and lie in the left half plane. The transfer function of the semi-integrating circuit can be seen as the nth approximant, truncated after nth level, of a real J-fraction and so all poles of this fraction are real, simple and have positive residues. Furthermore they all lie in the negative half of the real axis because the denominators of all the kth approximants are polynomials in s with positive coefficients [27].

In order to verify time domain expression (4.66) of a semi-integrating circuit, step input is applied to both designs, $n_1 = 30$ and $n_2 = 50$. Simulation results are compared to the step response obtained analytically. Analytical computation of step response of

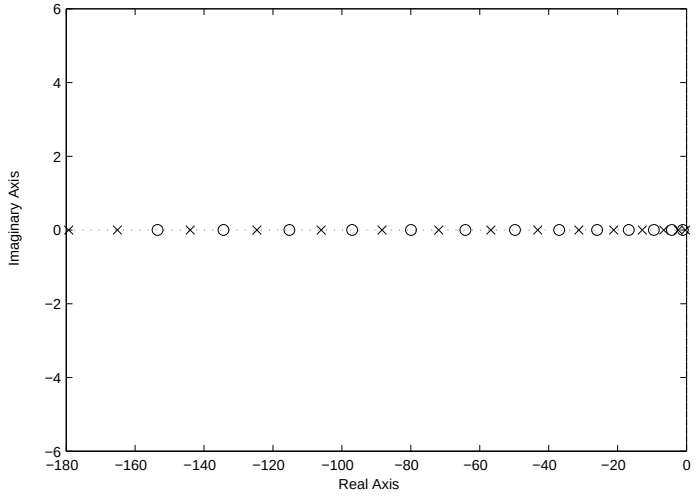

Figure 4.7. Pole-zero map of the transfer function of the semi-integrating circuit of $n_1 = 30$.

a fractional integrator is found by using the inverse Laplace transform

$$\mathscr{L}^{-1}\left\{\frac{1}{s^{\alpha}}\right\} = \frac{t^{\alpha}}{\Gamma(\alpha)}, \quad \alpha > 0 \tag{4.71}$$

By using (4.71), step response can be calculated analytically from

$$y(t) = \mathscr{L}^{-1}\left\{\frac{1}{s}\frac{1}{s^{\alpha}}\right\} = \mathscr{L}^{-1}\frac{1}{s^{1+\alpha}} = \frac{t^{\alpha}}{\Gamma(1+\alpha)}, \quad \text{for } \alpha = 0.5 \Rightarrow y(t) = \frac{t^{0.5}}{\Gamma(1.5)} \tag{4.72}$$

Step responses are given in Figure 4.8. According to (4.66) the both circuit designs can approximate a true semi-integrator only for a limited time interval. The intervals can be calculated as

$$6RC \leq t \leq \frac{1}{6}n^2RC \begin{cases} 0.06 \leq t \leq 1.53, & \text{for } n_1 = 30 \\ 0.06 \leq t \leq 4.17, & \text{for } n_2 = 50 \end{cases} \tag{4.73}$$

As it is observed from Figure 4.8, simulation results are in agreement with (4.73).

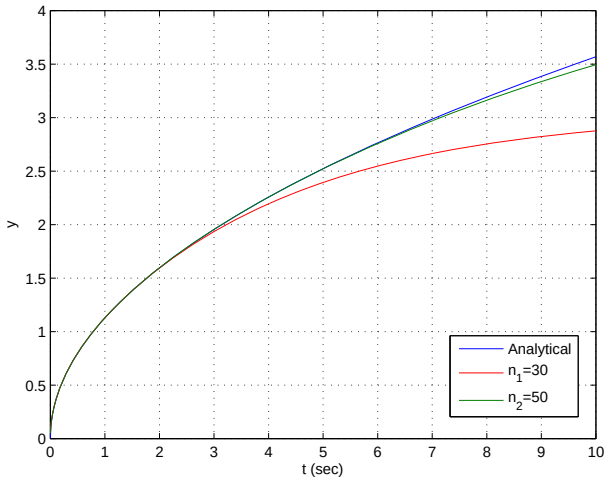

Figure 4.8. Step responses of semi-integrating circuits with $n_1 = 30$ and $n_2 = 50$.

4.2.2. Viscoelastic System of Bagley-Torvik

Viscoelastic system of Bagley-Torvik describes the motion of a large thin plate submerged in a Newtonian fluid. Mathematical model of this system is a fractional order differential equation which is originally formulated by R. L. Bagley and P. J. Torvik [9].

First the motion of a half-space Newtonian viscous fluid induced by a prescribed transverse motion of a rigid plate on the surface is considered. The equation of motion of the fluid is

$$\rho \frac{\partial v}{\partial t} = \mu \frac{\partial^2 v}{\partial z^2}, \qquad 0 < t < \infty, \ -\infty < z < 0 \tag{4.74}$$

where ρ is fluid density, μ is viscosity and $v(t, z)$ is transverse velocity, which is a function of time t and the distance z from fluid plate contact boundary (Figure 4.9).

It is assumed that the initial value of the velocity is zero, $v(0, z) = 0$, and as z goes to minus infinity the influence of the plate's motion vanishes, $v(t, -\infty) = 0$. The fluid's velocity at $z = 0$ is equal to the given velocity of the plate, $v(t, 0) = v_p(t)$.

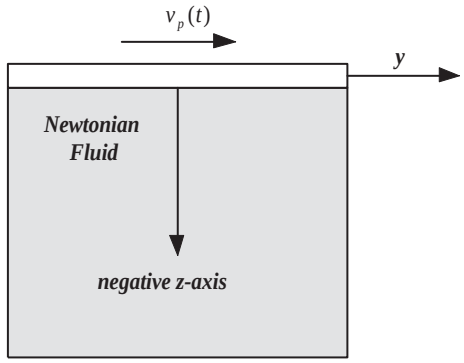

Figure 4.9. A rigid plate in a Newtonian fluid.

The following boundary-value problem is obtained by applying the Laplace transform (4.74).

$$\rho s V(s,z) = \mu \frac{\mathrm{d}^2 V(s,z)}{\mathrm{d}z^2}, \qquad V(s,0) = V_p(s),\ V(s,-\infty) = 0 \tag{4.75}$$

The solution of (4.75) is given as

$$V(s,z) = V_p(s) e^{z\sqrt{\frac{\rho s}{\mu}}} \tag{4.76}$$

Differentiating (4.76) with respect to z yields

$$\frac{\mathrm{d}V(s,z)}{\mathrm{d}z} = \sqrt{\frac{\rho s}{\mu}} V(s,z) \tag{4.77}$$

The stress $\sigma(t,z)$ can be expressed as

$$\sigma(t,z) = \mu \frac{\partial v(t,z)}{\partial z} \tag{4.78}$$

If the Laplace transform is applied to (4.78), the following equation in Laplace domain is obtained

$$\overline{\sigma}(s,z) = \mu \frac{\mathrm{d}V(s,z)}{\mathrm{d}z} = \sqrt{\mu \rho s}\ V(s,z) \tag{4.79}$$

where $\overline{\sigma}(s,z)$ denotes the Laplace transform of $\sigma(t,z)$. The equation (4.79) can be rewritten in the time domain as

$$\sigma(t,z) = \sqrt{\mu\rho}\ {}_0\mathscr{D}_t^{0.5} v(t,z) \tag{4.80}$$

(4.80) indicates that the stress at a given point at any time depends on the time history of the velocity at that point.

Now the actual viscoelastic system can be considered. As it is seen from Figure 4.10, there is a thin rigid plate of mass M which is immersed in a Newtonian fluid of infinite extent by an area of S and is connected by a massless spring of stiffness K to a fixed point.

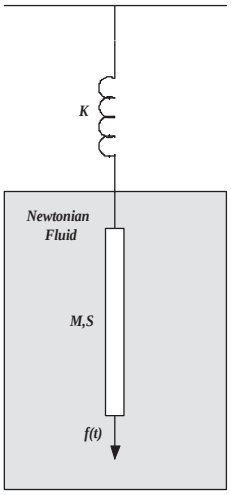

Figure 4.10. An immersed plate in a Newtonian fluid.

It is assumed that the spring does not disturb the fluid and the area of the plate is sufficiently large to produce the velocity field and stresses related to (4.80) in the fluid adjacent to the plate. When a forcing function $f(t)$ is applied to the plate, the displacement y of the plate is given as

$$My''(t) = f(t) - Ky(t) - 2S\sigma(t,0) \tag{4.81}$$

Substituting the stress given by (4.80) into (4.81) and using $v_p(t,0) = y'(t)$ gives the

following fractional order differential equation of Bagley-Torvik

$$\begin{aligned} & a_2 y^{''}(t) + a_1 \ {}_0\mathscr{D}_t^{1.5} y(t) + a_0 y(t) = f(t), \qquad t > 0 \\ & a_2 = M, \ a_1 = 2S\sqrt{\mu\rho}, \ a_0 = K, \ y(0) = 0, \ y^{'}(0) = 0 \end{aligned} \tag{4.82}$$

4.3. Comparison of Fractional Order Identification Methods

A semi-integrating circuit of $n = 90$ components is designed with the resistance and capacitance values equal to $R = 0.1\Omega$ and $C = 0.1F$ respectively. Then the arithmetic ladder network is placed in a negative feedback loop which yields the following system transfer function

$$G_0(s) = \frac{1}{\dfrac{1}{G_{\text{ladder}}(s)} + 1} \tag{4.83}$$

Three different input signals including a step, a periodic sum of sinusoids and a PRBS are applied to (4.83). Simulation step size is chosen to be 0.01 seconds. The periodic sum of sinusoids signal is generated for five frequencies that are selected in respect with the bandwidth of the system (4.83) which is calculated to be $\omega_B = 0.4802$.

$$\begin{aligned} & u(t) = \sum_{k=1}^{5} a_k \cos(\omega_k t + \phi_k), \\ & 0 \leq \omega_1 = 0.0126 \leq \omega_2 = 0.0880 \leq \omega_3 = 0.1508 \\ & \leq \omega_4 = 0.2262 \leq \omega_5 = 0.3016 \leq \omega_B = 0.4802 \end{aligned} \tag{4.84}$$

The sum of sinusoids signal and the PRBS are shown in Figure 4.11.

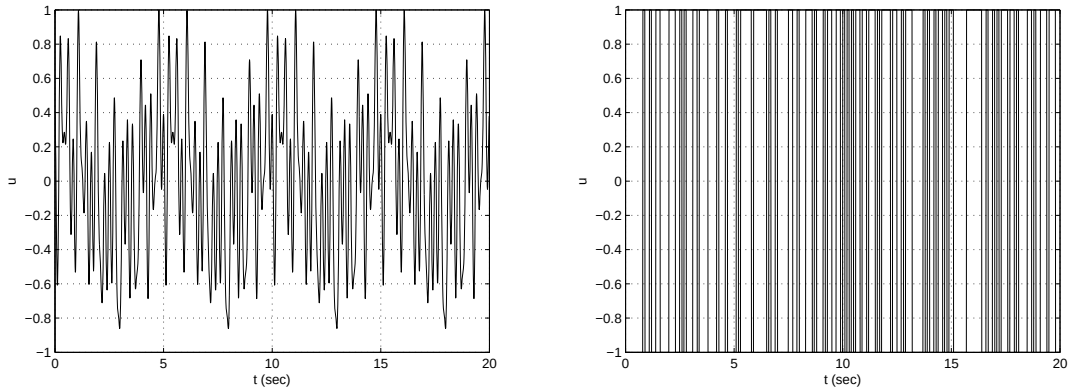

(a) Sum of Sinusoids (b) PRBS

Figure 4.11. Input Signals

Step response (Figure 4.12(a)) and sum of sinusoids response (Figure 4.12(b)) of the system are used in the estimation procedure while the PRBS response of the system is reserved for cross validation of the estimated models.

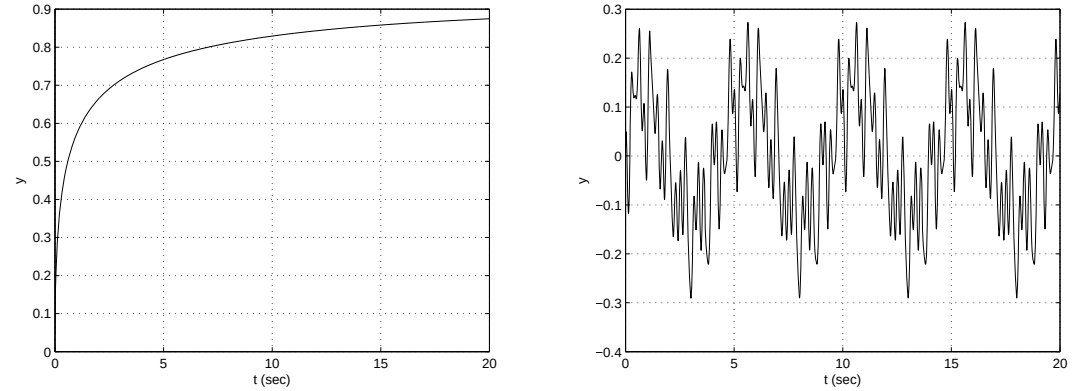

(a) Step Response (b) Sum of Sinusoids Response

Figure 4.12. Output Signals

The system (4.83) is to be identified with both a fractional order model and an integer first order process model

$$\hat{G}_{\mathrm{f}}(s) = \frac{b_0}{a_1 s^{0.5} + 1}, \qquad \hat{\theta}_{\mathrm{f}} = \begin{bmatrix} a_1 \\ b_0 \end{bmatrix}, \quad \hat{G}_{\mathrm{i}}(s) = \frac{b_0}{a_1 s + 1}, \qquad \hat{\theta}_{\mathrm{i}} = \begin{bmatrix} a_1 \\ b_0 \end{bmatrix} \tag{4.85}$$

Parameter estimations using linear regression methods of integer order and fractional order system identification are given for all input signals in Table 4.1.

Table 4.1. Parameter estimations using linear regression.

θ	Step Signal		Sum of Sinusoids		PRBS	
	$\hat{\theta}_{\mathrm{f1}}$	$\hat{\theta}_{\mathrm{i1}}$	$\hat{\theta}_{\mathrm{f2}}$	$\hat{\theta}_{\mathrm{i2}}$	$\hat{\theta}_{\mathrm{f3}}$	$\hat{\theta}_{\mathrm{i3}}$
a_1	0.9892	2.5269	1.0372	0.0839	0.3905	0.0914
b_0	0.9968	0.8512	1.0279	0.3928	0.4841	0.3917

The estimated fractional and integer order models for step and sum of sinusoids responses are compared to the measured system output for the PRBS input. While the fractional order models from step and sum of sinusoids responses fit the measured system output by 91.02 per cent and 91.42 per cent (Figure 4.13(a)), the fits for the integer order models are calculated to be 16.44 per cent and 64.09 per cent (Figure 4.13(b)).

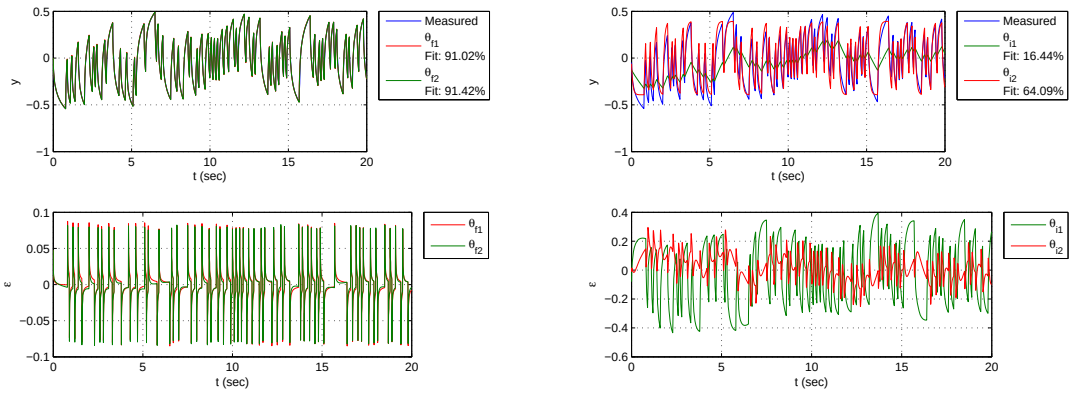

(a) Model outputs and prediction errors for fractional order models

(b) Model outputs and prediction errors for integer order models

Figure 4.13. Cross Validation with PRBS

The models constrcuted from the estimations with the PRBS input are compared to the measured step response of the system (see Figure 4.14). Although the models built from the PRBS response is expected to perform much better due to the high excitation order of a PRBS input, the fractional and integer order models estimated from the PRBS give very poor fits in cross validation with the step response (Figure 4.14).

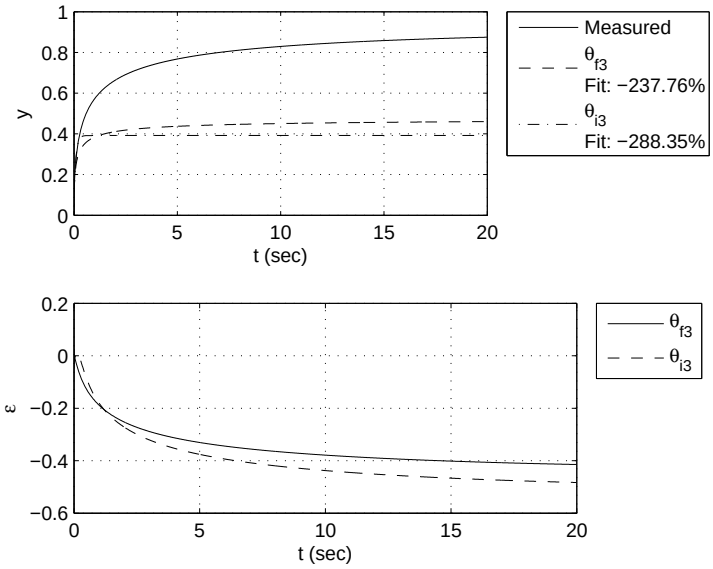

Figure 4.14. Cross Validation with Step Signal.

Grünwald-Letnikov definition (see Section 2.1.2.2) allows the parametrization of the model order. If the proposed fractional order model is rewritten in commensurate order form

$$\hat{G}_{\mathrm{f}}(s) = \frac{b_0}{a_1 s^{\alpha} + 1} = \frac{b_0}{a_1 s^{kq} + 1}, \qquad k = 1, \qquad \theta = \begin{bmatrix} q \\ a_1 \\ b_0 \end{bmatrix} \tag{4.86}$$

then iterative search method (see Section 4.1.1.2) can be applied to estimate the commensurate order of the model. The results of the estimations can be seen in Table 4.2.

Table 4.2. Iterative search of the parameters.

θ	$\hat{\theta}_{\mathrm{f4}}$(Step)	$\hat{\theta}_{\mathrm{f5}}$(Sum of Sinusoids)	$\hat{\theta}_{\mathrm{f6}}$(PRBS)
q	0.4974	0.5123	0.5696
a_1	0.9932	0.9391	0.7480
b_0	0.9999	0.9690	0.8757
$V(\theta)$	0.0032	0.0025	0.5212

The cross validation of the model estimated from step response data is given in Figure 4.15. The fit of the model is computed to be 90.78 per cent.

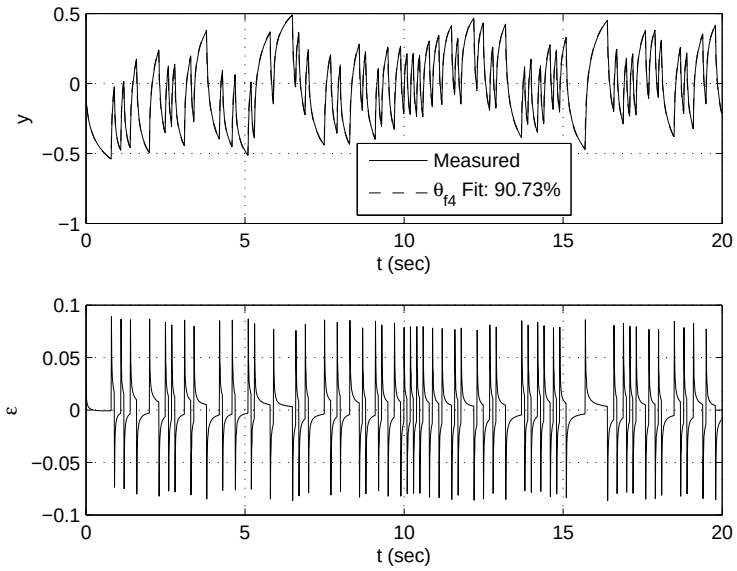

Figure 4.15. Cross validation of the model estimated by iterative search method.

Information about each iteration of the Levenberg-Marquardt algorithm including the number of function evaluations, norm of the residual vector, first order optimality measure, Levenberg-Marquardt parameter, ζ, and the norm of current step are given in Table 4.3. The values of the parameters for each iteration are plotted in Figure 4.16.

The parametric identification method of Levy (Section 4.1.2.1) requires the estimation of the frequency response of the system. Hence, first objective is to estimate the frequency response of the system by using a nonparametric frequency estimation method (see Section 3.2.2). Frequency response estimates calculated by ETFE and the true frequency response of the system are given in Figure 4.17.

As it can be seen from Figure 4.17, the frequency response estimates based on step and PRBS responses are not successful. This is due to the input signals being non-periodic. Nonparametric identification methods are very sensitive to the type of the input signal. ETFE gives crude estimations for non-periodic input signals. Levy's method cannot be applied using the step or PRBS input because of the large error between the true and estimated frequency responses.

Table 4.3. Iterative search of the parameters.

Iteration	Function Count	Residual	First Order Optimality	ζ	Norm of Step
0	4	979.726	1.27×10^3	10^{-2}	-
1	9	864.653	5.98×10^2	10^{-1}	1.67401
2	13	777.193	1.18×10^3	10^{-2}	2.24126
3	17	4.75377	4.61×10^1	10^{-3}	0.926439
4	21	0.248018	2.04×10^0	10^{-4}	0.50966
5	25	0.179024	1.45×10^1	10^{-5}	0.165549
6	29	0.00322674	7.84×10^{-2}	10^{-6}	0.0410263
7	33	0.0032205	1.6×10^{-4}	10^{-7}	0.000484942
8	37	0.0032205	1.86×10^{-7}	10^{-8}	1.6086×10^{-6}

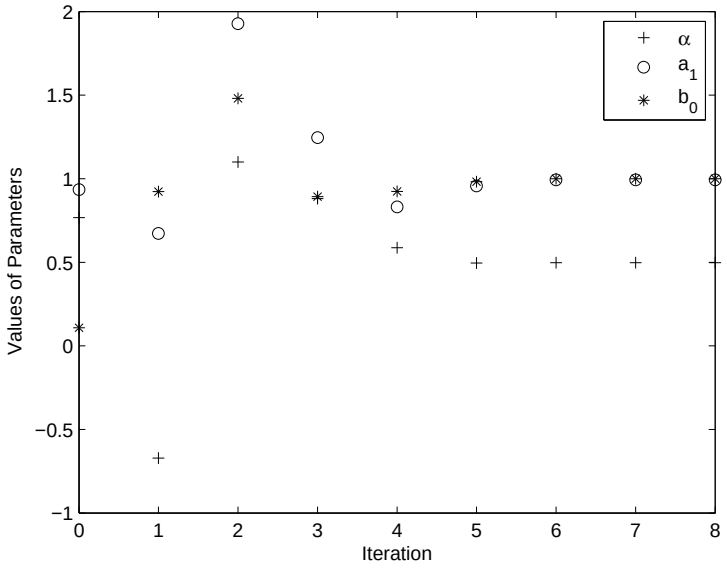

Figure 4.16. Parameter values of the iterative search for the step input

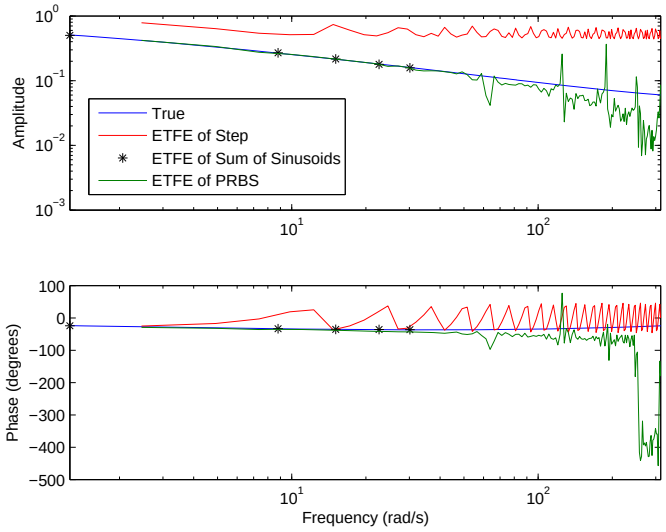

Figure 4.17. Frequency Response Estimation by ETFE

On the other hand, the frequency estimate based on the sum of sinusoids input signal is very successful and suitable for Levy's method since this input signal is a periodic signal. Applying Levy's identification method with and without Vinagre's weights yields the parameters given in Table 4.4.

Table 4.4. Frequency domain estimation of the parameters.

θ	Sum of Sinusoids	
	Levy	Vinagre
a_1	0.9290	1.0075
b_0	0.9391	0.9889

The fit of Levy's method with and without Vinagre's weights can be observed in frequency domain from Figure 4.18. The usage of Vinagre's weights do not improve the fit.

The PRBS input is applied to the estimated model (Table (4.4)) and the model output is compared with the measured system output (Figure 4.19). Although the usage of Vinagre's weights do not provide a much better fit in the frequency domain (Figure 4.18), the model acquired from estimation with the Vinagre's weights gives a slightly better fit in the time domain.

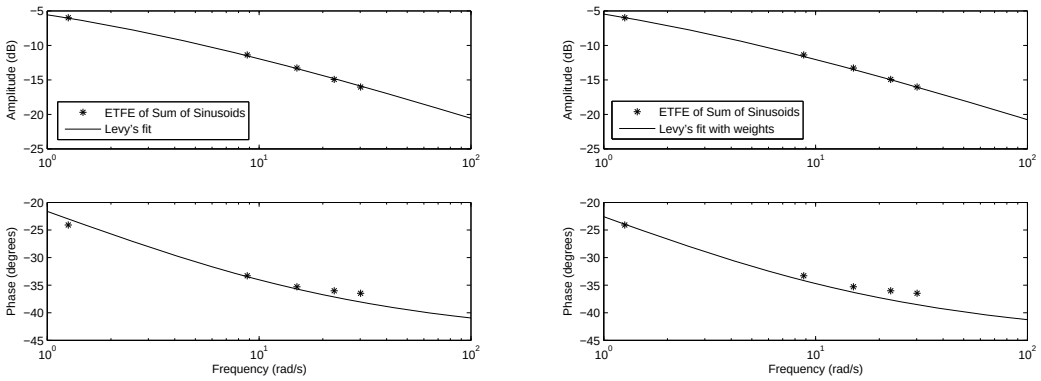

(a) Levy without weights (b) Levy with Vinagre's weights

Figure 4.18. Levy's fit in frequency domain with and without weights.

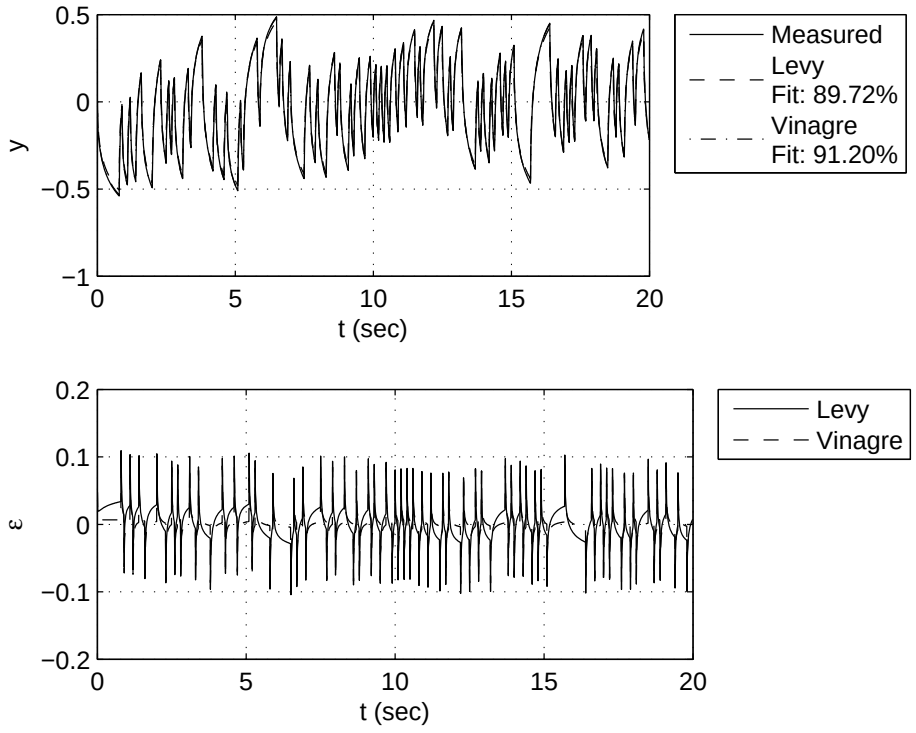

Figure 4.19. Cross validation for frequency domain estimation.

For a second experiment the arithmetic ladder circuit designed for $n = 90$, $R_l = 0.1\Omega$ and $C_l = 0.1F$ is extended with a series connection of a resistor and an inductance element (Figure 4.20).

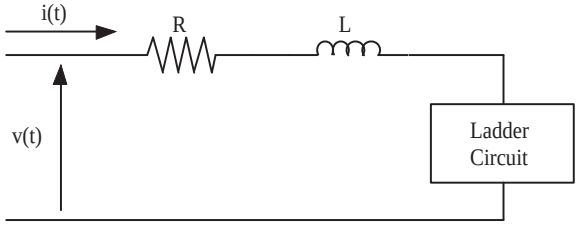

Figure 4.20. Ladder circuit extended with a series connection of a resistor and an inductance.

The equation that governs this circuit can be written as

$$v(t) \approx Ri(t) + L\frac{\mathrm{d}i}{\mathrm{d}t}(t) + \sqrt{\frac{R_l}{C_l}}\frac{\mathrm{d}^{-0.5}i}{\mathrm{d}t^{-0.5}}(t), \qquad \text{for } 6R_lC_l \leq t \leq \frac{1}{6}n^2R_lC_l \tag{4.87}$$

Choosing $R = 1\Omega$ and $L = 1H$ with $n = 90$, $R_l = 0.1\Omega$ and $C_l = 0.1F$ for the ladder circuit, the output current and input voltage relationship can be expressed in Laplace domain under zero initial conditions as

$$G(s) = \frac{I(s)}{V(s)} = \frac{s^{0.5}}{s^{1.5} + s^{0.5} + 1}, \qquad \text{for } 6R_lC_l \leq \frac{1}{s} \leq \frac{1}{6}n^2R_lC_l \tag{4.88}$$

Simulation is carried out with three different inputs: step, sum of sinusoids and PRBS. While the data collected from experiments with step and sum of sinusoids inputs are used for estimation, the data collected from the experiment with the PRBS are solely reserved for validation. The sum of sinusoids signal is composed of three sinusoids for the following frequencies

$$\begin{aligned} u(t) &= \sum_{k=1}^{3} a_k \cos(\omega_k t + \phi_k), \\ 0 \leq \omega_1 &= 0.063 \leq \omega_2 = 0.0126 \leq \omega_3 = 0.0251 \end{aligned} \tag{4.89}$$

The sum of sinusoids and the PRBS input signals are shown in Figure 4.21(a) and Figure 4.21(b) respectively.

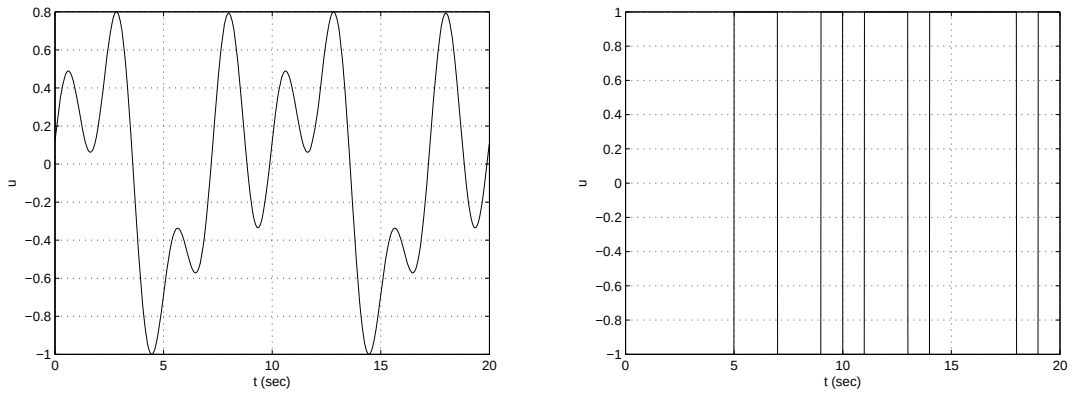

(a) Sum of sinusoids (b) PRBS

Figure 4.21. Input signals

A fractional order and an integer order model are proposed for the system.

$$\hat{G}_{\mathrm{f}}(s) = \frac{b_1 s^{0.5} + b_0}{a_2 s^{1.5} + a_1 s^{0.5} + 1}, \quad \hat{\theta}_{\mathrm{f}} = \begin{bmatrix} b_0 \\ b_1 \\ a_1 \\ a_2 \end{bmatrix}, \hat{G}_{\mathrm{i}}(s) = \frac{b_1 s + b_0}{a_2 s^2 + a_1 s + 1}, \quad \hat{\theta}_{\mathrm{i}} = \begin{bmatrix} b_0 \\ b_1 \\ a_1 \\ a_2 \end{bmatrix} \tag{4.90}$$

Parameter estimations using linear regression methods of integer order and fractional order system identification are given for all input signals in Table 4.5.

Table 4.5. Parameter estimations using linear regression.

θ	Step Signal		Sum of Sinusoids		PRBS	
	$\hat{\theta}_{\mathrm{f1}}$	$\hat{\theta}_{\mathrm{i1}}$	$\hat{\theta}_{\mathrm{f2}}$	$\hat{\theta}_{\mathrm{i2}}$	$\hat{\theta}_{\mathrm{f3}}$	$\hat{\theta}_{\mathrm{i3}}$
b_0	0.0709	0.1399	0.0358	0.2743	0.3554	0.2081
b_1	0.6223	241.480	0.9168	0.8854	-0.0474	1.2248
a_1	0.3686	3.4647	0.9031	1.5673	-0.0729	2.0894
a_2	0.4508	1.3633	0.9344	0.8034	0.0747	1.0872

The cross validation of the estimated models with the measured PRBS response can be observed from Figure 4.22. The first fractional order model estimated from the step response gives a poor fit of 56.28 per cent while the fractional order model and the integer order model estimated from the sum of sinusoids response fit the measured

output by 95.94 per cent and 92.15 per cent respectively. The simulation of the first integer order model estimated from the experiment with the step input is not shown because the fit of this model is computed to be -1.18×10^4 per cent.

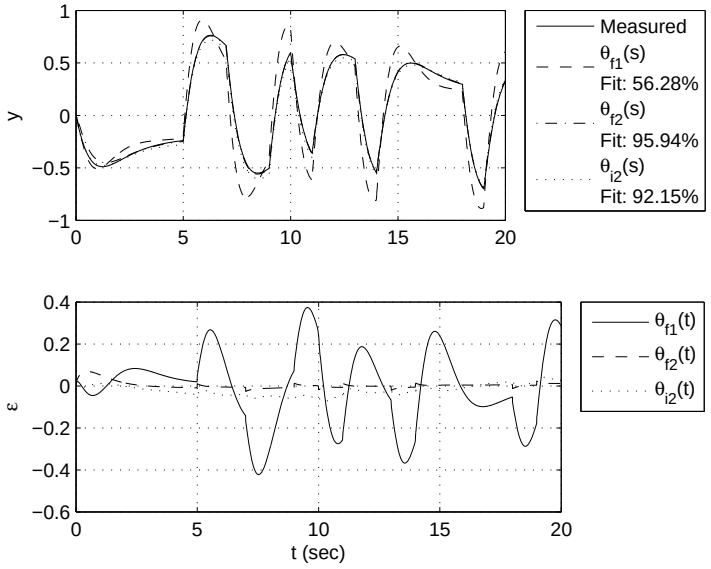

Figure 4.22. Model simulations and prediction errors for cross validation with PRBS response.

The estimated models from the PRBS response are compared to the measured step response of the system (see Figure 4.23). Although the input is a PRBS, the cross validation with the step response results in very poor fits (Figure 4.23).

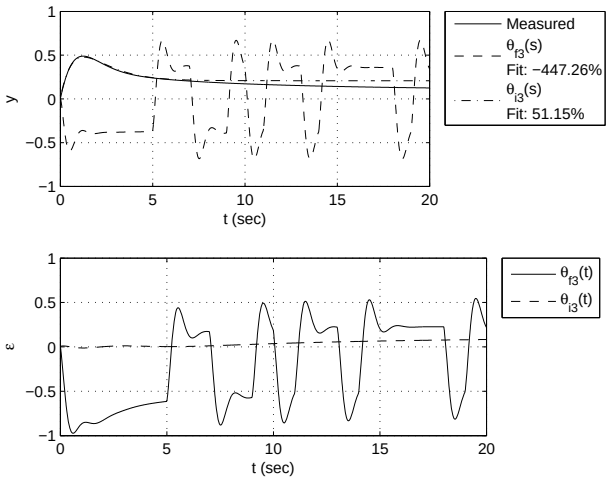

Figure 4.23. Cross Validation with Step Signal.

Iterative search method (see Section 4.1.1.2) can be applied to estimate the commensurate order of the model. The results of the iterative search method are given in Table 4.6.

Table 4.6. Iterative search of the parameters.

θ	$\hat{\theta}_{\text{f4}}$(Step)	$\hat{\theta}_{\text{f5}}$(Sum of Sinusoids)	$\hat{\theta}_{\text{f6}}$(PRBS)
q	0.4373	0.4969	0.4835
a_2	0.7644	0.9402	0.8926
a_1	0.3394	0.8768	0.6613
b_1	0.7963	0.9171	0.8279
b_0	-0.0091	0.0290	0.0389
$V(\theta)$	0.0024	0.0073	0.4851

The cross validation of the models estimated from step response and sum of sinusoids response is given in Figure 4.24. The fit of the model estimated from step response is computed to be 83.29 per cent, while the fit for the model estimated from sum of sinusoids response is found to be 97.19 per cent.

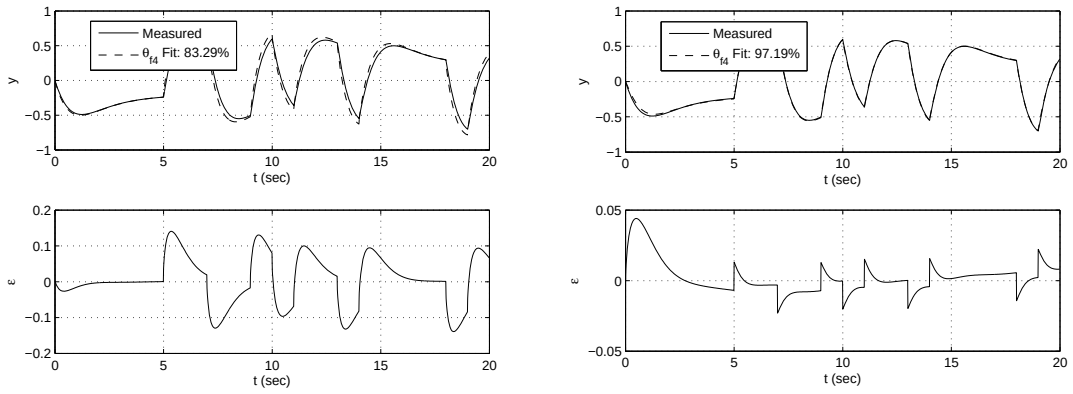

(a) Estimation from step response (b) Estimation from sum of sinusoids response

Figure 4.24. Cross validation of the models by iterative search method

Information about each iteration of the Levenberg-Marquardt algorithm including the number of function evaluations, norm of the residual vector, first order optimality measure, Levenberg-Marquardt parameter and the norm of current step are given in Table 4.7.

Table 4.7. Iterative search of the parameters.

Iteration	Function Count	Residual	First Order Optimality	ζ	Norm of Step
0	6	713.495	1.02×10^3	10^{-2}	-
1	12	0.527478	20	10^{-3}	0.819265
2	18	0.0114178	1.98	10^{-4}	0.236717
3	24	0.002472	0.0562	10^{-5}	0.115255
4	30	0.00243916	0.000311	10^{-6}	0.00594566
5	36	0.00243916	1.44×10^{-5}	10^{-7}	0.000207588
6	42	0.00243916	2×10^{-7}	10^{-8}	3.32872×10^{-7}

The values of the parameters of the estimations from step and sum of sinusoids responses are plotted for each iteration in Figure 4.25.

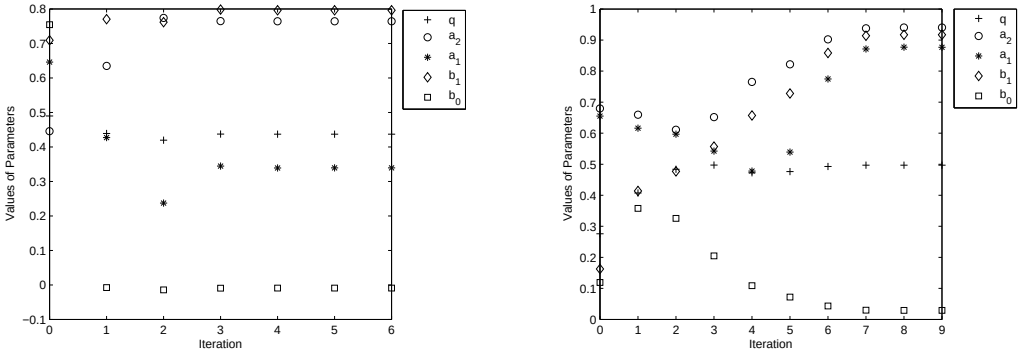

(a) Parameter values of θ_{f4} (b) Parameter values of $\theta_{\mathrm{f_5}}$

Figure 4.25. Parameter values of the iterative search for the step input

The frequency response is estimated by applying ETFE to the data gathered for different input signals. While the frequency estimation from the step and the PRBS responses are not satisfactory, the ETFE applied to the sum of sinusoids response yields successful magnitude and phase estimation at three frequencies (Figure 4.26).

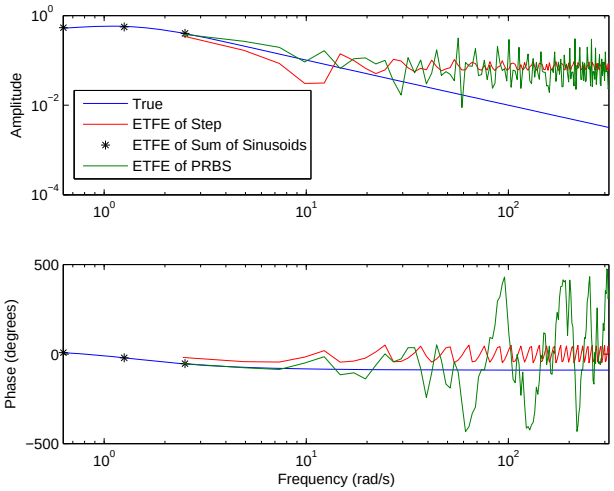

Figure 4.26. Frequency response estimation.

Levy's identification with and without Vinagre's weights yields the following parameters for the commensurate order model

$$G(s) = \frac{b_1 s^{0.5} + b_0}{a_3 s^{3\times 0.5} + a_2 s^{2\times 0.5} + a_1 s^{0.5} + 1}, \qquad \theta = \begin{bmatrix} b_1 & b_0 & a_3 & a_2 & a_1 \end{bmatrix}^T \tag{4.91}$$

Parameter estimations are given in Table 4.8.

Table 4.8. Frequency domain estimation of the parameters.

θ	Estimated Freq.		Exact Freq.
	Levy	Vinagre	Levy
b_1	1.3735	1.9066	1.0001
b_0	-0.1071	-0.2823	-0.0001
a_3	1.3412	1.8820	1.0001
a_2	-0.1551	-0.4323	0.0012
a_1	1.6047	2.4742	1.0001

The fit of Levy's method with and without weights is plotted in Figure 4.27.

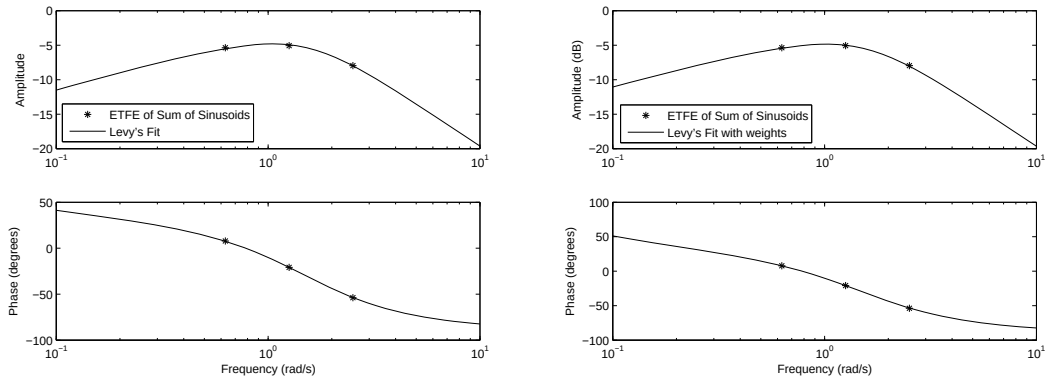

(a) Levy without weights (b) Levy with Vinagre's weights

Figure 4.27. Levy's fit in frequency domain with and without weights.

The simulation results of cross validation with PRBS are given in Figure 4.28.

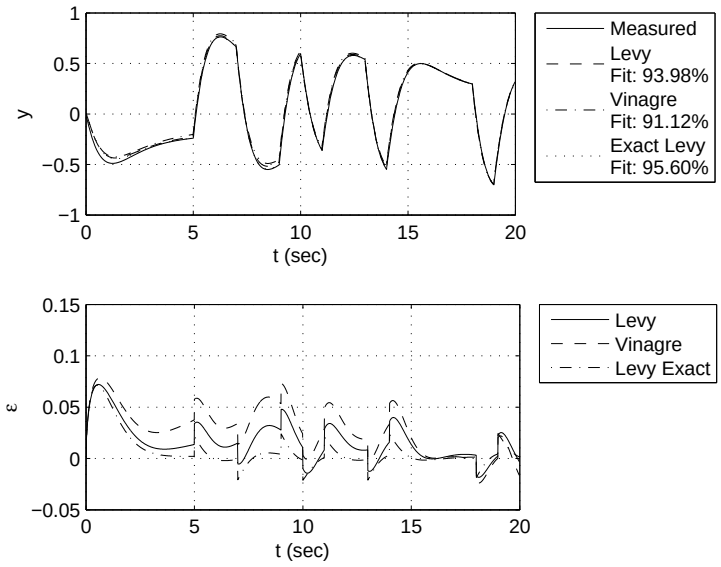

Figure 4.28. Cross validation of the models estimated in frequency domain.

For the third example, the motion of a large thin plate immersed in a Newtonian fluid is taken. The fractional order differential equation governing the system which is originally formulated by R. L. Bagley and P. J. Torvik [9] is also known as the Bagley-Torvik equation. The following initial value problem is considered for the Bagley-Torvik equation

$$y^{(2)}(t) + y^{(3/2)}(t) + y(t) = u(t), \qquad y(0) = y^{(1)}(0) = 0 \tag{4.92}$$

Step and sum of sinusoids input signals are used to create estimation data while the PRBS input signal is used to create the cross validation data. The frequencies of the sum of sinusoids signal are given as

$$u(t) = \sum_{k=1}^{5} a_k \cos(\omega_k t + \phi_k),\ 0 \leq \omega_1 = 0.0314 \leq \omega_2 = 0.0628 \leq \omega_3 = 0.1257 \leq \omega_4 = 0.1885 \leq \omega_5 = 0.2199 \tag{4.93}$$

The sum of sinusoids signal and the RBS signal is shown in Figure 4.29(a) and Figure 4.29(b) respectively.

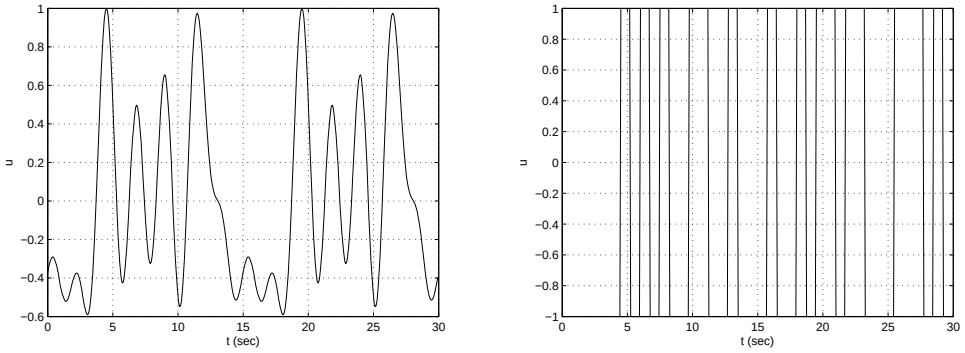

(a) Sum of sinusoids (b) PRBS

Figure 4.29. Input signals used for identification of the Bagley-Torvik system.

The suggested fractional and integer order models of the system are

$$G_{\mathrm{f}}(s) = \frac{b_0}{a_2 s^2 + a_1 s^{1.5} + 1}, \theta_{\mathrm{f}} = \begin{bmatrix} b_0 \\ a_1 \\ a_2 \end{bmatrix},\ G_{\mathrm{i}}(s) = \frac{b_0}{a_2 s^2 + a_1 s + 1}, \theta_{\mathrm{i}} = \begin{bmatrix} b_0 \\ a_1 \\ a_2 \end{bmatrix} \tag{4.94}$$

Estimated values of the parameters are shown in Table 4.9.

Table 4.9. Parameter estimations using linear regression.

θ	Step Signal		Sum of Sinusoids		PRBS	
	$\hat{\theta}_{\mathrm{f1}}$	$\hat{\theta}_{\mathrm{i1}}$	$\hat{\theta}_{\mathrm{f2}}$	$\hat{\theta}_{\mathrm{i2}}$	$\hat{\theta}_{\mathrm{f3}}$	$\hat{\theta}_{\mathrm{i3}}$
b_0	0.9950	1.0089	0.9933	1.064	0.9851	1.0588
a_1	0.9981	0.7228	0.9947	0.7427	0.9898	0.7020
a_2	1.0013	2.0543	0.9975	1.7255	0.9890	1.7358

Estimated models are compared to the measured output of the system for the PRBS input. The cross validation of fractional order models and integer order models are shown in Figure 4.30(a) and Figure 4.30(b) respectively. It is seen from Figure 4.30 that the estimated fractional order models fits the measured PRBS response better than their integer order counterparts.

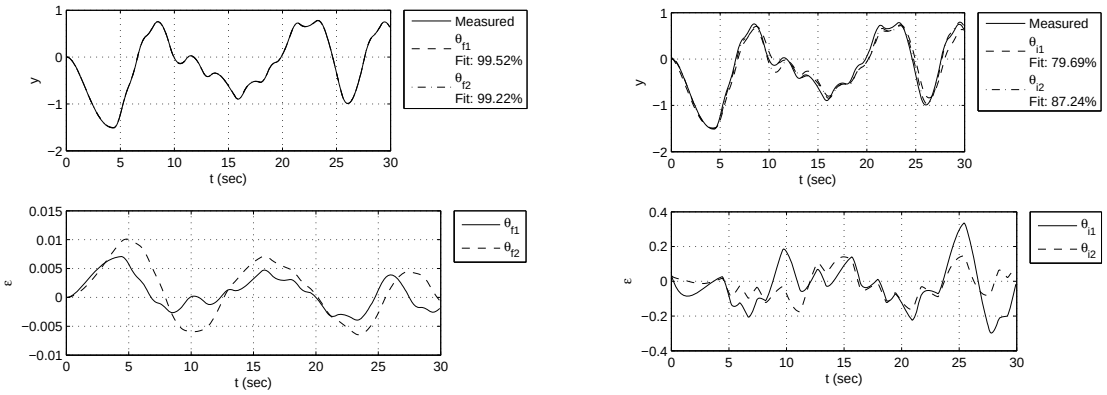

(a) Fractional Order Models

(b) Integer Order Models

Figure 4.30. Cross validation of fractional order and integer order models.

The model estimated from the PRBS response is simulated using the step input and the model output is compared to the measured output (Figure 4.31).

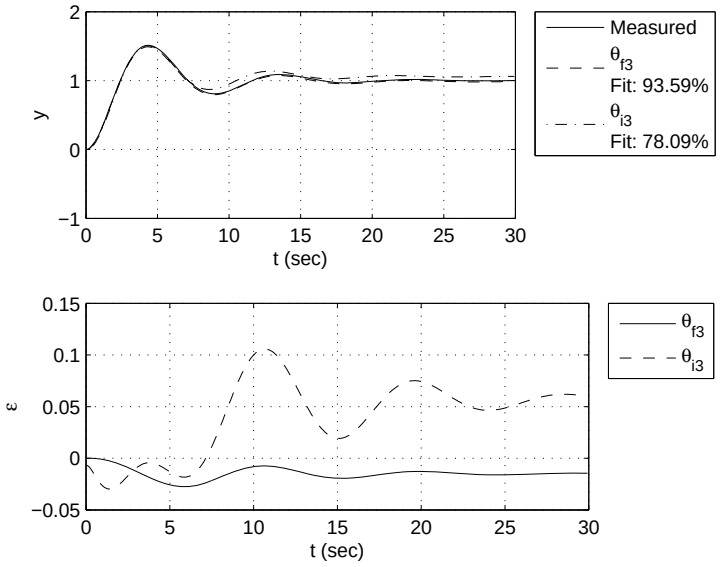

Figure 4.31. Cross validation with step input.

Iterative search method (see Section 4.1.1.2) can be applied to estimate the commensurate order of the model. As it is seen in Table 4.10, the fractional order is successfully estimated.

Table 4.10. Iterative search of the parameters.

θ	$\hat{\theta}_{\mathrm{f4}}$(Step)	$\hat{\theta}_{\mathrm{f5}}$(Sum of Sinusoids)	$\hat{\theta}_{\mathrm{f6}}$(PRBS)
q	0.5000	0.5000	0.6111
a_4	1.0000	1.0000	0.0790
a_3	1.0000	1.0000	1.5369
a_2	0.0000	0.0000	0.4118
a_1	0.0000	0.0000	-0.0349
b_0	1.0000	1.0000	0.9974
$V(\theta)$	7.9496×10^{-21}	1.5230×10^{-19}	4.2896×10^{-5}
Iteration Number	11	38	14

The cross validation of the models estimated from step response and sum of sinusoids response is given in Figure 4.32. The fit of the model estimated from step response is computed to be 98.0421 per cent, while the fit for the model estimated from sum of sinusoids response is found to be 98.04 per cent.

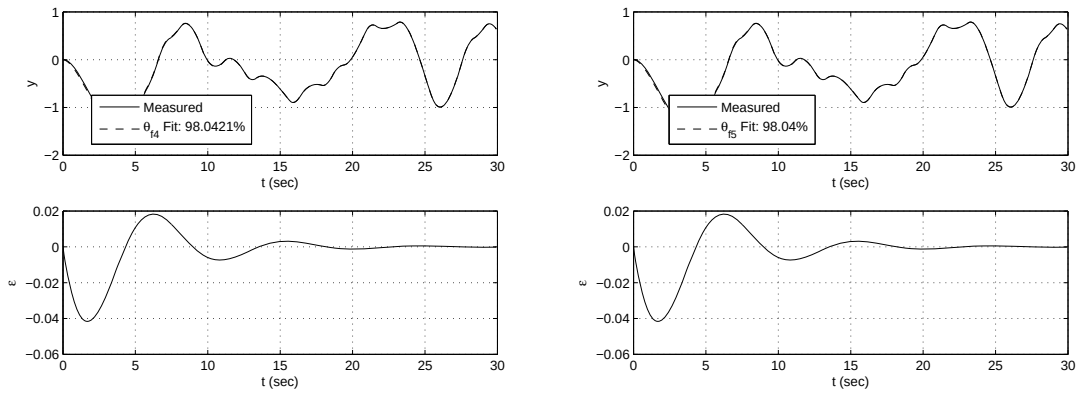

(a) Estimations from step response (b) Estimations from sum of sinusoids response

Figure 4.32. Cross validation of the models estimated by iterative search method.

Information about each iteration of the Levenberg-Marquardt algorithm including the number of function evaluations, norm of the residual vector, first order optimality measure, Levenberg-Marquardt parameter and the norm of current step are given in Table 4.11. The values of the parameters of the estimations from step and sum of sinusoids responses are plotted for each iteration in Figure 4.33.

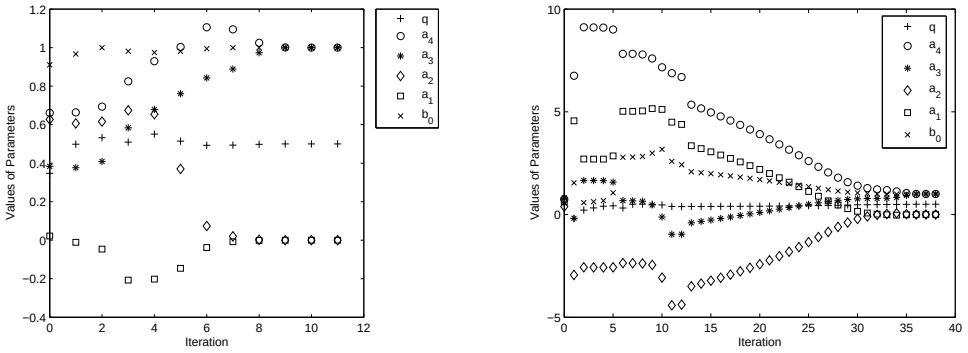

(a) Parameter values of θ_{f4} (b) Parameter values of $\theta_{\mathrm{f_5}}$

Figure 4.33. Parameter values of the iterative search for the step input

Table 4.11. Iterative search of the parameters.

Iteration	Function Count	Residual	First Order Optimality	ζ	Norm of Step
0	7	23.0868	60.9	10^{-2}	-
1	18	6.474	22.2	10^{2}	0.165676
2	25	4.0639	5.41	10	0.0741707
3	32	1.33118	22.9	1	0.279395
4	39	0.102718	9.83	10^{-1}	0.149097
5	46	0.0173818	2.15	10^{-2}	0.311744
6	53	0.00373819	1.7	10^{-3}	0.342721
7	60	7.71691×10^{-6}	0.00172	10^{-4}	0.0779465
8	67	7.1552×10^{-6}	0.0343	10^{-5}	0.111126
9	74	1.44585×10^{-7}	0.00686	10^{-6}	0.0351178
10	81	6.15896×10^{-13}	1.95×10^{-5}	10^{-7}	0.00128476
11	88	7.94964×10^{-21}	1.76×10^{-9}	10^{-8}	3.08508×10^{-6}

The frequency response estimation of Bagley-Torvik systems is shown in Figure 4.34. While the estimations from step and PRBS responses cannot be used for frequency domain curve fit, the estimation from sum of sinusoids response can be used in Levy's method.

Levy's identification with and without Vinagre's weights is applied for the following commensurate order model

$$G(s) = \frac{b_0}{a_4 s^{4\times 0.5} + a_3 s^{3\times 0.5} + a_2 s^{2\times 0.5} + a_1 s^{0.5} + 1}, \; \theta = \begin{bmatrix} b_0 & a_4 & a_3 & a_2 & a_1 \end{bmatrix}^T \quad (4.95)$$

Parameters are estimated as given in Table 4.12. The fit of Levy's method with and without weights is plotted in Figure 4.35.

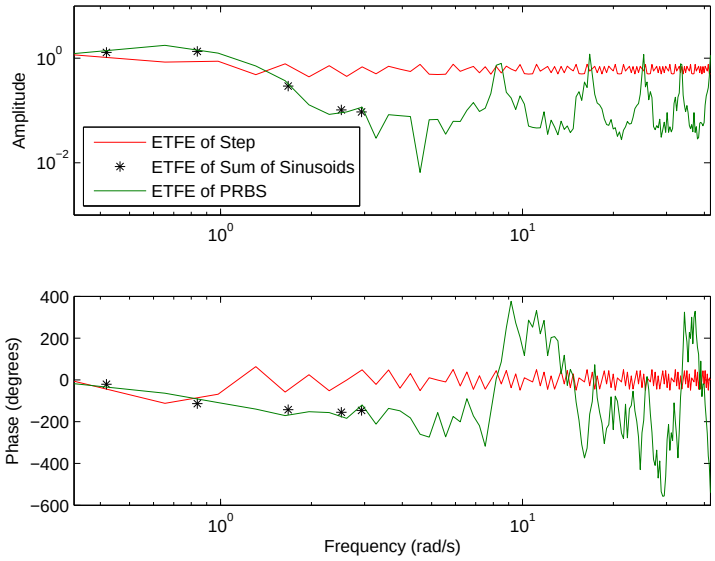

Figure 4.34. Frequency response estimation of Bagley-Torvik system.

Table 4.12. Frequency domain estimation of the parameters.

θ	Levy	Vinagre
b_0	0.4610	0.6621
a_4	0.6085	0.8709
a_3	-0.3606	0.0356
a_2	1.7182	1.1907
a_1	-1.3645	-0.8205

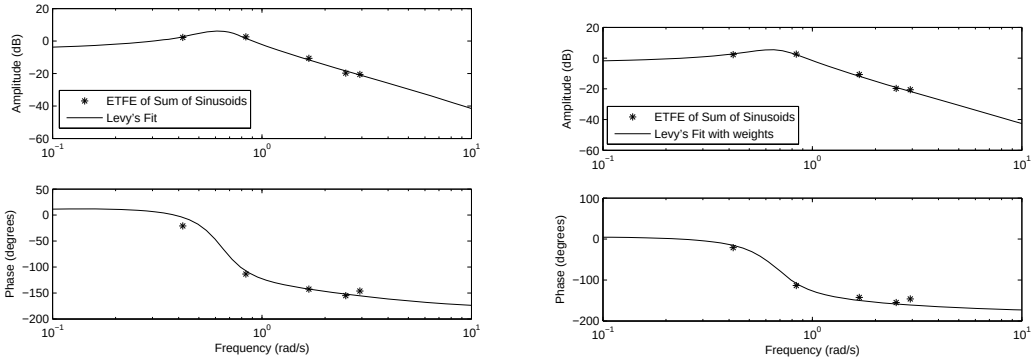

(a) Levy without weights

(b) Levy with Vinagre's weights

Figure 4.35. Levy's fit in frequency domain with and without weights.

The models estimated from frequency domain are simulated with the PRBS input. The simulation results are given in Figure 4.36.

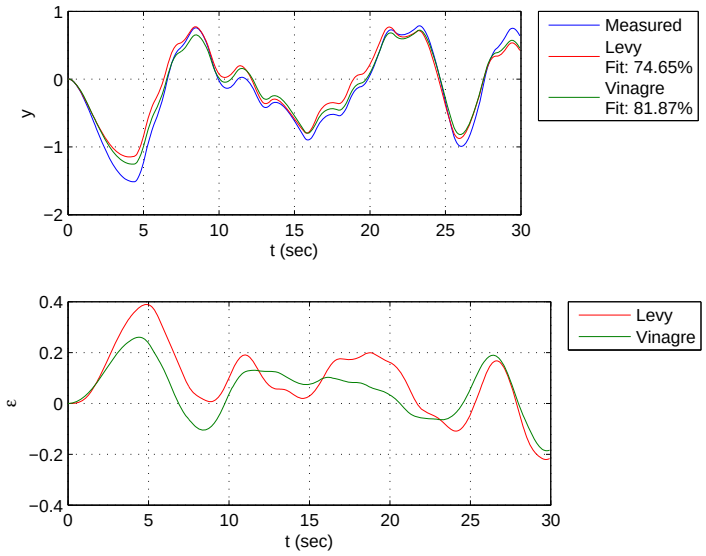

Figure 4.36. Cross validation of the model estimated in frequency domain.

Experiments performed on the given benchmark systems have shown that each method has its own advantages and disadvantages. Time domain methods can be applied directly to the gathered system input-output data while frequency domain methods require the estimation of the frequency response of the system. Frequency response of the system can be estimated by nonparametric frequency domain methods but these methods yield good estimation for only periodic signals. Simulations have also revealed that the usage of Vinagre's weights do not always improve the frequency domain fit. Time domain method of linear regression is easy to apply and the parameters can be estimated successfully by a least squares (LS) solution as long as the input is persistently exciting. Grünwald-Letnikov definition allows the parametrization of the commensurate order of the system. However, this method requires a numerical search routine in order to estimate the parameters. Only local solution can be guaranteed by the numerical methods. The advantages and disadvantages of the given fractional order parametric identification methods are summarized in Table 4.13.

Table 4.13. Comparison of fractional order parametric identification methods

Domain	Methods	Advantages	Disadvantages
Time	Linear Regression	is simple to apply, solution is given by least squares	input signal must be sufficiently exciting
	Iterative Search	can be used to determine commensurate order, can be applied to ill-conditioned data	solution is local, global solution is not guaranteed, model must be in commensurate form
Freq.	Levy	a good frequency domain fit results in good time domain fit	only works with sinusoidal input, low frequency fit may be poor
	Levy with weights	may improve low frequency fit by weights	only works with sinusoidal input, improvement is not guaranteed

5. A HEURISTIC PROCEDURE FOR IDENTIFYING AN UNKNOWN LINEAR DETERMINISTIC SYSTEM

Nonparametric methods should be applied as a first step in identifying an unknown linear deterministic system. Time domain methods of impulse and step response analysis can be used to find out important properties of a system such as delay time, gain, time constant, and order. For example in the case of a delayed system delay time can be computed by observing system's first response to the impulse or step input. If it is not possible to change the input signal of the system or apply inputs like impulse or step, time domain method of correlation analysis can be applied in order to estimate the impulse or step responses of these systems. Although the correlation analysis depends on the input signal being sufficiently exciting and can only give crude estimates in the presence of noise, properties of the system like delay time, gain and order can still be identified by analysing an estimated impulse or step response. In addition to impulse and step response analysis, an estimate of frequency response of the system can also be used to gain insight into the unknown system. By looking at resonance peaks, high frequency roll-off and phase shift in an estimated frequency response, system order and delay time can be recognized.

In order to find a mathematical model for the system, a parametric method has to be applied. If some insight regarding the system order is available by the information gathered from the nonparametric methods or by priori knowledge about dynamics of the system, then deciding on the form of the model to be used in the parametric method is easier. However, if it is not possible to determine the structure of the model, as a principle starting with a simpler first order integer model or fractional models whose orders are less than one and using linear regression method to estimate the parameters of the model is always recommended. Grünwald-Letnikov's definition which allows the parametrization of the system order can be applied with both a first order integer model and a fractional model whose order is less than one. Then system order can be estimated by a numerical method. If the estimated models give unsatisfactory results

in the validation tests, the structure of the proposed integer or fractional model must be changed. The procedure can be outlined as

- If model structure cannot be determined, apply nonparametric methods to gain insight into the system
  - If possible apply an impulse or step input and try to determine system properties such as delay time, gain, and system order by analyzing impulse or step response of the system
  - If it not possible to apply an impulse or step input, use correlation analysis to estimate impulse or step response of the system
  - Properties of the system can also be recognized by analyzing an estimated frequency response of the system
- If some insight into the system, use that insight to propose a model structure for the system and then by using a parametric method either in time domain or frequency domain estimate the parameters of the model
- If it is not possible to determine a model structure, start out with either a first order integer model or a fractional model whose order is less than one and by using linear regression in time or frequency domain estimate the parameters of the model
  - Grünwald-Letnikov's definition which allows the parametrization of the system's order can be used with simpler integer or fractional models and the system's order can be estimated by a numerical method
- For validation, models obtained under various conditions in various model structures should be simulated and compared with the measured system output

6. CONCLUSIONS

In this thesis fractional calculus and its potential as a tool for system identification have been investigated. Definitions and properties of fractional calculus as well as fractional order differential equations and their solutions have been studied. It is seen that the initial condition problem can dramatically change the solution of the fractional order differential equation. While the usage of the RL definition introduces initial conditions which are not physically interpretable, the usage of Caputo's initial conditions from integer order differential equations changes the solution. The lack of physical interpretation of the RL initial conditions is a serious issue which makes it unclear how to measure them experimentally. However, the solutions obtained from these two different definitions coincide for zero initial conditions. For non-zero initial conditions the problem remains and a review of the literature has shown that researchers either use the Caputo's definition, or consider only the case of zero initial conditions. Thus, the usage of zero initial conditions, where the same solution is obtained regardless of the definition, has been preferred in this study in order to avoid the initial condition problem.

System identification with integer order models has been reviewed. A survey of nonparametric and parametric methods based on minimizing the prediction error has been conducted. A delayed second order process model with random binary input disturbed by white noise has been selected as a benchmark system to compare the performances of the surveyed identification methods. First, nonparametric methods have been applied to the gathered data in order to gain an insight into the system. Nonparametric methods of time and frequency domains have resulted in crude estimations of impulse, step and frequency response of the system due to the fact that these methods neglect the presence of noise. Nevertheless through analyzing these crude estimations, delay time, system order and complexity of the system's poles have been identified. It is seen that nonparametric identification can give critical information about the system to be identified as long as the estimates are good enough to extract meaningful information. Then different model structures are proposed based on the

insight gained through nonparametric identification and the parameters of these structures are estimated by parametric identification methods. The performances of the different model structures are compared by using the validation data. The comparison between different model structures has revealed that selection of the correct model structure determines the success of the parametric methods. An outline of conclusions drawn from the review of integer order system identification is given as

- Input signal must be persistently exciting for a successful identification. Identification methods are applied on the system's response to the input signal. If the input signal is not persistently exciting, then the gathered data will be ill-conditioned and the identification will fail.
- Nonparametric methods are very sensitive to the type of the input signal. If the input signal is not persistently exciting, then nonparametric methods give crude estimations. For nonperiodic input signals the estimations obtained through frequency domain methods are still crude even if the input signal is persistently exciting.
- Nonparametric methods give large estimation errors in the presence of noise. The nonparametric methods do not take noise into account in their calculations.
- System properties such as delay time, gain, time constant and order can be identified through nonparametric identification.
- Parametric identification methods are less sensitive to the type of the input signal than the nonparametric identification methods.
- Success of parametric methods depend on the structure of the chosen model. If the selected model structure is close to the true model of the system, then the model parameters are estimated successfully regardless of the input signal.

After reviewing integer order system identification, attention is given to fractional order system identification. Various parametric identification techniques which use fractional order models have been investigated. The analyzed methods consist of linear regression, iterative search using Grünwald-Letnikov definition, and Levy's frequency domain curve fitting with and without weights. Studies have uncovered the fact that the given methods are extensions of the parametric identification methods with integer

order models. As for the nonparametric identification, it is seen that they can be directly applied without any modification. For comparing the performances of the presented identification techniques, semi-integrating circuits and viscoelastic system of Bagley-Torvik have been chosen as benchmark systems. Identification experiments have been carried out with three systems: a semi-integrating circuit in a negative feedback loop, a semi-integrating circuit in series connection with a resistance and an inductance element and the viscoelastic system of Bagley-Torvik. Three input signals including a step, a periodic sum of sinusoids and a random binary signal are applied to each system. The data from the step and sum of sinusoids response are used in the estimation procedure while the data gathered from the experiment with the random binary signal are reserved for the cross validation of different models. A fractional order and an integer order model is proposed for each system and then the parameters of each model are estimated for both step and sum of sinusoids experiments by applying the given identification methods. Comparisons have shown that

- From the perspective of models, the proposed fractional order models are better at predicting the outputs of the systems than the proposed integer order models. It may be possible to find a higher integer order model which better fits the validation data but complexity of a model increases as its order increases.
- In the case of semi-integrating circuits the order of the true model is very high which makes it very hard to work on these systems. The proposed fractional order model benefits from model order reduction. Fractional order models may provide efficient modeling and thus easier simulation of such systems.
- Persistency of excitation from integer order system identification does not work for fractional order models. In system identification with integer order models, the persistency of excitation demands that the level of excitation of the applied input signal must be at least equal to or higher than the order of the proposed model in order for a successful estimation. If the order of the proposed fractional model is equal to or less than one as in the case of the first system, the step input signal, of whose excitation level is one, yields good estimation results that are in agreement with the persistency of excitation from integer order system identification. However, PRBS input, whose excitation level is much more greater

than the excitation level of the step input signal, results in ill-conditioned data which prevents successful estimation.

- Nonparametric identification methods from integer order system identification can be directly applied to fractional order systems, while parametric methods need to be modified in order to work with fractional order models.
- Each fractional parametric method has its own advantages and disadvantages. While time domain identification methods can be directly applied to the gathered data, frequency domain methods of Levy with and without weights requires the estimation of the frequency response of the system first.
- Frequency domain methods depends on the nonparametric methods from integer order system identification for estimating the frequency response of the system. This dependency brings a serious constraint on the type of the input signal since nonparametric methods are very sensitive to the type of the input signal.
- Using Vinagre's weights in Levy's method does not guarantee an improvement in the frequency domain fit and even in some cases poorer fits are obtained through the usage of weights.
- Time domain method of linear regression is simply to apply and the parameters can be easily estimated by a LS solution.
- Iterative search by using Grünwald-Letnikov's definition is a significant method for allowing the estimation of the system order as a model parameter. However, this method implements numerical schemes in the search of the parameter vector. The numerical search routines can only guarantee convergence to a local solution of the minimization problem. In order to find the global solution there is no other way than to re-run the numerical search routine for different initial parameter values.

Persistency of excitation needs to be redefined for fractional order models. As a future work, further research into this open area is encouraged.

APPENDIX A: EXISTENCE AND UNIQUENESS THEOREMS FOR FODEs

In this appendix the existence and uniqueness of solutions of initial value problems for linear fractional differential equations are given. The theorems and their proofs are given in [9].

The initial value problem is given as

$$
\begin{aligned}
&{}_0\mathscr{D}_t^{\sigma_n} y(t) + \sum_{j=1}^{n-1} p_j(t) {}_0\mathscr{D}_t^{\sigma_{n-j}} y(t) + p_n(t) y(t) = f(t), \quad (0 < t < T < \infty) \\
&\left[{}_0\mathscr{D}_t^{\sigma_k - 1} y(t) \right]_{t=0} = b_k, \quad k = 1, \ldots, n
\end{aligned} \tag{A.1}
$$

The fractional derivatives in the equation (A.1) are sequential derivatives (A.2).

$$
\begin{aligned}
&{}_a\mathscr{D}_t^{\sigma_k} \equiv {}_a\mathscr{D}_t^{\alpha_k} \, {}_a\mathscr{D}_t^{\alpha_{k-1}} \cdots {}_a\mathscr{D}_t^{\alpha_1} \\
&{}_a\mathscr{D}_t^{\sigma_{k-1}} \equiv {}_a\mathscr{D}_t^{\alpha_{k-1}} \, {}_a\mathscr{D}_t^{\alpha_{k-2}} \cdots {}_a\mathscr{D}_t^{\alpha_1} \\
&\sigma_k = \sum_{j=1}^{k} \alpha_j, \quad k = 1, 2, \ldots, n \\
&0 < \alpha_j \leq 1, \quad j = 1, 2, \ldots, n
\end{aligned} \tag{A.2}
$$

The forcing function is bounded, $f(t) \in L_1(0, T)$ (A.3). It is further assumed that $f(t) \equiv 0$ for $t > T$.

$$
\int_0^T |f(t)| \mathrm{d}t < \infty \tag{A.3}
$$

In the first step, the case of zero coeficients are considered $p_k(t) \equiv 0$.

Theorem 1. If $f(t) \in L_1(0,T)$, then the equation (A.4) has the unique solution $y(t) \in L_1(0,T)$, which satisfies the initial conditions (A.1).

$$ {}_0\mathscr{D}_t^{\sigma_n} y(t) \equiv f(t) \tag{A.4} $$

Proof. The Laplace transform of the equation (A.4) is given in (A.5).

$$ s^{\sigma_n} Y(s) - \sum_{k=0}^{n-1} s^{\sigma_n - \sigma_{n-k}} \left[{}_0\mathscr{D}_t^{\sigma_{n-k}-1} y(t) \right]_{t=0} = F(s) \tag{A.5} $$

Using the initial conditions (A.1) the Laplace tranform can be written as (A.6).

$$ Y(s) = s^{-\sigma_n} F(s) + \sum_{k=0}^{n-1} b_{n-k} s^{-\sigma_{n-k}} \tag{A.6} $$

The solution in the time domain can be obtained by applying the inverse Laplace transform (A.7).

$$ y(t) = \frac{1}{\Gamma(\sigma_n)} \int_0^t (t-\tau)^{\sigma_n - 1} f(\tau) \mathrm{d}\tau + \sum_{k=0}^{n-1} \frac{b_{n-k}}{\Gamma(\sigma_{n-k})} t^{\sigma_{n-k}-1} \tag{A.7} $$

If $n-k$ is replaced with i, the solution is shown in (A.8).

$$ y(t) = \frac{1}{\Gamma(\sigma_n)} \int_0^t (t-\tau)^{\sigma_n - 1} f(\tau) \mathrm{d}\tau + \sum_{i=1}^{n} \frac{b_i}{\Gamma(\sigma_i)} t^{\sigma_i - 1} \tag{A.8} $$

Once the solution expressed by (A.8) is substituted into the equation (A.1), it is observed that $y(t)$ satisfies the initial conditions and thus the existence of the solution is proved. □

Theorem 2. If $f(t) \in L_1(0,T)$ and $p_j(t)$ are continuous functions in the closed interval $[0,T]$, then the initial value problem (A.1) has a unique solution $y(t) \in L_1(0,T)$.

Proof. The initial value problem is assumed to have a solution $y(t)$ (A.9).

$$ {}_0\mathscr{D}_t^{\sigma_n} y(t) = \varphi(t) \tag{A.9} $$

Using Theorem 1 the solution of (A.9) is obtained as (A.10).

$$ y(t) = \frac{1}{\Gamma(\sigma_n)} \int_0^t (t-\tau)^{\sigma_n - 1} \varphi(t) \mathrm{d}t + \sum_{i=1}^{n} b_i \frac{t^{\sigma_i - 1}}{\Gamma(\sigma_i)} \tag{A.10} $$

If $y(t)$ (A.10) is substituted into the initial value problem (A.1), the function $\varphi(t)$ is obtained as the Volterra integral equation of the second kind (A.11).

$$ \begin{aligned} &\varphi(t) + \int_0^t K(t,\tau)\varphi(\tau)\mathrm{d}t = g(t) \\ &K(t,\tau) = p_n(t)\frac{(t-\tau)^{\sigma_n - 1}}{\Gamma(\sigma_n)} + \sum_{k=1}^{n-1} p_{n-k}(t)\frac{(t-\tau)^{\sigma_n - \sigma_k - 1}}{\Gamma(\sigma_n - \sigma_k)} \\ &g(t) = f(t) - p_n(t)\sum_{i=1}^{n} b_i \frac{t^{\sigma_i - 1}}{\Gamma(\sigma_i)} - \sum_{k=1}^{n-1} p_{n-k}(t) \sum_{i=k+1}^{n} b_i \frac{t^{\sigma i - \sigma_k - 1}}{\Gamma(\sigma_i - \sigma k)} \end{aligned} \tag{A.11} $$

Since the functions $p_j(t)$ are continuous in $[0,T]$, then the kernel $K(t,\tau)$ can be expressed in the form of a weakly singular kernel (A.12).

$$ K(t,\tau) = \frac{K^*(t,\tau)}{(t-\tau)^{1-\mu}} \tag{A.12} $$

$K^*(t,\tau)$ is continuous for $0 \le t \le T$, $0 \le \tau \le T$, and $\mu = \min\{\sigma_n, \alpha_n\}$. The function, $g(t)$ can be written similarly in the form (A.13).

$$ g(t) = \frac{g^*(t)}{t^{1-\nu}} \tag{A.13} $$

$g^*(t)$ is continuous in $[0,T]$ and $\nu = \min\{\alpha_1, \alpha_2, \ldots, \alpha_n\}$.

The equation (A.11) with the weakly singular kernel (A.12) and the function $g(t) \in L_1(0,T)$ has a unique solution. According to Theorem 1, the unique solution $y(t) \in L_1(0,T)$ can be determined using (A.10). In many applied problems the zero

initial conditions on the function $y(t)$ and its integer-order derivatives are used. For this particular case it is supposed that there exist $m-1$ number of zero initial conditions, $m-1 \leq \sigma_n < m$ (A.14).

$$y^{(j)}(0) = 0, \qquad j = 0, 1, \ldots, m-1 \tag{A.14}$$

All sequential fractional derivatives are replaced with the Riemann-Liouville fractional derivatives of the same order σ_k (A.15).

$${}_0\mathscr{D}_t^{\sigma_n} y(t) + \sum_{j=1}^{n-1} p_j(t)\, {}_0\mathscr{D}_t^{\sigma_{n-j}} y(t) + p_n(t) y(t) = f(t) \tag{A.15}$$

□

Theorem 3. If $f(t)$ and $p_j(t)$ are continuous functions in the closed interval $[0, T]$, then the initial condition problem (A.15), where $m-1 \leq \sigma_n < m$ and $\sigma_n > \sigma_{n-1} > \cdots > \sigma_1 > 0$ has a unique solution $y(t)$, that is continuous in $[0, T]$.

APPENDIX B: STOCHASTIC PROCESSES

A stochastic process is a sequence of random variables with a joint probability distribution function (PDF). Some well-known definitions are given for a stochastic process, $x(n)$ (B.1).

$$\begin{aligned}
&\text{Mean} : m_x(n) = E\{x(n)\} \\
&\text{Correlation} : R_x(n) = E\left\{x(n_1)x^T(n_2)\right\} \\
&\text{Covariance} : C_x(n_1, n_2) = E\left\{(x(n_1) - m_x(n_1))(x(n_2) - m_x(n_2))^T\right\} \\
&\text{Variance} : R_x(n, n) - E^2(x(n))
\end{aligned} \tag{B.1}$$

If $x(n)$ is a wide-sense stationary (WSS) process, the following properties hold (B.2).

$$\begin{aligned}
m_x(n) &= m_x = \text{constant } \forall\, n \\
R_x(n_1, n_2) &= R_x(n_1 - n_2)
\end{aligned} \tag{B.2}$$

The stochastic processes with the following assumptions are called quasi-stationary processes (B.3).

$$\begin{aligned}
E\{x(n)\} &= m_x(n),\ |m_x(n)| \leq C\ \forall n \\
E\{x(n)x(r)\} &= R_x(n, r),\ |R_x(n, r)| \leq C \\
\lim_{N\to\infty} \frac{1}{N} \sum_{n=1}^{N} R_x(n, n-\tau) &= R_x(\tau),\ \forall \tau
\end{aligned} \tag{B.3}$$

The first two properties are satisfied trivially since $x(n)$ is a stochastic process. For the third property a symbol $\overline{E}$ is introduced in order to ease the notation (B.4).

$$\overline{E}\{x(n)x(n-\tau)\} = R_x(\tau) = \lim_{N\to\infty} \frac{1}{N} \sum_{n=1}^{N} x(n)x(n-\tau) \tag{B.4}$$

$x(n)$ is a deterministic signal and that means it is a bounded sequence. Thus the limit

in (B.4) exits.

If a stochastic process is expressed as the sum of two other stochastic processes, $x(n) = x_1(n) + x_2(n)$, then the mean and correlation of $x(n)$ can be found as (B.5).

$$\begin{aligned} \overline{E}\{x(n)\} &= m_{x_1} + m_{x_2} \\ \overline{E}\{x(n)x(n-\tau)\} &= R_{x_1} + R_{x_2} + 2m_{x_1}m_{x_2} \end{aligned} \tag{B.5}$$

APPENDIX C: TRANSFER FUNCTION OF LTI SYSTEM

Using the z transform ($z = e^{j2\pi f}$, $|f| \leq \frac{1}{2}$) the output of a LTI system can be written as

$$y(n) = \sum_{k=1}^{\infty} g(k)u(n-k) \Rightarrow Y(z) = G(z)U(z) \tag{C.1}$$

where $G(z)$ is described by

$$G(z) = \sum_{k=1}^{\infty} g(k)z^{-k} \tag{C.2}$$

$G(z)$ is called the discrete time transfer function of the linear system.

The relationship of the distrubance term can also be expressed in the z-domain with the discrete time transfer function, $H(z)$.

$$H(z) = \sum_{k=0}^{\infty} h(k)z^{-k} \tag{C.3}$$

The continuous time representation of a linear system can be obtained by applying the Laplace transform to the impulse response function. Once the transformation is applied, the continuous time transfer function $G_c(s)$ describes the relationship between the input and the output.

$$Y(s) = G_c(s)U(s) \tag{C.4}$$

For identification of systems described by continuous time transfer functions, it is neccessary to go from continuous time representation to discrete time representation

$$G_c(s) \rightarrow G_T(z) \tag{C.5}$$

T (C.5) denotes the sampling interval. If the input is piecewise constant over the sampling interval, the transformation is accomplished without any approximation. Otherwise, there exists several discrezation schemes. For example the most simple approximation is of Euler's

$$G_T(z) \approx G_c\left(\frac{z-1}{T}\right)$$

while the Tustin's formula is given as

$$G_T(z) \approx G_c\left(\frac{2}{T}\frac{z-1}{z+1}\right)$$

The transfer function $G(z)$ is stable if

$$G(z) = \sum_{k=1}^{\infty} g(k)z^{-k}, \qquad \sum_{k=1}^{\infty} |g(k)| < \infty \tag{C.6}$$

This corresponds to $G(z)$ being analytic on and outside the unit circle for $|z| \geq 1$.

REFERENCES

1. L. Ljung, *System identification: theory for the user*, Englewood Cliffs, New Jersey: Prentice-Hall, 1987.

2. T. T. Hartley, C. F. Lorenzo and H. K. Qammar, "Chaos in a Fractional Order Chua System", Cleveland, Ohio, 1996.

3. S. Westerlund, "Dead Matter Has Memory!", *Physica Scripta*, vol. 43, pp.174-179, 1991.

4. T. Machado and A. Galhano, "Fractional Dynamics: A Statistical Perspective", *Journal of Computational and Nonlinear Dynamics*, 3, 021201-5, 2008.

5. K. S. Miller and B. Ross, *An Introduction to The Fractional Calculus and Fractional Differential Equations*, New York: Wiley, 1993.

6. K. B. Oldham and J. Spanier, *The Fractional Calculus*, San Diego, California: Academic Press, 1974.

7. L. Ljung, "Perspectives on System Identification", in *Proceedings of the 17th IFAC World Congress,* Seoul, Korea, 2008.

8. M. Gevers, "A Personal View of The Development of System Identification: A 30-year Journey Through an Exiciting Field", *IEEE Control Systems Magazine*, vol. 26, pp. 93-105, 2006.

9. I. Podlubny, *Fractional Differential Equations*, San Diego, California: Academic Press, 1999.

10. A. A. Kilbas, H. M. Srivastava, and J. J. Trujillo, *Theory and Applications of Fractional Differential Equations*, Amsterdam: Elsevier, 2006.

11. I. Petráš, I. Podlubny, P. O'Leary, Ľ. Dorčák and B. Vinagre, *Analogue Realization of Fractional Order Controllers*, Kosice: Technical University of Kosice, 2002.

12. D. Xue and Y. Chen, *Solving Applied Mathematical Problems with MATLAB*, Boca Raton: CRC Press, 2008.

13. I. Podlubny, "Matrix Approach to Discrete Fractional Calculus", *Fractional Calculus and Applied Analysis*, 4, 3, pp. 359-386, 2000.

14. T. Söderström and P. Stoica, *System Identification*, London: Prentice Hall International, 1989.

15. R. Malti, M. Aoun, J. Sabatier and A. Oustaloup, "Tutorial on System Identification using Fractional Differentiation Models", in *14th IFAC Symposium on System Identification,* Newcastle, Australia, pp. 606-611, 2006.

16. O. Cois, A. Oustaloup, T. Poinot and J. L. Battaglia, "Fractional State Variable Filter for System Identification by Fractional Model", in *IEEE 6th European Control Conference*, Porto, Portugal, 2001.

17. T. Poinot and J. C. Trigeassou, "Identification of Fractional Systems Using an Output-Error Technique", *Nonlinear Dynamics*, 38, pp. 133-154, 2004.

18. A. Oustaloup, P. Melchior , P. Lanusse, O. Cois and F. Dancla, "The CRONE toolbox for Matlab", in *Proceedings of the 41st IEEE Conference on Decision and Control*, Las Vegas, Nevada, USA, pp. 240-245, 2002.

19. B. M. Vinagre, C. A. Monje and A. J. Calderón, "Fractional Order Systems and Fractional Order Control Actions", in *41st IEEE Conference on Decision and Control*, Las Vegas, USA, 2002.

20. O. Cois, A. Oustaloup, E. Battaglia and J.-L. Battaglia, "Non Integer Model from Modal Decomposition for Time Domain System Identification", in *Proceedings of 12th IFAC Symposium on System Identification*, Santa Barbara, USA, 2000.

21. The MathWorks, "Optimization Toolbox^{TM} 4 User's Guide", *The MathWorks*, 2009.

22. D. Valerio and J. Sa da Costa, "Identification of Fractional Models from Frequency Data", *Advances in Fractional Calculus: Theoratical Developments and Applications in Physics and Engineering*, pp. 229-242, 2007.

23. M. D. Ortigueira, D. Valerio, and J. Sa da Costa, "Identifying a transfer function from a frequency response", in *ASME 2007 International Design Engineering Technical Conferences & Computers and Information in Engineering Conference*, Las Vegas, Nevada, USA, 2007.

24. D. Valerio, "Ninteger 2.3 Fractional Control Toolbox for Matlab", *Universidade Técnica de Lisboa Instituto Superior Técnico*, 2005.

25. T. Poinot, J. C. Trigeassou, "A method for modelling and simulation of fractional systems", *Elsevier: Signal Processing*, 83, pp. 2319-2333, 2003.

26. M. Aoun, R. Malti, F. Levron and A. Oustaloup, "Numerical simulations of fractional systems", in *Proceedings of DETC'03 ASME 2003 Design Engineering Technical Conferences & Computers and Information in Engineering Conference*, Chicago, Illinois, USA, 2003.

27. M. S. Takyar and T. T. Georgiou, "The fractional integrator as a control design", in *Proceedings of the 46th IEEE Conference on Decision and Control*, New Orleans, LA, USA, pp. 239-244, 2007.